TAMPEREEN TEKNILLINEN YLIOPISTO
TAMPERE UNIVERSITY OF TECHNOLOGY

SAMI VEHMASVAARA

COMPENSATION STRATEGIES IN CABLED RURAL NETWORKS

Master of Science Thesis

Examiner: Professor Pekka Verho
Examiner and topic approved by the Faculty Council of Computing and Electrical Engineering on 7th November 2012

ABSTRACT

TAMPERE UNIVERSITY OF TECHNOLOGY
Master of Science Degree Programme in Electrical Engineering
VEHMASVAARA, SAMI: Compensation strategies in cabled rural networks
Master of Science Thesis, 97 pages
February 2013
Major: Power systems and market
Examiner: Professor Pekka Verho
Keywords: compensation, reactive power, petersén coil, shunt reactor, earth fault

The medium voltage network of Finland is experiencing major changes in the near future as the overhead lines are replaced with cables. The reason for the extensive cabling is the new suggestions for distribution network operators' quality of supply, which were set by the Ministry of Employment and the Economy. Cabling sets a number of practical and technical challenges to distribution network operators. From the technical point of view, cables generate a significant amount of reactive power and earth fault current, which were the main research interests of this thesis.

The purpose of the thesis was to find an optimal way to compensate both reactive power and earth fault currents in extensively cabled networks. The thesis studied, what is the actual need for compensation and how should it be implemented optimally in a techno-economic way. The study was carried out by using PSCAD-simulation software and making calculations based on the results.

The study revealed that there is a certain need for reactive power compensation. The main reason is Fingrid's fee for inputting reactive power in the main grid, which can cause major costs as the amount of cabling increases. Another reason is the power losses due to reactive power flow, which can be effectively limited with the correct selection and placement of shunt reactors. The reactive power compensation should be implemented by using centralized shunt reactors. Distributed shunt reactors did not appear to be profitable in the normal branched feeders. Instead, they should be used with over 50 km straight feeders.

The distributed earth fault current compensation should be implemented with distributed Petersén coils. The centralized earth fault compensation should be carried out with a combination of adjustable Petersén coils and centralized shunt reactors. It is possible to use a shunt reactor for earth fault compensation if its neutral point is grounded. However, substations should always first have an adjustable Petersén coil before grounding the shunt reactors in order to keep the correct compensation degree.

TIIVISTELMÄ

TAMPEREEN TEKNILLINEN YLIOPISTO
Sähkötekniikan koulutusohjelma
VEHMASVAARA, SAMI: Maaseudun kaapeliverkon kompensointistrategiat
Diplomityö, 97 sivua
Helmikuu 2013
Pääaine: Sähköverkot ja -markkinat
Tarkastaja: Professori Pekka Verho
Avainsanat: kompensointi, loisteho, sammutuskela, shunttireaktori, maasulku

Työ- ja elinkeinoministeriö on määrittänyt verkkoyhtiöille uudet suositukset toimitusvarmuudesta, jotka tulevat muuttamaan Suomen keskijänniteverkon rakennetta merkittävästi lähitulevaisuudessa. Käytännössä suositukset ohjaavat säävarman verkon rakentamista, jonka seurauksena suuri osa ilmajohdoista tullaan korvaamaan maakaapeleilla. Kaapeloinnin haasteina ovat sen käytännön toteutus sekä sähkötekninen toimivuus. Tämän diplomityön pääaiheina olivat kaapeleiden merkittävä loistehon tuotanto sekä suuret maasulkuvirrat, mitkä kuuluvat kaapeloinnin teknisiin haasteisiin.

Työn tavoitteena oli kehittää optimaalinen tapa kompensoida loistehoa ja maasulkuvirtoja kaapeloidussa keskijänniteverkossa. Työssä tutkittiin, mikä on kompensoinnin todellinen tarve ja miten sen toteutus voidaan optimoida teknis-taloudellisesti. Työ tehtiin pääosin suorittamalla PSCAD-simulointeja, ja tekemällä tuloksiin pohjautuvia laskelmia.

Työssä havaittiin, että loistehon kompensoinnille on todellinen tarve. Pääsyynä ovat Fingridin asettamat maksut loistehon siirrolle kantaverkkoon päin, jotka saattavat aiheuttaa merkittäviä kustannuksia kaapelimäärän lisääntyessä. Toisena syynä ovat loistehon siirrosta aiheutuvat tehohäviöt, joita voidaan tehokkaasti rajoittaa oikeilla reaktorivalinnoilla ja sijoituksella. Tulosten mukaan loistehon kompensointi tulisi toteuttaa pääosin keskitetysti sähköasemilla tai kytkinasemilla. Hajautettujen shunttireaktorien käyttö on taloudellista vain yli 50 km pitkillä säteittäisillä lähdöillä.

Maasulkuvirran hajautettu kompensointi tulisi toteuttaa hajautetuilla sammutuskeloilla. Keskitetty maasulkuvirran kompensointi kannattaa toteuttaa säädettävien sammutuskelojen ja shunttikelojen yhdistelmänä. Tähtikytkentäisiä shunttireaktoreja voidaan myös käyttää maasulkuvirran kompensointiin, jos niiden tähtipiste maadoitetaan. Pelkillä shunttireaktoreilla ei kuitenkaan voida hoitaa keskitettyä maasulkuvirran kompensointia, sillä säädettävää sammutuskelaa tarvitaan verkon oikean kompensointiasteen säilyttämiseen.

PREFACE

This Master of Science Thesis was written for Elenia Oy during the time between June 2012 and January 2013. The examiner of the thesis was Professor Pekka Verho from the Department of Electrical Engineering and the supervisor was M.Sc. Juho Uurasjärvi from Elenia Oy.

First of all, I want to thank the company for giving me an opportunity to write the thesis about such an interesting and current topic. The thesis process has been extremely educational and useful for me. A great thank goes to my supervisor Juho Uurasjärvi who have given helpful feedback and guided the work in the right direction. I am also grateful for all other colleagues who have given me advice and opinions during the work, especially for Hanna-Mari Pekkala. My examiner Pekka Verho also deserves great thanks for giving supportive feedback and new ideas for the development of the work.

I want to thank all of my friends with whom I have spent awesome time during the studies. Special thanks to Vesa Hälvä for his useful comments for this thesis and also for being an invaluable friend in our common study path. Last but not least, I want to express my sincere gratitude for my family who have always believed in me and showed their unbending support during my studies and life.

Tampere,
January 9th, 2013

Sami Vehmasvaara

CONTENTS

SYMBOLS AND ABBREVIATIONS

A, B, C, D	Transmission constants
C	Capacitance
C_0	Line capacitance
C_l	Present value of power losses
E	Fault voltage source
f	Frequency
G	Conductance
H	Loss price
L	Inductance
I	Current
I_{comp}	Compensation capacity
I_f	Fault current
I_{Rf}	Resistive part of the earth fault current
I_{RL}	Current in coil resistance
I_{R0}	Current in coil's parallel resistance
I_R	Receiving-end current
I_S	Sending-end current
P	Active power
p	Interest rate
P_{cu}	Load losses of the transformer
P_{cun}	Nominal load losses of the transformer
P_0	No load losses
P_{max}	Maximum active power
P_R	Receiving-end active power
P_S	Sending-end active power
Q_C	Reactive power generated by capacitor
Q_h	Transformers' reactive power losses
Q_L	Reactive power consumed by reactor
Q_{losses}	Reactive power losses
Q_M	One hour average of reactive power
Q_{max}	Maximum reactive power
Q_R	Receiving-end reactive power
Q_S	Sending-end reactive power
Q_s	Reactive power window output limit

Q_{s1}	Reactive power window output limit
R	Resistance
r	Loading increase rate
R_0	Coil's parallel neutral point resistance
R_e	Parallel connection of R_L and R_0
R_f	Fault resistance
R_L	Coil resistance
R_m	Earthing resistance
S	Apparent power
S_N	Apparent power of the largest generator
S_n	Nominal apparent power
S_R	Receiving-end complex power
S_S	Sending-end complex power
t_k	Peak usage time
T	Review period T
U	Voltage
U_a	Phase A voltage
U_b	Phase B voltage
U_c	Phase C voltage
U_{a1}	Phase A positive sequence voltage
U_{b1}	Phase B positive sequence voltage
U_{c1}	Phase C positive sequence voltage
U_{a2}	Phase A negative sequence voltage
U_{b2}	Phase B negative sequence voltage
U_{c2}	Phase C negative sequence voltage
U_{a0}	Phase A zero sequence voltage
U_{b0}	Phase B zero sequence voltage
U_{c0}	Phase C zero sequence voltage
U_k	Touch voltage
U_m	Earthing voltage
U_{ph}	Phase voltage
U_N	Nominal line voltage
U_s	Step voltage
U_0	Neutral point voltage
V_R	Receiving-end voltage

V_S	Sending-end voltage
W_{Gen}	Net active power production
W_{Output}	Output active energy
X	Reactance
X_C	Capacitor reactance
X_L	Coil reactance
x_k	Relative short circuit reactance
X_{Wye}	Reactance of a wye-connected shunt reactor
X_{Delta}	Reactance of a delta-connected shunt reactor
Y	Shunt admittance
Z	Series impedance
Z_0	Zero sequence impedance
Z_1	Positive sequence impedance
Z_2	Negative sequence impedance
Z_c	Characteristic impedance
Z_{T1}	Positive sequence impedance of rural networks
Z_{T2}	Negative sequence impedance of rural networks
Z_{T0}	Zero sequence impedance of rural networks
Z_π	The corrected series impedance
α	The angle of the transmission constant A
β	The angle of the transmission constant B
δ	Sending-end voltage angular displacement
ω	Angular speed
κ	Capitalization factor
CC	Covered cable line
DSO	Distribution system operator
OHL	Overhead line
RMS	Root mean square
SIL	Surge impedance loading

1. INTRODUCTION

The distribution network in Finland is experiencing major changes in a next few years. The winter storms Tapani and Hannu caused serious damage to the distribution network in 2011. The damages were severe especially in the eastern part of Finland and they caused the outages of two weeks for the customers at worst. As a result, the Ministry of Employment and the Economy had a report done about suggestions for the new criteria for the quality of supply. The report suggests that over 6 hour outages are not allowed for the customers in city areas and over 24 hour outages are not allowed in the rural areas during major disturbances. 50 % of the customers of DSO have to meet these conditions before the end of 2019, 75 % of the customers before 2023 and all customers before 2027. Practically, this means that many of the present overhead line networks have to be replaced with cable networks in order to withstand the weather conditions and avoid long outages. The goal is challenging since most of the Finnish medium voltage network is currently overhead line. (Ministry of Employment and The Economy 2012)

Elenia Oy is a second largest distribution network operator in Finland and serves 408 000 customers. The network area is almost 50 000 m^2 and the area extends from Karkkila to Hailuoto in the area of 100 municipalities. Early 2013, Elenia Verkko Oy was merged to Elenia Oy together with Elenia Asiakaspalvelu Oy and Asikkalan Voima Oy. Consequently, Elenia Oy includes all operations from above companies at the moment. Elenia has cabled all new medium voltage lines since 2009 and currently has a cabling degree of approximately 12 % in the medium voltage network. The intention of Elenia is to increase the speed of cabling so that the criteria will be met according to the quality of supply criteria.

Although the idea about the weatherproof network is tempting, there are some challenges with the cabling. For example, the repairing of the cable faults is significantly slower than with overhead lines and the location of the fault is more difficult to find out since they are underground. Another issue is the price of cable installation, which may become very expensive if the soil is rocky or otherwise difficult to dig. In addition to the practical issues, there are technical limitations and new phenomena caused by the cabling, which are the main themes and the motivation of this thesis.

Firstly, cables complicate the protection and safe use of the network by increasing

the total earth fault currents in the network. Besides increasing the total earth fault current, cables also increase the resistive part of the current, which can not be compensated centrally at the substation. Both of these endanger the human safety in the network, which is not acceptable. Secondly, cables generate a significant amount of reactive power. This is a new phenomenon in the medium voltage network since the network has traditionally consumed reactive power instead. When more cables are installed in the network and the reactive power balance turns from inductive to capacitive, it can result in several problems.

It is possible to decrease the affects of the above technical issues by adding compensations devices to the network. The earth fault current compensation has been studied in the extensive cabled network in a previous thesis made for Elenia (Pekkala 2010) and in Sweden (Guldbrand 2009). However, reactive power compensation has studied less in the medium voltage network since it has not been a concern before. Therefore, the main focus of this thesis is at reactive power and earth fault compensation comes as a secondary subject.

Chapters 2, 3 and 4 discuss the theoretical background of the research theme. The second chapter describes the basic electricity theory about the power lines and the power transmission in the network. The third chapter discusses the earth fault phenomenon and presents the new challenges, which have to be considered when more cables are installed in the network. The fourth chapter concerns essential topics about the reactive power such as information about the main grid connection, the challenges of the growing reactive power and devices, which can be used to compensate reactive power. The fifth and sixth chapter include the applied part of the thesis. The fifth chapter introduces the initial data and describes the tools, which are used in the thesis. The sixth chapter presents the results, which consist of four different section and a conclusion section of them.

2. REPRESENTATION OF TRANSMISSION LINES

The fundamental theory of this thesis is introduced in this chapter. In order to simulate and analyze different situations in the distribution network, components and lines of the network have to be modeled mathematically. In this thesis, cables' modeling and power flow in the network play a major role. Additionally, symmetrical components are needed to represent asymmetrical fault situations in the network. The first section is about the general modeling of the transmission lines, in which three different models are introduced. The second section is the derivation of the power flow equations and representing two phenomenon related to it, surge impedance loading and Ferranti-effect. The last section introduces symmetrical components, which are used later in the earth fault chapter.

2.1 Models of transmission lines

One of the most important things in the analysis of the power lines is the relation between current and voltage. Their mutual behavior depends on numerous matters and there has to be a model in order to handle them mathematically. There are four parameters, which are used to describe the characteristics of power lines: resistance, inductance, capacitance and conductance. Resistance represents the ohmic losses of the line. Inductance describes magnetic interactions between different circuits formed in the power line. Capacitance of the power line has to be considered due to earth proximity that generates an electrical field between them. Conductance represents the leakage current of the isolation, which can be noticed as active power losses. However, in spite of having a constant value, conductance depends highly on the weather conditions, which makes its value difficult to estimate. Therefore, it is rarely used and often neglected. Impedance $Z = R + jX$ consists of resistance and inductance and admittance $Y = G + jC$ consists of conductance and capacitance. (Kothari & Nagrath 2010)

In principle, the presented parameters are distributed evenly throughout the power line. This means that power lines should be analyzed in infinite small elements. However, it would make calculations quite complicated and for that reason, simplified models are often used. Transmission lines can be modeled in different ways depending on their length and the type of the line. Of course, all models can

be used for all kinds of line types such as cables and overhead lines but the accuracy of the model will suffer. Consequently, the characteristics of the line type should be considered when choosing the correct model. (Grainger & Stevenson 1994)

Impedances and admittances are usually presented in matrix form with transmission constants A, B, C and D. These constants allow to represent the network as a "black box", which is presented in figure 2.1. V_S and I_S represent voltage and current in the sending-end and V_R and I_R in the receiving-end respectively. The constants can be calculated for short- and medium length lines easily by multiplying the parameters with the length of the lines. There is a connection between constants, $AD - BC = 1$. (Kothari & Nagrath 2010)

$$\begin{bmatrix} \underline{V}_S \\ \underline{I}_S \end{bmatrix} = \begin{bmatrix} \underline{A} & \underline{B} \\ \underline{C} & \underline{D} \end{bmatrix} \begin{bmatrix} \underline{V}_R \\ \underline{I}_R \end{bmatrix}$$

When the matrices are dismantled, the equations will be

$$\underline{V}_S = \underline{A}\underline{V}_R + \underline{B}\underline{I}_R \tag{2.1}$$

$$\underline{I}_S = \underline{C}\underline{V}_R + \underline{D}\underline{I}_R. \tag{2.2}$$

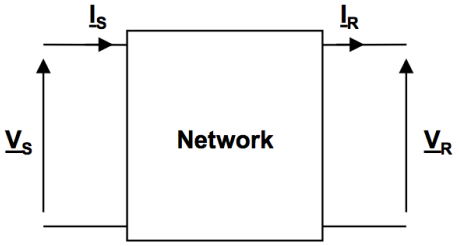

Figure 2.1. *Power line representation with transmission constants*

Short lines can be modeled with single impedance and the admittances can be neglected. In this case, the black box is replaced with single impedance, which consists of the resistive and inductive part. This model is only valid for shorter than 100 km overhead lines. The equivalent circuit is presented in figure 2.2.

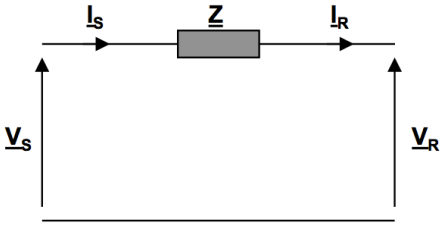

Figure 2.2. *Short line equivalent circuit*

Therefore, the transmission constants will get the following values

$$A = D = 1$$
$$B = Z$$
$$C = 0.$$

However, the short line presentation is not always accurate enough. A more accurate model is a pi- or t-section, which are presented in figure 2.3. These models are normally used for medium length transmission lines. Both models are convertible to each other but pi-section is used more because it is easier to use in calculations. Overhead lines lengths 100-250 km is usually modeled with a pi-section (Kothari & Nagrath 2010). In case of cables, pi-section should be used up to 15 km lengths (Manitoba HVDC Reasearch Centre 2010). Pi-section is used later on this thesis as a primary model.

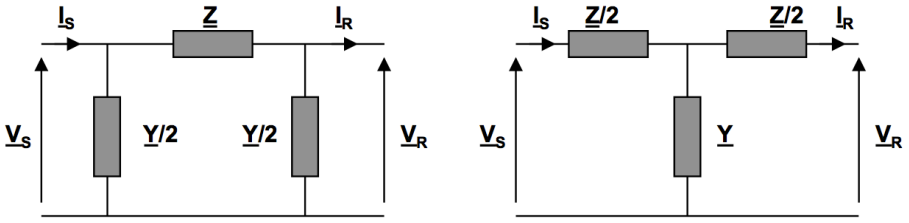

Figure 2.3. *Medium line equivalent circuit, pi- and t-section*

When using pi-section, the transmission constants will be

$$\underline{A} = \underline{D} = 1 + \frac{\underline{ZY}}{2}$$
$$\underline{B} = \underline{Z}$$
$$\underline{C} = Y(1 + \frac{\underline{ZY}}{4}). \tag{2.3}$$

With over 250 km overhead lines, long line equations have to be used since the wave nature of electricity (Kothari & Nagrath 2010). Long line equations assume that parameters are distributed uniformally throughout the power line and several pi-sections are connected in series. This makes equations quite complicated. Therefore, an easier way is to use correction factors, which consider correctly the wave behavior of the power lines. The correction factors are presented in equations (2.4) and (2.5) (Guldbrand 2009). The usage of transmission values is similar to pi-section. The long line equations are mainly needed only in the transmission network. However, the equations are required also in the distribution network when long cables have to modeled accurately.

$$Z_\pi = Z\frac{\sinh(G)}{G} \tag{2.4}$$

$$Y_\pi = \frac{Y}{2}\frac{\tanh(\frac{G}{2})}{\frac{G}{2}} \tag{2.5}$$

As mentioned before, all power line models are not suitable for all types of conductors because there are some essential differences between overhead lines and cables. For overhead lines, the series impedance is a lot greater than the line capacitance and therefore, the short line model can often be used. However, the characteristics of cables are slightly different because of the high line capacitance and the short line model have seldom an adequate accuracy. The difference between cables and overhead lines can be understood with the formula (2.6), which can be used to calculate the capacitance of a cylinder. (Aro et al. 2011)

$$C = \frac{2\pi\epsilon_r\epsilon_0 l}{ln\frac{r_u}{r_s}} \tag{2.6}$$

ϵ_r is the relative static permittivity, ϵ_0 is the permittivity of the vacuum, r_u is the radius of the conductor, r_u is the total radius and l is the length of the cylinder. In case of overhead lines, the gap between earth and power line can be assumed to be the distance to another electrode. A good average is 9 m for normal overhead lines and the radius of the conductor shall be 0,02 m. The intermediate agent is air, so the ϵ_r would be 1. Therefore, the capacitance of this overhead line is

$$C_o = l \cdot \frac{2\pi\epsilon_0 \cdot 1}{ln\frac{9+0{,}02}{0{,}02}} = 1{,}027 \cdot l.$$

Next, the area of the conductor is kept at constant and the capacitance value is calculated for a cable. Generally, cables consist of different layers, which all have a different ϵ_r and in principle all of these layers should be taken into consideration. For the simplicity, only one layer is calculated. If the isolation is assumed to be totally PEX-plastic, ϵ_r would be 2,9. The radius of the conductor is still 0,02 m and the total radius including the sheath can be assumed to be 0,05 m. Therefore the capacitance of the cable would be

$$C_c = l \cdot \frac{2\pi\epsilon_0\epsilon_r}{ln\frac{0{,}05}{0{,}02}} = 19{,}88 \cdot l.$$

The capacitance value of the cable is almost 20 times greater with these approximations. If the calculation was made accurately, the nearby wires and other layers of the cable should be considered. Additionally, dimensions of the lines affect remarkably on the outcome. Usually, the capacitance is 50-100 times greater than in overhead lines (Elforsk 2006). However, the installation, soil and bonding affect on cables' behavior and the alternation of the characteristics is clearer than

with overhead lines. In addition, the loading capacity of the cables is determined by thermal limits unlike overhead lines, which can be overloaded momentarily and the limiting factor is often the voltage regulation. On the other hand, overhead lines have a greater load capacity when comparing conductors with a same area. (Elovaara & Haarla 2011)

2.2 Power flow equations

Power flow equations are essential when analyzing transmission lines. The simplified version of the flow equations, which is based on the short line model, is usually adequate especially with overhead lines. However, it is not accurate enough for cables because the capacitance of the cables is considerable compared with overhead lines. Therefore, the equations should be derived in a more general form by using the pi-section.

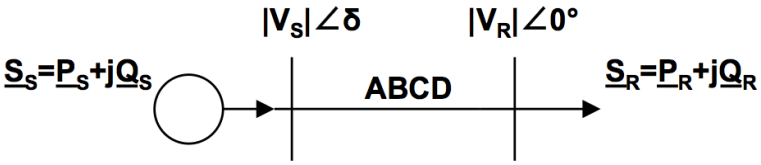

Figure 2.4. *Example network (Bastman 2011)*

A presented situation in figure 2.4 is considered. Complex power S_S goes through the transmission line and S_R is the received power at the end of the line. The angle of the receiving-end voltage is assumed to be 0° and the sending-end voltage leads it by δ. According to the figure, complex powers for sending- and receiving-end are

$$S_S = P_S + jQ_S = \underline{V}_S \underline{I}_S{}^*$$
$$S_R = P_R + jQ_R = \underline{V}_R \underline{I}_R{}^*.$$

The transmission line is modeled with pi-section constants A,B,C,D, which were presented in equation (2.3). As these constants are placed in matrix (2.2), the following equations can be written for sending- and receiving-end currents

$$I_R = \frac{1}{|B|}\underline{V}_S - \left|\frac{A}{B}\right|\underline{V}_R$$
$$I_S = \frac{\underline{D}}{\underline{B}}\underline{V}_S - \frac{1}{\underline{B}}\underline{V}_R.$$

Next the transmission constants are marked with $\underline{A} = |A|\angle(\alpha)$, $\underline{B} = |B|\angle(\beta)$ and $\underline{D} = |D|\angle(\alpha)$. The angles represent the angle displacement of the constants'

impedances. When placing the constants in above current equations and then to the apparent power equation S_R, complex powers will be

$$S_R = \frac{|V_S||V_R|}{|B|}\angle(\beta - \delta) - \frac{|A|}{|B|}|V_R|^2\angle(\beta - \alpha)$$
$$S_S = \frac{|V_S||V_R|}{|B|}\angle(\beta - \alpha) - \frac{|A|}{|B|}|V_R|^2\angle(\beta + \delta).$$

After separating the real and imaginary parts, we will get equations for active and reactive powers for sending- and receiving end

$$P_R = \frac{|V_S||V_R|}{|B|}\cos(\beta - \delta) - \frac{|A|}{|B|}|V_R|^2\cos(\beta - \alpha) \tag{2.7}$$
$$Q_R = \frac{|V_S||V_R|}{|B|}\sin(\beta - \delta) - \frac{|A|}{|B|}|V_R|^2\sin(\beta - \alpha) \tag{2.8}$$
$$P_S = \frac{|D|}{|B|}|V_S|^2\cos(\beta - \alpha) - \frac{|V_S||V_R|^2}{|B|}\cos(\beta + \delta) \tag{2.9}$$
$$Q_S = \frac{|D|}{|B|}|V_S|^2\sin(\beta - \alpha) - \frac{|V_S||V_R|^2}{|B|}\sin(\beta + \delta). \tag{2.10}$$

These are the general forms of the power flow equations. As can be seen, all power flows can be calculated when voltages and line parameters and their angles are known. However, equations are not always necessarily used in this general form and simplifications can be made to shorten the equations if the situation enables it. For example in case of overhead lines, the influence of the shunt capacitances can usually be neglected and the equations become simpler.

2.2.1 Surge impedance loading

As seen in section 2.1, power lines have both capacitive and inductive characteristics. They are opposite phenomenon in case of the reactive power because capacitors generate reactive power and inductors consume it. It is important to notice that the shunt capacitors generate reactive power proportional to the phase voltage. The total reactive power generated by three phases can be calculated with

$$Q_C = 3\frac{U_{ph}^2}{X_C}, \tag{2.11}$$

in which the U_{ph} represents the phase voltage and X_C represents the impedance of the shunt capacitors. However, the series inductors of three phases consume reactive

power proportional to phase current according to

$$Q_L = 3I^2 X_L, \tag{2.12}$$

in which I represents the phase current and X_L represents the impedance of the series inductor. Since the phenomenon are opposite, there has to be a balanced loading condition when the line consumes the same amount of the reactive power it generates. If the above equations are set to equal,

$$Q_C = Q_L \Longleftrightarrow 3I^2 X_L = 3\frac{U_{ph}^2}{X_C} \Longleftrightarrow \frac{U_{ph}^2}{I^2} = X_L \cdot X_C = \frac{2\pi f L}{2\pi f C} = \frac{L}{C}.$$

If both sides of the last equation are squared, the *characteristic impedance* will be

$$Z_c = \sqrt{\frac{U_{ph}^2}{I^2}} = \sqrt{\frac{L}{C}}. \tag{2.13}$$

With this impedance, the power line operates on its natural loading and the reactive power balance is zero at both ends. If the resistance of the power line is assumed to be zero, the voltage profile of the line would be flat. In other words, there is no angular displacement in either voltage or current in any part of the power line. This leads to the definition of *surge impedance loading* (SIL), which is presented in equation (2.14). SIL is not proportional to the length of the power line; it only depends on the characteristic values of the line and the voltage. SIL is approximately 10 times larger for cables compared with overhead lines in the distribution network because of the higher values of capacitances (Elovaara & Haarla 2011). (Bastman 2011)

$$SIL = 3\frac{(U_{ph}/\sqrt{3})^2}{Z_c} = \frac{U^2}{Z_c} \tag{2.14}$$

However, there are some limitations in the above equation. Firstly, the equation 2.14 is correct only with lossless lines whose resistance is zero. The assumption of the lossless line can usually be made in the transmission network, in which the resistance is really small compared to inductance values. In the distribution network, resistance can not be neglected because of the smaller conductor areas and therefore the larger resistance values. Secondly, the theoretical SIL definition assumes that the loading is purely resistive at the end of the power line and only active power is transferred. However, the loading consists rarely of mere resistance and usually there is also some inductance. In this case, the surge impedance loading point is not the same as in equation (2.14) and it depends on the power factor of the loading. If the power factor of the loading is below one, the balance of the reactive power is achieved with a smaller active power value in the sending point. So the more the

loading consumes reactive power, the less active power can be transferred in order to maintain the voltage level in the receiving end. Still, it has to be kept in mind that the theoretical SIL definition considers only the power line so the influence of the loading is usually observed separately.

The above limitations of the surge impedance loading can be understood with the power flow theory and pi-sections. The pi-section presented in section 2.1 is assumed to represent a power line. The phasor diagram in figure 2.5 describes a situation when the power line works on its natural loading and the loading is purely resistive and resistance is not neglected. The capacitive current $I_{Y/2}$ and the inductive current I_{ZX} compensate each other and as a result, there is no angular displacement between the voltage and the current in neither receiving- nor sending-end. The series resistance causes a voltage drop between sending and receiving end as expected.

The phasor diagram in figure 2.6 describes a situation when the power line works on its natural loading and the loading is slightly inductive. Because of the inductance of the loading, there is an angle between the current and the voltage in the receiving end. In this situation, the transferred active power has to be smaller in order to maintain the voltage level in the receiving end and in order to keep the reactive power balance in zero in the sending end. When there is no reactive power coming from the sending-end, the demanded reactive power has to come from the shunt capacitances. Therefore, the $I_{Y/2}$ capacitive current phasors are longer than the I_{ZX} inductive current phasor. As a result, there is no angular displacement between the voltage and the current in the sending-end. It should be noticed that both of the phasors diagrams are overwhelmed in order to makes the principle clear. The ratios between the phasors would be different in a real situation.

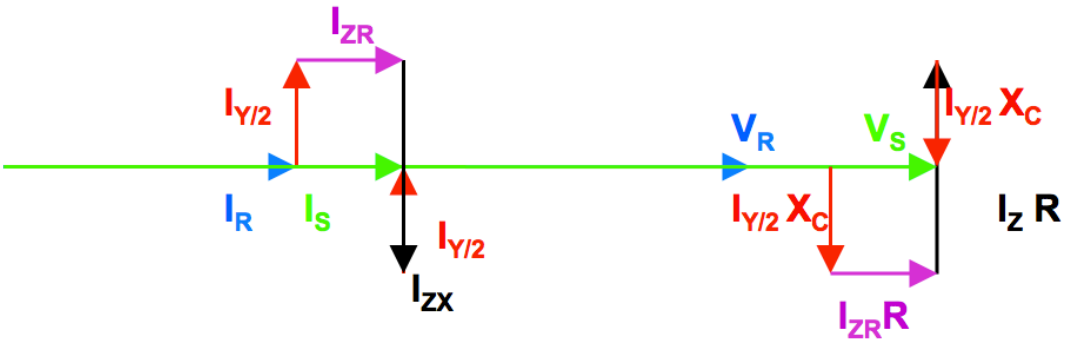

Figure 2.5. *Phasor diagram of natural loading situation with a purely resistive loading*

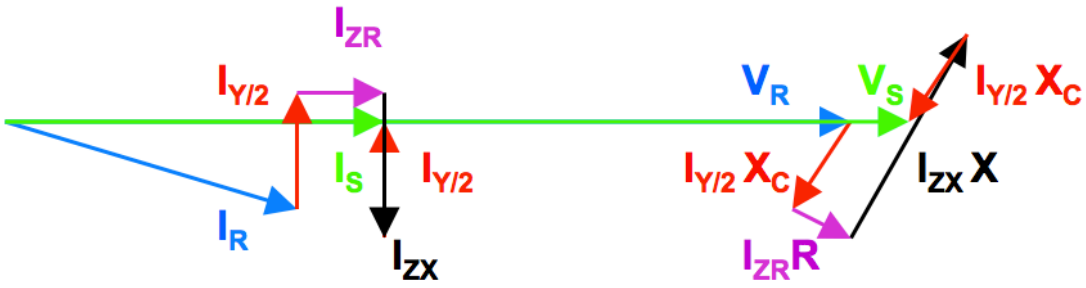

Figure 2.6. *Phasor diagram of natural loading situation with a slightly inductive loading*

2.2.2 Ferranti-effect

Ferranti-effect is a phenomenon caused by the recharging current of the line capacitances. When the power line is considerably long or it has a remarkable line capacitance value, the voltage rises towards to the receiving end. The phenomenon can be explained in detail with long line equations but it is not relevant in the scope of this work. A simpler explanation is gained if the whole capacitive current is assumed to go to the capacitance in the receiving end in no-load situation. The phasor diagram in figure 2.7 describes the situation. As the receiving end current is zero, the current going to the line capacitance is purely capacitive and causes a negative voltage drop across the series inductance. As a result, the voltage in the receiving end is greater compared to the sending end. (Kothari & Nagrath 2010, Kannus 2012)

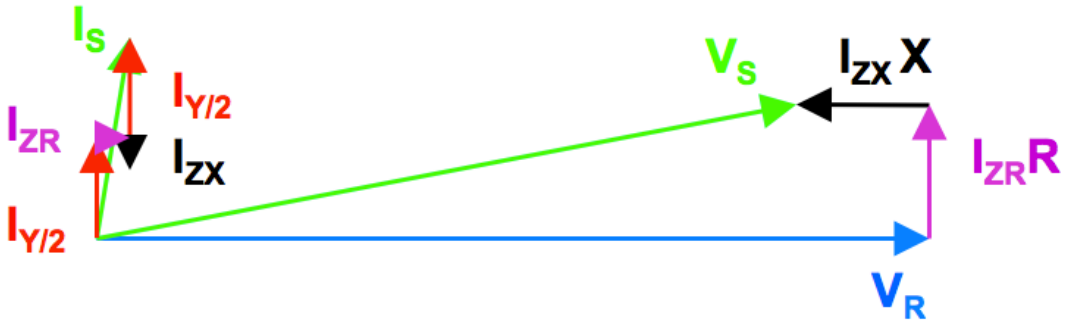

Figure 2.7. *Phasor diagram for a no-load situation in the power line*

The strength of Ferranti-effect depends on the values of line capacitances. Besides the line type, line capacitance is also proportional to the length of the power line so the phenomenon is stronger with longer lines. As mentioned earlier, cables have considerable higher values of capacitance over the inductance part of the series impedance. Therefore, Ferranti-effect is considerable stronger with cables.

2.3 Symmetrical components

Normally the three-phased network is assumed to have a symmetrical loading, which means that voltages and currents of all phases have the same magnitude and a 120° phase displacement to each other. The voltage phasor diagram of a symmetric loading is presented in figure 2.8. All phasors are rotating to counter-clockwise according to the sinusoidal wave. The symmetrical loading makes it possible to analyze all three phases of the network with a single phase equivalent circuit. This makes the calculations a lot simpler and saves time. Single phase calculations are often adequate for normal condition analysis. (Bastman 2011)

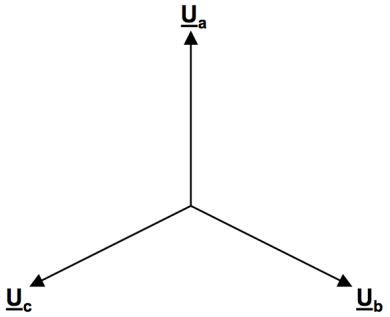

Figure 2.8. *Voltage phasors in a symmetrical loading situation*

However, the network is not always symmetrical. The state of the network can change to asymmetrical during an asymmetrical fault such as an earth fault and a two-phased short-circuit. After this, the calculations can not be made with a single phase equivalent circuit any more because the assumption about the identical equivalent circuit in all phases is not valid. The options are either to calculate everything separately in three phases or to use symmetrical components. Symmetrical components are a good option when there is only one fault in the network. If several faults occur at the same time, calculations become complicated.

The idea of symmetrical components is to replace asymmetrical voltage or current phasors with three independent symmetrical systems per phase. This is done with three different sequence systems; positive, negative and zero sequence system. As a result, it is possible to analyze the network effectively and quite easily in a single circuit. Without a fault in the network, only the positive sequence system exists and the circuits of the other sequence system are open. The negative sequence system is equivalent to the positive system but the order and angles of the phases are reversed. In the zero sequence system, all phases have the same angle and magnitude.

All sequence systems can be presented as a Thevenin's equivalent circuit and they are presented in figure 2.9. The positive system includes an imagined voltage source and a Thevenin's impedance. The negative system has negative sequence Thevenin's impedance and no voltage source. The zero sequence system includes

zero sequence Thevenin's impedance but it might also have fault resistance if it exists. The sequences are independent on one another and the value of each sequence's impedance is defined by the components in the network. (Elovaara & Haarla 2011)

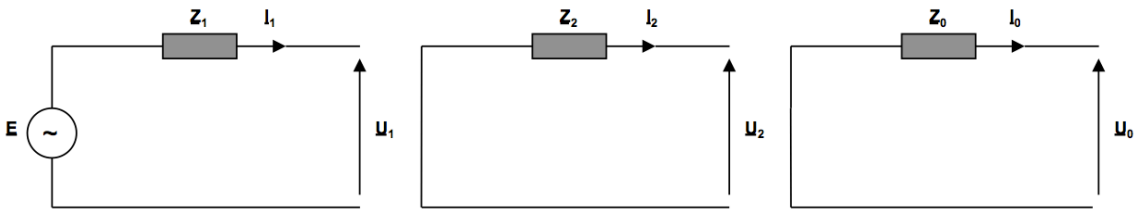

Figure 2.9. *Positive-, negative- and zero sequence system*

An example of asymmetric voltages is given in figure 2.10 and these phasors are combined in figure 2.11. Subindex 1 desbribes the positive sequence, 2 is the negative sequence and 0 is the zero sequence network. U_a, U_b and U_c represent the voltages in phases A, B and C. (Bastman 2011)

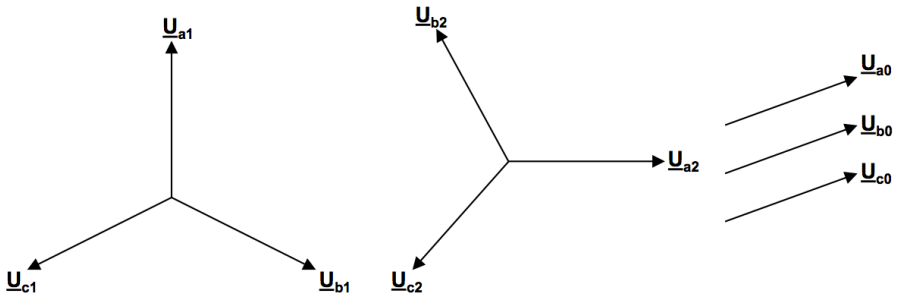

Figure 2.10. *Positive-, negative- and zero sequence system during a fault (Bastman 2011)*

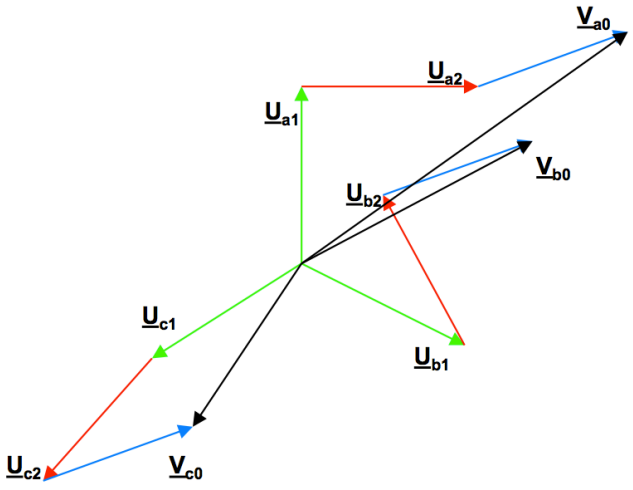

Figure 2.11. *Combined phasors from figure 2.10 (Bastman 2011)*

When using symmetrical components in mathematical analysis, they are usually presented in the matrix form. The equations can be simply derived from the basic definitions of the sequence networks. As mentioned, phase voltages have a 120° phase displacement to each other and it can be described with the operator $\alpha = e^{j120} = 1\angle 120°$. The phase order in the positive sequence system is assumed to be abc and in the negative sequence system acb. Therefore, the phase voltages of each sequence system can be written with the α operator when choosing phase a as a reference. (Kothari & Nagrath 2010)

$$\begin{array}{lll} \underline{U}_{a1} & \underline{U}_{b1} = \underline{\alpha}^2 \underline{U}_{a1} & \underline{U}_{c1} = \underline{\alpha} \underline{U}_{a1} \\ \underline{U}_{a2} & \underline{U}_{b2} = \underline{\alpha} \underline{U}_{a2} & \underline{U}_{c2} = \underline{\alpha}^2 \underline{U}_{a2} \\ \underline{U}_{a0} & \underline{U}_{b0} = \underline{U}_{a0} & \underline{U}_{c0} = \underline{U}_{a0} \end{array}$$

Now the phase voltages of the asymmetric situation can be written as a sum of the sequence networks.

$$\begin{aligned} \underline{U}_a &= \underline{U}_{a1} + \underline{U}_{a2} + \underline{U}_{a0} = \underline{U}_{a1} + \underline{U}_{a2} + \underline{U}_{a0} \\ \underline{U}_b &= \underline{U}_{b1} + \underline{U}_{b2} + \underline{U}_{b0} = \underline{\alpha}^2 \underline{U}_{a1} + \underline{\alpha} \underline{U}_{a2} + \underline{U}_{a0} \\ \underline{U}_c &= \underline{U}_{c1} + \underline{U}_{c2} + \underline{U}_{c0} = \underline{\alpha} \underline{U}_{a1} + \underline{\alpha}^2 \underline{U}_{a2} + \underline{U}_{a0} \end{aligned}$$

The above equations can be written in the matrix form:

$$\begin{bmatrix} \underline{U}_a \\ \underline{U}_b \\ \underline{U}_c \end{bmatrix} = \begin{bmatrix} 1 & 1 & 1 \\ \underline{\alpha}^2 & \underline{\alpha} & 1 \\ \underline{\alpha} & \underline{\alpha}^2 & 1 \end{bmatrix} \begin{bmatrix} \underline{U}_{a1} \\ \underline{U}_{a2} \\ \underline{U}_{a0} \end{bmatrix}$$

The phase currents of each network are respectively:

$$\begin{bmatrix} \underline{I}_{a1} \\ \underline{I}_{a2} \\ \underline{I}_{a0} \end{bmatrix} = \frac{1}{3} \begin{bmatrix} 1 & \underline{\alpha} & \underline{\alpha}^2 \\ 1 & \underline{\alpha}^2 & \underline{\alpha} \\ 1 & 1 & 1 \end{bmatrix} \begin{bmatrix} \underline{I}_a \\ \underline{I}_b \\ \underline{I}_c \end{bmatrix}$$

These matrices allow to solve the voltages and currents of each sequence system from the original phase voltages or currents. Symmetrical components are generally used in the transmission network analysis. However, the matrix forms of the equations are usually not needed in the distribution network because the earthing system is different (Bastman 2011). This is discussed in detail in the next chapter.

3. EARTH FAULTS

An earth fault is a fault situation, in which one or two phases are connected to the ground. During an earth fault, voltages change to asymmetrical according to figure 3.1. U_{L1}, U_{L2} and U_{L3} are phase voltages in phases 1, 2 and 3 and $U_{L1}{}'$ and $U_{L2}{}'$ are line voltages in phases 1 and 2 during the fault. The fault is assumed to happen in phase 3. The neutral point of the network can change along the half circle depending on the voltage drop due to fault resistance R_f and fault current I_f. The neutral point voltage is marked with U_0. If the fault resistance is zero, the fault is called solid and the voltage of the neutral point has the magnitude of the phase voltage. Consequently, the magnitude of the voltage in the faulted phase is zero and the voltage in other two healthy phases will rise to the level of line voltage. If the fault resistance differs from zero, the voltage of the faulted phase is above zero and the neutral point voltage is below the phase voltage depending on the place of the neutral point. Fault resistance varies normally between 0 Ω and 100 kΩ but it can be even more. There are no requirements for the sensitivity of earth fault detection in Finland. However, the Finnish Electricity Association recommends, the detection of 500 Ω faults. In Elenia, there is a capability to detect up to 5 kΩ earth faults (Pekkala 2010). Good examples for causes of earth faults are a tree leaning on the line or a bird on the cover of the transformer. (Lakervi & Partanen 2008)

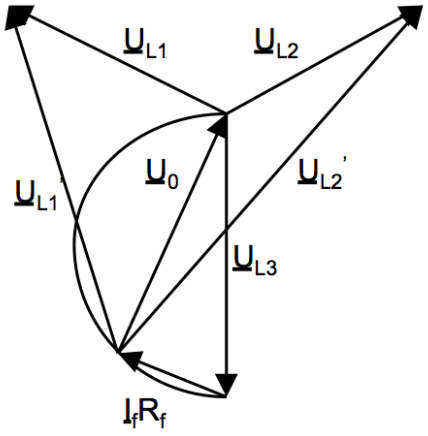

Figure 3.1. *Voltage phasors during earth fault (Lakervi & Partanen 2008)*

Earth fault current is generated by line capacitances because the electrical circuit formed during the earth fault closes through them. The magnitude of the earth

fault current is not dependent on the fault location and it is impossible to locate an earth fault solely based on the fault current. There are no accurate mathematical methods for location because the whole galvanic network behind the main transformer generates a fault current and it flows towards the fault point. Therefore, the earth fault current has the same magnitude, which is mainly proportional to the length and type of feeders from the substation. The capacitance of overhead lines is mainly the same for all types of conductors (6 nF/km/phase) and they generate earth fault current 0,067 A/km per phase. Cables generate a lot more earth fault current due to high values of line capacitance. Typical earth fault currents generated by cables vary between 2,7 - 4 A/km. Values depend on the geometry and the structure of the cables and it is always mentioned in the specifications of cables. (Lakervi & Partanen 2008)

3.1 Single phase earth fault

A single phase earth fault is the most common earth fault type and at the same, it is the most common fault in the medium voltage network. The behaviour of the network during an earth fault depends highly on the earthing system. Two different systems are used in Finland and therefore the theory of a single phase earth fault is presented in two subsections.

3.1.1 Isolated neutral system

In isolated neutral systems, there is not straight connection between ground and the neutral point of the transformer. Besides shunt capacitances, the connection to ground exists only via high impedance equipment such as voltage transformers or surge arresters. Since the impedance is quite high, earth fault currents are relatively low in isolated systems. In principle, the network could temporarily continue operating during an earth fault because there would not be any technical limitations for it. However, this is not possible with the modern distribution network due to its large size and it would cause problems for human safety. In Finland, the isolated system is the most used system in the medium voltage network because of poor earthing conditions. Poor earthing conditions increase the touch voltages on the fault location and therefore endanger human safety during an earth fault. Isolated neutral system is also the cheapest and easiest option for an earthing system. (Lakervi & Partanen 2008)

An earth fault in the isolated neutral system is presented in figure 3.2. One can see that the earth fault current flows from shunt capacitances C to the transformer and goes around the neutral point towards the fault point. If there were other feeders fed by the transformer, they would generate earth fault current towards the

fault location as well. The earth fault circuit closes in ground through a possible fault resistance R_f. As was expressed in figure 3.1, U_0 rises to the magnitude, which depends on the fault resistance. The larger the fault resistance is, the smaller the fault current and neutral point voltage are. Voltage source E has been drawn to the circuit only for mathematical reasons.

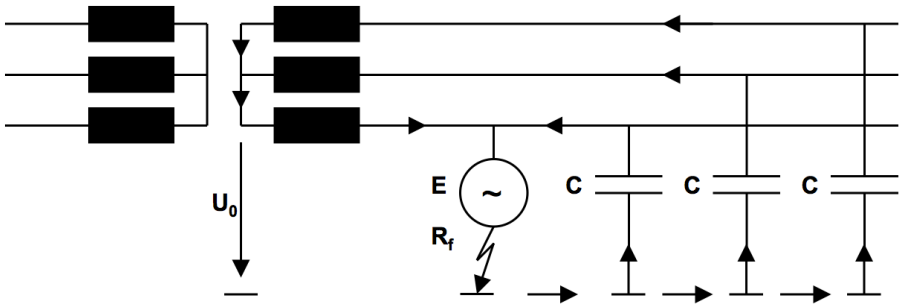

Figure 3.2. *Earth fault in isolated neutral system*

The same earth fault is presented with equivalent circuits of symmetrical components in figure 3.3. The positive-, negative- and zero sequences are connected in series with each other and in parallel with the fault resistance. The networks are modelled with a pi-section, and the series impedances are neglected because the line is assumed to be short. The neutral point displacement voltage is also marked to the zero sequence network. The equivalent circuit simplifies to a circuit in figure 3.4. (Guldbrand 2009)

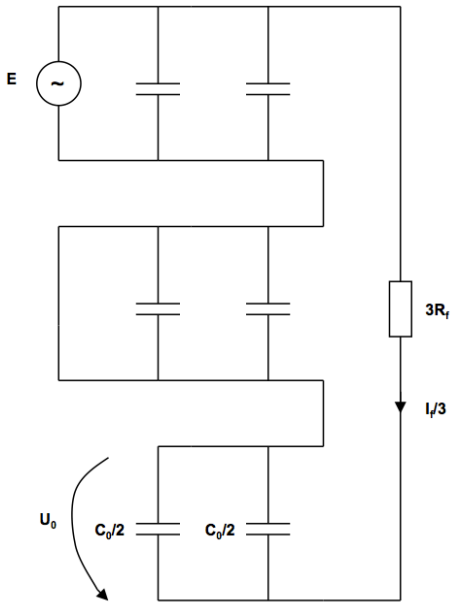

Figure 3.3. *Symmetrical networks for earth fault current in isolated neutral system*

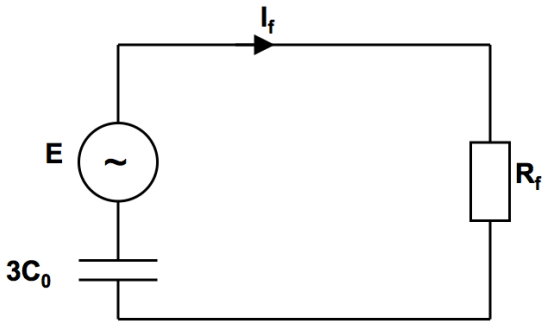

Figure 3.4. *Equivalent circuit for earth fault current in isolated neutral system*

Now it is easy to solve the fault current from the simplified circuit with equation (3.1). If the current is disassembled to real and imaginary parts, the equation will get the form (3.2). The neutral point displacement voltage U_0 can be calculated with the equation (3.3). (Guldbrand 2009)

$$\underline{I}_f = \frac{j3\omega C_0}{1 + R_f j3\omega C_0} \cdot \underline{E} \tag{3.1}$$

$$\underline{I}_f = \underline{I}_{Rf} + \underline{I}_C = \frac{R_f(3\omega C_0)^2}{1 + (R_f 3\omega C_0)^2} \cdot E + j\frac{3\omega C_0}{1 + (R_f 3\omega C_0)^2} \cdot E \tag{3.2}$$

$$\underline{U}_0 = \frac{1}{1 + j\omega C_0 R_f} \cdot \underline{E} \tag{3.3}$$

If the fault is solid ($R_f = 0\ \Omega$) and the equations simplify to (3.4) and (3.5). It can be seen that in a solid earth fault, the fault current is purely capacitive and the zero sequence voltage is the same as the phase voltage. A solid fault is more a theoretical case because in practise some fault resistance always exists.

$$\underline{I}_f = \underline{I}_{Rf} + \underline{I}_C = j3\omega C_0 \cdot E \tag{3.4}$$

$$\underline{U}_0 = \underline{E} \tag{3.5}$$

One problem in the isolated system is fairly steep recovery voltage, which means the voltage in the fault location after the fault has been cut off. Although the fault currents are relatively low, the rising speed of the recovery voltage is high. Therefore, it is not likely for an arc to extinguish itself, which increases the probability of the re-ignition of the voltage. This is because there is no inductance, which would decrease the rising speed of the wave. Additionally, the phase voltages of the healthy phases will rise to the magnitude of the main voltage. In the worst case, this might cause secondary failures because of the over voltages. (Nikander 2002)

3.1.2 Compensated neutral system

Compensated neutral system is a special version of the isolated neutral system. It has a coil at the neutral point of the network, which works as a compensator for earth fault current. The idea is to produce an inductive current, which has opposite phase displacement compared with the capacitive current. As a result, the inductive current cancels the capacitive current and the total earth fault current will decrease. Another name for compensation coil is Petersén coil. In principle, Petersén coils can be placed on any place at the network, where a neutral point is available.

In Finland, the 110 kV high voltage network is totally compensated and at the moment a part of 20 kV network as well. However, isolated systems are constantly changed to compensated ones by placing compensation coils to the substations. The increasing cabling of the distribution network is an important factor, which increases the interest towards compensated systems since cables generate a lot more earth fault current compared to overhead lines. Using the compensation coil is yet only economic to use it in straight networks, not in ring networks. Communication would be needed to sending-end and receiving-end of the power line to achieve selective relay protection in the ring networks. (Bastman 2011)

An earth fault in a compensated system is presented in figure 3.5. The situation is otherwise the same as in the isolated system but now the fault current flows through the Petersén coil and the parallel resistance as well.

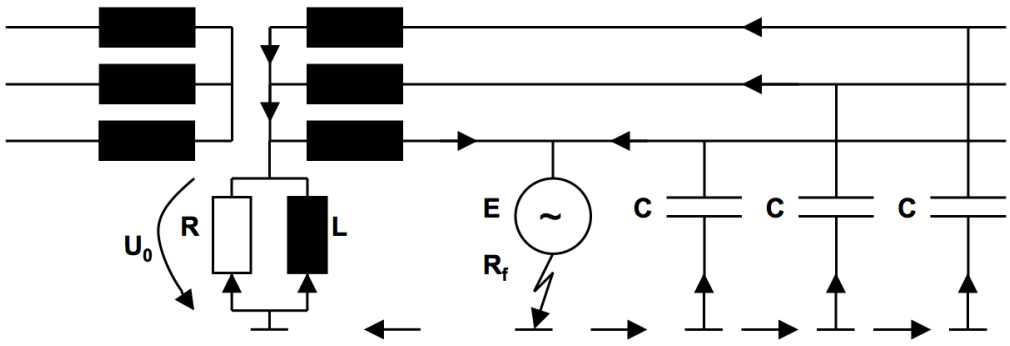

Figure 3.5. *Earth fault in compensated neutral system*

The symmetrical networks and the simplified equivalent circuit are presented in figure 3.6 and figure 3.7. The series impedances of the pi-section are neglected again because of the short length of the line. Now the coil's resistance and inductance have appeared to the zero sequence system. R in the zero sequence system includes both R_L, which is the natural resistance of the coil and R_0, which is the parallel resistance. The purpose of the parallel resistance is explained later.

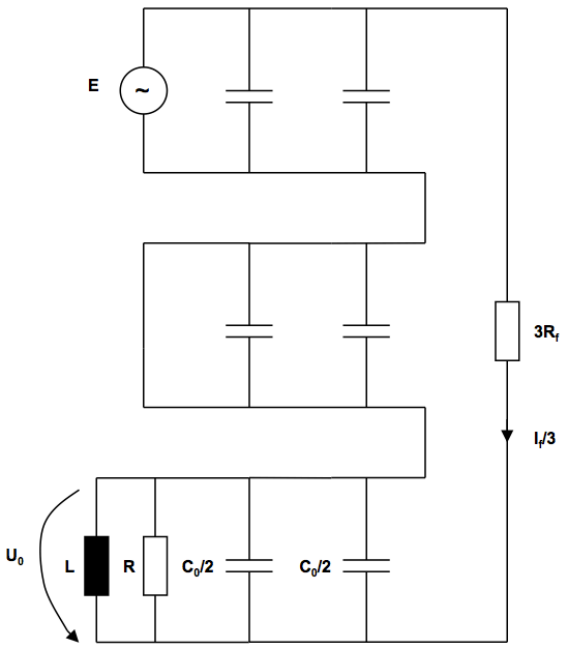

Figure 3.6. *Symmetrical networks for earth fault current in compensated neutral system*

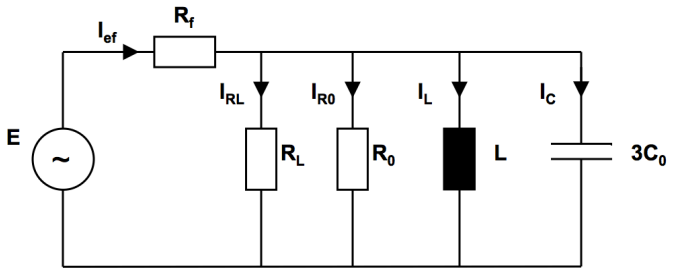

Figure 3.7. *Equivalent circuit for earth fault current in compensated neutral system*

Now the equations for the earth fault current and the zero sequence voltage can be written according to the equivalent circuit. The earth fault current is given in equation (3.6) and the equation of the zero sequence voltage in equation (3.7). (Guldbrand 2006)

$$I_{ef} = I_{RL} + I_{R0} + I_L + I_C = \frac{R_e(R_f R_e + 1) + R_f {X_e}^2 + jX_e}{(R_f R_e + 1)^2 + (R_f X_e)^2} \tag{3.6}$$

$$U_0 = \frac{I_{ef}}{\sqrt{(\frac{1}{R_e})^2 + \left(3\omega C_0 - \frac{1}{\omega L}\right)^2}} \tag{3.7}$$

In which

$$R_e = \frac{R_L + R_0}{R_L \cdot R_0}$$
$$X_e = 3\omega C_0 - \frac{1}{\omega L}.$$

The whole capacitive current should not, however, be compensated by matching the inductance perfectly (100 %) with the network's capacitance. This would endanger the network for resonance. Therefore, the compensation degree is kept under compensated, at 95 % in Finland. It would also possible to use the network as overcompensated as in Sweden but it would require different setting for relay protection. This is because the earth fault protection is based on angular displacement be tween the zero sequence voltage and the zero sequence current. If the network would be over compensated in Finland and an earth fault would be noticed, the whole substation would disconnect if the relays were set to under compensated settings. (Elovaara & Haarla 2011)

When using Petersén coils in the network, it is more likely for arcs to extinguish by themselves. This is because Petersén coils lower the rising speed of the recovery voltage when an earth fault occurs besides limiting the fault current. Therefore the probability of arc's self-extinction increases and the arc can extinguish at the first zero point of the sinusoidal wave. This reduces the number of reclosings and therefore improves the power quality. However, remarkable advantage is not gained until the compensation degree is over 75 %. (Nikander 2002)

3.2 Earth fault compensation

An earth fault is not particularly difficult situation from the distribution system operator's (DSO) point of view. It normally does not do any serious damage to the network components and in principle the network could be temporary used for a short time. A larger and limiting threat is the danger of people touching a live part such as the safety earthing during an earth fault. Sometimes it is even enough to stand near the fault location. When an earth fault occurs, the current starts the flow to the ground in the fault location. The flowing current causes a *touch voltage* in the fault location due to earthing resistance. A person will be exposed to the touch voltage if she/he touches the earthing electrode because there is a potential difference between the touching spot and person's leg. Consequently, a part of the fault current flows through a person. Touch voltage U_m can be calculated with equation (3.8). Naturally, higher earthing resistance R_m will cause higher touch

voltage and the danger is larger. (Elovaara & Haarla 2011)

$$U_m = I_f \cdot R_m \tag{3.8}$$

Figure 3.8 represents the potential distribution around the energized electrode. V represents the potential on both sides of the electrode and I_m is the current through the electrode. U_m is the earthing voltage and it depends on the conductivity of the soil and the amount of copper in the ground. U_k is the touch voltage, which is the experienced voltage by a person when touching the electrode. U_s is the step voltage, which is the potential difference between person's legs. As can be seen from the picture, both step and touch voltage depends on the horizontal distance from the electrode. (Elovaara & Haarla 2011)

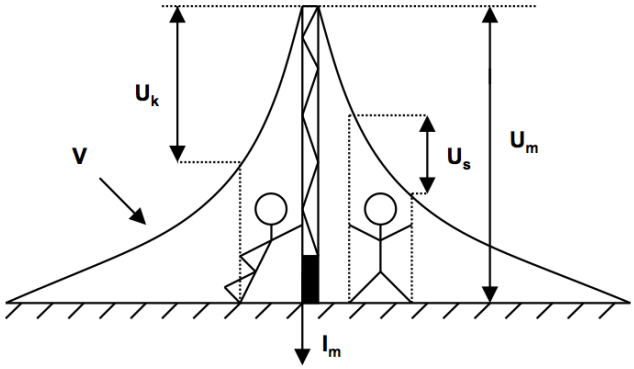

Figure 3.8. *Potential around the earth electrode (Lakervi & Partanen 2008)*

Touch voltages are dangerous for humans because touching the electrode will cause a current flowing through a person. Alternating current is especially dangerous for a human because already after a current of 5 mA, muscular contractions start to happen and loosening from the energized part might become impossible. If 30 mA flows through a person, the probability of ventricle fibrillation increases remarkably. Another important factor is the time the persons touches the live part. The longer the time the larger is the probability of getting the ventricle fibrillation. SFS 6001 standard defines the allowed clearing times and the corresponding touch voltage values, which are calculated with 10 % probability of ventricle fibrillation. Clearing times and allowed touch voltages are presented in figure 3.9. (Elovaara & Haarla 2011)

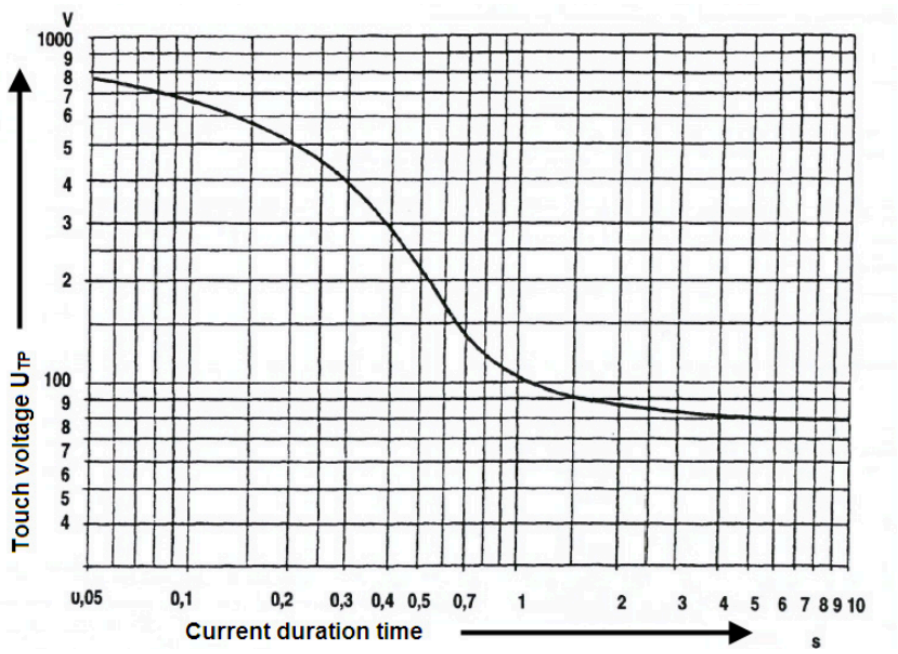

Figure 3.9. *Allowed touch voltage as a function of current duration time (SFS 2005)*

Besides touch voltage, the current through a person is inversely proportional to body's impedance, which does not behave linearly. Body's impedance depends on e.g. touching area, moisture, frequency and current path and of course, there is some natural variation between different people. For example, hand-to-hand impedance with a large touching area and dry hands is 3,3 kΩ at 50 V and 0,8 kΩ at 700 V. Standard limits are calculated with the average values. (Elovaara & Haarla 2011)

Lowering touch voltages is possible by lowering the earthing resistance, lowering earth fault current or shortening the clearing times (Mörsky 1993). Shortening the clearing times naturally gives less time for faults to disappear by themselves and therefore causes more reclosing operations. Lowering the earthing resistance is usually the most expensive way to lower the fault current because more copper has to be put to underground in several locations. The third option is to lower the earth fault currents with Petersén coils. This is often the optimal solution. As mentioned before, Petersén coils lowered the total earth fault current by compensating the capacitive current. Centralized and distributed compensation are presented in detail in the following two subsections.

3.2.1 Centralized compensation

Centralized compensation is located in the substation and it is supposed to compensate the earth fault current generated by all feeders or a part of them. The compensation coil is placed to secondary winding's neutral point of the main transformer if

it exists. However, in Finland 110/20 kV main transformers are Ynd-coupled so the upper voltage side is star-coupled and lower voltage side delta-coupled. This means that the main transformers do not have a natural neutral point so it has to be created if one wants to implement a compensation coil. The problem would be solved if Ynyn-coupled transformers were used instead but they can not be used in parallel with Yd-coupled ones, which are the most common type in Finland. One drawback of the neutral point equipped main transformers is the limited loading capacity of the neutral point. The neutral point does not necessarily withstand large earth fault currents from extensive cabled networks. A virtual neutral point can also be created by using an earthing transformer, which is Znyn-coupled. It creates a neutral point and the Petersén coil can be connected between the earthing transformer and the ground. The earthing transformer allows the easy disconnection if Petersén coil has been damaged for a reason. (Pekkala 2010)

Earth fault current can not transfer to 100 kV or to 0,4 kV network from the medium voltage side. This is because of distribution transformers are normally Dy-coupled and as stated before, the main transformers are Yd-coupled. This means that earth fault current has no route from the lower voltage side to the upper side or vice versa. As a result, earth fault in the high or low voltage network do not have to be considered in the medium voltage side.

Petersén coils have an extra parallel resistance as well. It is used to artificially increase the active component of the earth fault current during a fault so that the relay can see the fault and disconnect the faulted feeder selectively. Without the extra resistance, an earth fault would disconnect the whole substation after the neutral point displacement voltage relay trips. The extra resistance can be connected to network all the time or it can be connected only during faults for a certain time depending on the desired purpose. (Mörsky 1993)

The network has to have a compensation degree of 95 % even though the topology would change. This is usually implemented with the self adjustable coils. Adjustment of the coil is carried out by measuring the zero sequence voltage at the neutral point. The inductance of the coil can be changed by differing the air gap in core of the coil. When the capacitance of the network increases, also the inductance is increased with a certain time delay. The adjustment range of the inductance is pretty wide, usually 10-100 %. (Pekkala 2010)

3.2.2 Distributed compensation

Earlier, the distributed network consisted mainly of the overhead lines, which leaded to low earth fault currents and there was no need for other than centralized compensation in some cases. However, as the cabling has increased, there has been a new need for compensating the earth fault currents locally. One reason for this is the

lack of compensation capacity in the substations. A new centralized compensation coil is a large investment already as itself and as the existing compensation is usually placed in the station service feeder, a new coil would sometimes require a totally new feeder. Also, the old smaller coil may remain useless after the replacement. In addition to high earth fault currents, long cable feeders have a problem of causing a part of the earth fault current to become resistive. This is discussed more in the next section. These two reasons have brought fairly new distributed compensation coils to the market.

Distributed compensation coils are basically small Petersén coils, which are located in the secondary substations. However, Petersén coils require a neutral point from the network, which is seldom found from the distribution transformers in Finland since most of them are Dy-coupled. If distributed Petersén coils are desired to be used, an existing transformer has to be either replaced with a ZNzn- or Zn(d)yn-coupled one or a new earthing transformer has to be installed. The coil is placed between ground and the earthing transformer as in centralized compensation. It is also essential, that the earth fault current does not flow to the low voltage side. As a result, distributed Petersén coils are always put to the 20 kV side and they have to be separated from low voltage side with a stabilization delta coupling. (Pekkala 2010)

Distributed coils have usually a fixed compensation capacity and they can only be adjusted when the transformer is offline. A common capacity of earth fault current compensation is 5-15 A. The lack of adjustability is normally not a problem because distributed compensation coils are installed in compensate a certain part of the feeder. Therefore if a part of the feeder is disconnected from the network, the feeder will not become over compensated.

3.3 Challenges of extensive cabling in rural area networks

Traditionally, cabling has been focused on the urban areas due to practical reasons such as space saving and relatively short distances. Rural area has not been cabled diligently before because it has not been economically beneficial. However, the prices of cable installation have gone down and there is a pressure to build most of new lines underground due to recommendations of the weather-proof network. Therefore, much wider areas will be cabled, which will raise new kinds of challenges.

The large amount of overhead lines in rural areas has made it possible to analyze earth fault situations with simplified methods. Also, there are a few assumptions, which have been valid with a adequate accuracy. Firstly, the total length of the network has defined the total earth fault current without concerning the lengths of single feeders. Secondly, the series impedances of the power lines have always been neglected in earth fault calculations and the fault current is assumed to be almost purely capacitive and directly proportional to the line length. This means that the

whole earth fault current could have been compensated by using Petersén coils in principle. Thirdly, the zero sequence voltage has depended solely on the neutral point resistance and fault resistance. Fourthly, the location of the fault have not affected on network's behavior. (Guldbrand 2009)

These assumptions are not necessarily valid when analyzing long cable feeders and the extensive cabled network. They are discussed in detail in the following subsections.

3.3.1 Long cable feeders

In the urban network, there are usually several short feeders in one substation. It is justified to assume that one feeder can be modeled with a single pi-section. The sequence network systems in an urban network are presented in figure 3.10. Z_{T1} is the positive , Z_{T2} is the negative and Z_{T0} is the zero sequence network. Because of the short length, the series impedance can be considered as meaningless due to large line capacitance when analyzing an earth fault situation. When the series impedance is removed, the line capacitances are in parallel and they can be added together. Therefore, the total earth fault current can be calculated from this capacitance. The specifications of the cables define the capacitance value per kilometer so it is easy to calculate the total earth fault current. Therefore, the assumption that the length of the network defines the total earth fault current is valid.

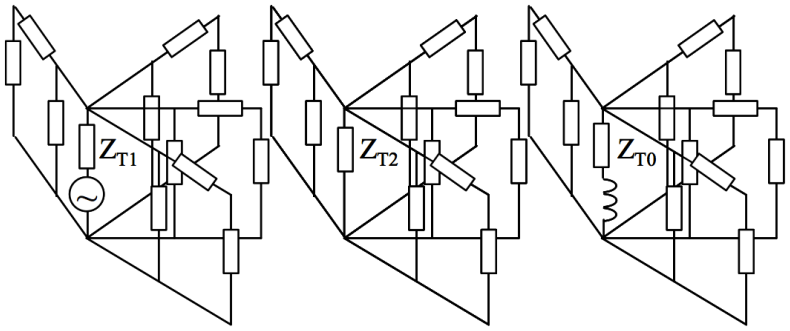

Figure 3.10. *Positive-, negative- and zero sequence systems in urban network (Guldbrand 2009)*

However, feeders are usually much longer in rural networks and the series impedance can not be neglected any more. The equivalent sequence circuits are presented in figure 3.11. Because of the length, a single feeder has to be modeled with several pi-section connected in series. This makes the situation more complicated because the series impedances are connected in series. When the series impedance is taken into consideration, the earth fault current is no longer solely capacitive. (Guldbrand 2009)

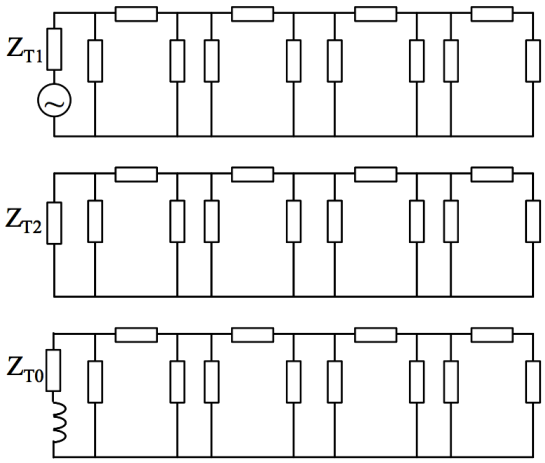

Figure 3.11. *Positive-, negative- and zero sequence systems in rural network (Guldbrand 2009)*

An example is given in figure 3.12. A 10 kV cable is considered, which is the 95 mm^2 XLPE cable. Impedance and its argument are described with a function of cable length with a short line model (pure capacitance) and with pi-sections. It is easy to see that more accurate modeling with pi-section changes the situation significantly with longer cable lengths. The absolute value of zero sequence impedance does not change remarkably when the length of the cable increases. Instead, the angle of the current changes. As a result, earth fault current has now a resistive part in addition to the capacitive part. The total earth fault current remains the same as before but only the capacitive part of the current can be compensated with Petersén coils. Consequently, the uncompensated resistive part raises touch voltages and it might cause danger to people. (Guldbrand 2009)

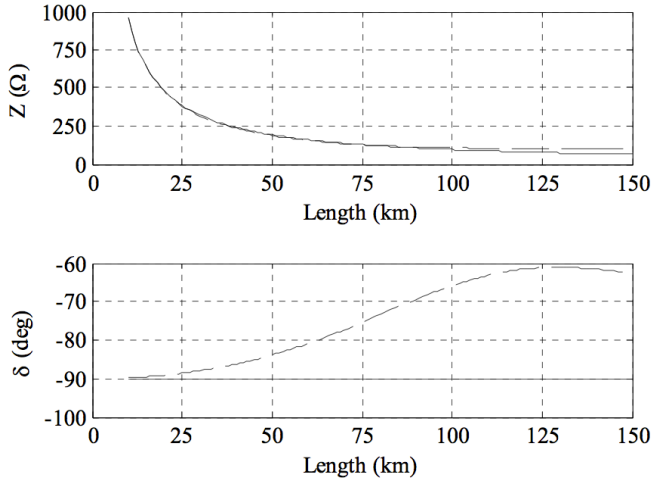

Figure 3.12. *Magnitude and argument of the equivalent zero sequence impedance of cables modelled by pi-sections (dashed) and capacitance only (solid) (Guldbrand 2009)*

3.3.2 Influence of fault location

According to conventional earth fault analysis, the neutral point displacement voltage is the same everywhere in the network and independent on the fault location. This is a consequence of the same assumption that series impedances can be neglected because of the short cable distances. According to this assumptions, there is no voltage drop in the zero sequence voltage. However, as explained in the previous section, long cable feeders have to be modeled with several pi-sections and series impedances can not be neglected. As a result, the voltage drop exists in the zero sequence system and it has to be considered.

The series impedance consists of the inductive and resistive part. The resistive part causes a voltage drop and the inductive part compensates a part of the capacitive fault current. Because of the resistive component of the earth fault current, the zero sequence voltage is not the same in all parts of the network. Now the fault location defines the magnitude of the zero sequence voltage in the substation. For example, if the fault is located at the end of the feeder, the voltage at the transformer's neutral point is less than at the fault point. In some cases, this might lead to failure to detect the fault and since the true zero sequence voltage of the fault location is not known. (Guldbrand 2009)

4. REACTIVE POWER CONTROL

Reactive power is the second component of the apparent power and a consequence of the angular displacement between voltage and current. Unlike active power, it cannot be used to do work or utilize by electric devices. Since the apparent power consists of both active and reactive power, reactive uses the same bandwidth with active power and therefore, it limits the transmission of active power. Additionally, reactive power affects directly on the voltage level of the network. The more reactive power the higher the voltage is. Because of these reasons, the transmission of reactive power should always be minimized in order to transfer active power efficiently. Generally, the volume of reactive power can simply be controlled by either adding capacitive or inductive components to the network. (Elovaara & Haarla 2011)

The increasing cabling of the distribution network increases the volume of reactive power in the network. Usually, cables operate under their natural loading and therefore generate more reactive power than they consume. This is due to the high line capacitance value of the cables. It raises many new challenges since traditionally the distribution network has considered to be a drain of reactive power. This chapter discusses the affects of reactive power excess due to extensive cabling and a method used to minimize the transmission of the reactive power. In the first section, the principles of the main grid connection are introduced including both active and reactive power regulations and requirements. The second section is about the affects of the cabling from the distribution system operator point of view. The third section concerns shunt reactors, which are used for the compensation of reactive power.

4.1 Main grid connection

The Finnish main grid is operated by Fingrid, which also owns the major power links to foreign countries. Fingrid is responsible for operation supervision, operation planning, maintenance, development of the main grid and electricity market development. The main grid exists at three different voltage levels: 400 kV, 220 kV and 110 kV and almost all of the power lines are overhead lines. The major part of consumed electricity in Finland is transferred through the main grid. The main grid has certain stability limits, which are possible to exceed if the active or reactive power is transferred too much or too less into the grid. In order to use the main grid effectively and economically, Fingrid has to supervise the usage of reactive and

active power and set limits for the clients. (Fingrid 2012)

4.1.1 Active power transmission

The consumption of electricity, in other words, the demanded active power affects directly on the frequency of the network and it is a global quantity for a single synchronous system (Elovaara & Haarla 2011). If the generation of active power is kept at constant and the demand is increasing, the frequency of the network starts to decrease. Vice versa, the frequency increases when the demand decreases. Frequency is usually corrected by increasing or decreasing the generation of active power or in the emergency situation, cutting the consumption. In normal conditions when the frequency deviation is less than 0,1 Hz, the automatic primary control takes care of the frequency control. Especially water power generators are used for this purpose due to their fast response time. If the deviation goes over 0,1 Hz, the manual secondary control takes over and the responsible operator of Fingrid connects more reserve generators to the main grid. Frequency is allowed to deviate in the range of 49,5..51,5 Hz in normal conditions, which is also the requirement limit for clients to cope with. In exceptional conditions, the frequency is possible to deviate in the range of 47,5...53 Hz. (Fingrid 2012)

Nowadays the transmission of active power consists of two different fees, a use of grid fee and a consumption fee. The connection fee is constant and paid monthly for every connection point regardless of the transferred energy. The consumption fee is based on the consumption of active power and it is calculated per MWh. The use of grid fee is taken into account every time active power is either taken from or fed to the main grid. The evolution of fees for the past years is listed at table 4.1.

Table 4.1. *Fees for the main grid service 2008-2012 (Fingrid 2012)*

Consumption fee	**2008**	**2009**	**2010**	**2011**	**2012**	
Winter period	2,16	2,28	2,40	2,52	3,48	€/MWh
Other times	1,08	1,14	1,20	1,26	1,74	€/MWh
Use of grid fee						
Output from grid	0,66	0,68	0,70	0,72	0,80	€/MWh
Input into grid	0,30	0,30	0,30	0,30	0,50	€/MWh
Connection point fee	1000	1000	1000	1000	1000	€/month

4.1.2 Reasons for reactive power limitations

Reactive power and voltage are both local quantities and they are directly connected to each another. In other words, voltage level is controlled by adjusting the amount of reactive power in the network. If a connection point is consuming a lot of reactive power, voltage drops and if it produces reactive power, voltage raises. Since reactive

power is a local quantity, it should be generated locally to minimize the unwanted effects. The amount of reactive power can be decreased by placing reactors and increased by placing capacitors in different spots of the network. Combinations of them exist as well, which control the voltage level by automatically adjusting the reactance of the device. These are called FACTS-devices. Another ways to adjust the voltage level are the on-load tap changer of the main transformer and over magnetized synchronous generators. (Elovaara & Haarla 2011)

Fingrid's policy of reactive power is somewhat different from active power. Fingrid encourages clients to limit their reactive power input/output by setting a reactive power window for each connection point. The ideal input/output would be zero. The main purpose of limitations is to ensure the stability of the main grid and maintaining the voltage balance. Clients are driven to stick within these limits so stability would not be threatened during the normal use. There are also other reasons, which are achieved with voltage balance such as better reliability, power quality and lower losses (Elovaara & Haarla 2011). The limits of allowed voltage deviation are presented in table 4.2. Within these limits, the stability is maintained. (Fingrid 2012)

Table 4.2. *Allowed voltage levels in the main grid (Fingrid 2012)*

Voltage level	Lower limit	Upper limit
400 kV	380 kV	420 kV
220 kV	215 kV	245 kV
110 kV	105 kV	123 kV

During a disturbance, voltage tends to drop and reactive power is needed to support the voltage. Because of this, there has to be a reserve capacity of reactive power in case of a disturbance so that the voltage of the main grid will not collapse. All generators larger than 10 MVA connected to the 400 kV grid are required to reserve all of their reactive power capacity for the disturbance reserve. Generators connected to voltage levels of 110 kV and 220 kV have to reserve half of their reactive power capacity for a disturbance. (Bastman 2011)

4.1.3 Reactive power control method

Fingrid makes a reactive power contract for every connection point, where the customer is connected to the main grid. If there are several connection points, which are electrically close to each other from Fingrid point of view, Fingrid forms a monitoring area. The reactive power windows of single customers in the same monitoring area are summed together and the whole area is observed with common reactive power limits. This allows clients to decide how they will share the consumption and production of reactive power. (Fingrid 2012)

Every monitoring area has a limit for the output and input of reactive power, in which it is free to transfer reactive power. If these limits are exceeded, the exceeded volume will be charged. The exceedings are measured in hours per month. Under 10 hours of exceedings per month are allowed for free if the reactive power limit has not exceeded double the limit. Still, every exceeding has to be explained and clarified for Fingrid. Additionally, reactive power fees are not charged in exceptional situations such as starting a generator, a fault in the lower voltage side, a significant starting or stopping a process or a major disturbance. All of these incidents have to be reported to Fingrid in forehand if it is possible. (Fingrid 2012)

The principle figure of reactive power window limits is presented in figure 4.1. Q_{s1} is the reactive power input limit and Q_s is the reactive power output limit. As can be seen, the limit of reactive power input to the main grid is independent on the active power consumed. On the other hand, the reactive power output depends on the consumed active power and it can be 16 % of the active power at maximum. An example exceeding is drawn with arrows and the price to pay is marked on the horizontal axle. Output and input limits can be calculated with formulas (4.1), (4.2) and (4.3). The formula, which gives a larger result, is chosen from two above Q_s formulas. (Fingrid 2012)

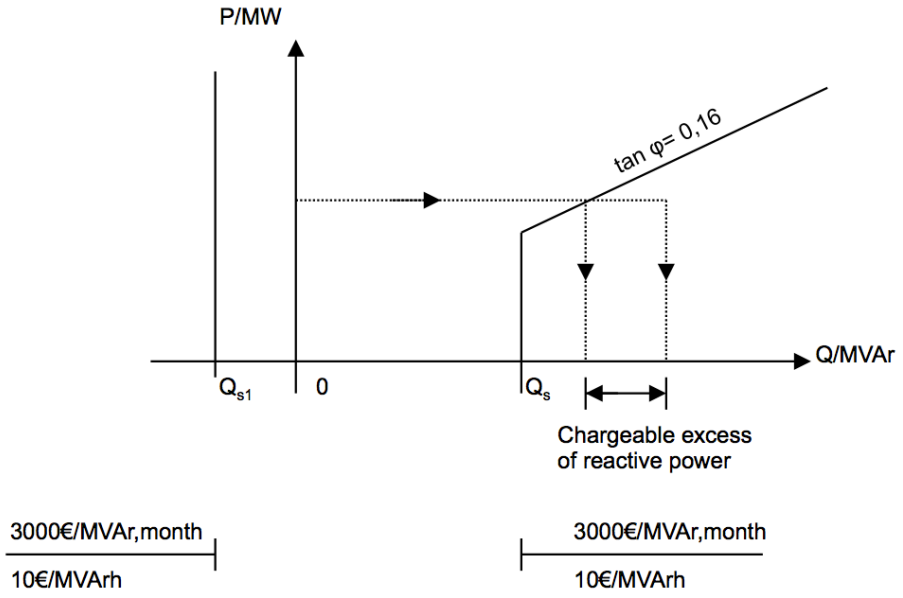

Figure 4.1. *Fingrid's pricing model for reactive power (Fingrid 2012)*

$$Q_s = W_{Output} \cdot \frac{0,16}{t_k} + \frac{0,025 \cdot W_{Gen}}{5000} \tag{4.1}$$

$$Q_s = W_{Output} \cdot \frac{0,16}{t_k} + 0,1 \cdot S_N \tag{4.2}$$

$$Q_{s1} = -0,25 \cdot Q_s \tag{4.3}$$

Where

t_k = peak usage time

- 7000 h for process industry
- 6000 h for other industry
- 5000 h for other consumption

W_{Output} = output active power (MWh)
W_{Gen} = net active power production

- If the largest generator is smaller than 10 MVA $\Rightarrow W_{Gen}$=0

S_N = apparent power of the largest generator

- $0,1 \cdot S_N \leq 30$ MVA
- If the largest generator is smaller than 10 MVA $\Rightarrow S_N$=0

The chargeable price of reactive power exceeding consists of the usage fee and energy fee. Reactive power measurements are carried out at every connection point and the average value of the hour is used in calculations. The usage fee is calculated from the largest exceeding of the month by using formulas (4.4), (4.5) and (4.6). The principle is to calculate the difference between the maximum exceeding and the window limit and multiply the result with 3000 €. The energy fee is calculated from every hour exceeding so that all exceeding hours have to be paid for. The energy fee can be calculated by multiplying the consumed reactive energy by 10 €/MVArh. (Fingrid 2012)

- If $P \leq Q_s/0,16$ and $Q > Q_s$, the usage fee is

$$(Q - Q_s) \cdot 3000\ €/MVAr \tag{4.4}$$

- If $P > Q_s/0,16$ and $Q/P > 0,16$, the usage fee is

$$(Q - 0,16 \cdot P) \cdot 3000\ €/MVAr \tag{4.5}$$

- If $|Q| > |Qs1|$

$$(|Q| - |Q_{s1}|) \cdot 3000\ €/MVAr \tag{4.6}$$

Where

$Q = Q_M + Q_h$
Q_M = one hour average of reactive power
Q_h = transformers' reactive power losses, concerned if the power measurements are done in lower voltage side
P = one hour average of active power

4.2 Influences of reactive power growth due to extensive cabling

Extensive cabling brings challenges to earth fault situations, which were explained in section 3.3. In addition to these, the reactive power generation of the cables has to be considered. As mentioned earlier, cables generate a remarkable amount of reactive power and their surge impedance loading limit is relatively high. This means that cables often operate under their natural loading limit and they cause a surplus of reactive power to the network. There are several different phenomena, which are consequences from the excess of reactive power.

These phenomena are fairly new in the medium voltage network and they have not been researched much yet. Elforsk carried out a study in 2006 about the influences of extensive cabling in Sweden. The focus point of the report was at the challenges related to earth faults but reactive power excess was also considered. The topic was also examined in Pekkala's M.Sc. thesis 2010, which was focused on earth fault management.

4.2.1 Reactive power transfer to the upper voltage network

The first possible problem is the reactive power balance at Fingrid connection points. As described in subsection 4.1.3, Fingrid has set limits for reactive power output and input. Traditionally there have not been problems with the input limits but the situation is about to change as the cabling of the medium voltage network is taken forward. When more capacitive load is added to the network, the reactive power balance moves towards capacitive at the connection point. Problems may occur especially during light loading situations with long cable feeders and a large amount of cable in a single substation.

Fingrid was interviewed in order to find out if the policy of reactive power control will be changed in the near future. According to Fingrid, the present control method and the window limits have just been renewed and they do not have plans of changing the policy. The present control method has worked well and therefore, the window limits are not planned to tighten in the future. Neither the zero tolerance of reactive power window, which has been used in Central Europe, will not be taken in use in

the future. Fingrid has also noticed that there is a gentle trend of an increasing reactive power input to the network. Reactive power limits have been a problem for some DSOs who work in the city areas and their guess is that the rest of the DSOs will probably follow after. (Fingrid 2012)

4.2.2 Power losses

As discussed in the previous subsection, the surplus of reactive power starts to flow towards the upper voltage network when the loading situation is light. In addition to problems with reactive power balance in the substation, the flow causes active power losses in power lines. Theoretically, reactive power is the second part of the complex power in addition to active power according to

$$S = \sqrt{P^2 + Q^2}.$$

The increase of the reactive power increases the total complex power as well regardless of the sign of reactive power. In case of power lines, if the voltage level of the network is assumed to be constant, the total current has to increase according to Ohm's law. The increasing current warms the cable up and a part of electrical energy turns into heat energy. As a result, the reactive power excess increase is seen as active power losses. These losses increase the demand for active power from the upper voltage level and of course, this increases the costs of losses. It is also considerable that the loading capacity of cables is determined by thermal limits and therefore reactive power reduces cables' transferring capacity.

In Elforsk report 2006, the reactive power was simulated in different networks. A 260 km long 24 kV idle cable network generated approximately 8 MVAr surplus of reactive power during a light loading condition and caused 0,16 MW losses. The simulations showed also that a 60 km idle straight cable had losses of 35 kW while the same value is 4 kW for a 30 km cable. This shows that the losses due to reactive power depend highly on the length of single feeders and it is not profitable to transfer it long distances. The reason for the significant rise of losses is the squared current in the power equation $P = 3RI^2$.

Another concern is the power losses in the main transformer. When power is flowing through the transformer, it generates active and reactive power losses due to series impedance $Z = R + jX$. Active power losses can be divided into two parts; no-load and load losses. No load losses are due to the whirling currents, which are caused by changing the magnetic field at the iron core. No load losses are only dependent on the voltage level. Load losses are heat losses, which are generated at the resistance of the coils. They depend on the loading according to the equation

(4.7). (Korpinen 2012)

$$P_{cu} = (\frac{S}{S_n})^2 \cdot P_{cun} \tag{4.7}$$

4.2.3 Voltage rise

Voltage rise is a consequence of Ferranti-effect, which was explained in subsection 2.2.2. During light loading conditions, voltage rises towards the end of the cable because of the capacitive charging current. Again, the reason is the line capacitance of the cable. The phenomenon exists also with overhead lines but the effect is not noticeable in the medium voltage network. Instead, it is apparent in the high voltage network, in which it can cause a breakdown at the end of long lines if reactors are not used as loads (Elovaara & Haarla 2011). Naturally, the voltage displacement would transfer to the low voltage side. It is also noticeable that the voltage rise cannot be seen or fixed from the substation with tap changers because they see voltage level as normal in the bus. This might lead to too high voltage levels on the customer side.

Elforsk simulations showed that the voltage rise is the highest when the first third from the feeding station is overhead line and the rest two thirds are cabled. A simulation was made for 12 kV line with the first third from the substation overhead line and the rest two thirds cabled. In this situation, the voltage rise can be 4 % at maximum, which is acceptable. In Pekkala's master thesis 2010, the voltage rise was also simulated with light loading. A single feeder was examined and cabled amount was increased with 5 km steps from the end of the 60 km length feeder. The result was the same as in Elforsk report; the voltage rise was at the highest when one thirds from the station were overhead line. However, the voltage rise was only minor. (Pekkala 2010, Elforsk 2006)

4.2.4 Reactive power from customers' aspect

Reactive power is often quite an invisible concept for normal household users. This is mainly because low voltage customers are not charged for reactive power consumption. However, this is not the case with customers with the medium voltage connection. They have a fee for electricity distribution, the basic fee per month, active power fee and reactive power fee (Elenia 2012).

The reactive power fee for medium voltage customers is often at least double the active power fee. So from the customers' point of view, reactive power output is not beneficial. As a result, it is often less expensive for customers to compensate their own reactive power when the continual costs of reactive power can be minimized. Capacitor banks are a common solution to increase the power factor and reduce the

intake of reactive power. Since the purchase of the compensation devices depends entirely on the customer and DSO does not work as a middleman, DSO does not have information about its customers' compensation devices.

A surplus of reactive power is more likely to exist in the future network due to extensive cabling. It may lead to situations, in which reactive power is compensated with reactors by the DSO on the network side and customers compensate their own reactive power usage with capacitor banks. It is self evident that it is pointless to compensate the reactive power to the opposite directions. One possibility might be to make a special contract with the customer. The customer would be allowed to use a certain volume of reactive power for free or customers compensation would be accessible to use from the control center of the DSO. This would be beneficial for both parties. Contracts of this kind could come into questions with really long cable feeders, which would have to be compensated any way.

4.3 Shunt reactors

In principle, there are two types of compensation devices for reactive power compensation, which change the compensation degree in different directions. They can be statically connected to the network but also adjustable combinations of them are available. Capacitors generate reactive power and they are used to rise the voltage level. Shunt capacitors are mainly used locally in the overhead line networks for load compensation. Series capacitors are used to compensate the power line electrically shorter to increase the transferring capacity if the lines are physically long. (Elovaara & Haarla 2011)

Reactors are electrically the opposite to capacitors and they are used for consuming reactive power. In the high voltage network, they are used especially during light loading conditions in order to limit the voltage rise at the end of the line. However, shunt reactors can be used for other purposes as well: the filter of harmonics, current limiter or - compensator of reactive power. Shunt reactors are available for all voltage levels but naturally the ones for lower voltage levels are cheaper. Therefore, shunt reactors are often placed in the tertiary winding of the transformer in the high voltage network to reduce the costs. There are also available reactors, which are placed directly shunt to the bus or to the line.

4.3.1 Core and insulation

Basically, the core and insulation define the characteristics of the reactor. Reactors can be built either with a gapped core or with an air core. The inductance of the air core reactors is linear because air allows the magnetic field density to increase evenly. This makes their behavior easy to predict and therefore simpler to dimension. The

core of gapped core reactors is made of ferromagnetic material such as iron, which makes the reactor prone to saturation after a certain current limit. At the saturation point, the inductance of the reactor will reduce and the current will increase. This might cause a breakdown of the device if it is not protected properly. It is possible to build gapped core reactors as adjustable with a tap changer by varying the amount of circuits of the coil. (Elovaara & Haarla 2011)

Most of the reactors placed in the high voltage network are air core dry type ones in Finland. They are assembled from three one-phase coils, which are cylindric, concentric and equal high. Single phase coils are placed at a symmetric triangle when symmetric impedance is gained. The solution is also optimal for minimizing the spreading magnetic field. The conductor layers are nowadays covered with fiber-glass and separated from each other with aluminum sticks. The coils have to have a strong structure because of the Lorentz force. A large advantage of air core reactors is the constant inductance due to the air core, which makes reactors' behavior easy to predict and decreases the switching transient problems. Oil immersed air core reactors have a closed structure and they are significantly smaller than dry type ones. The structure resembles a normal distribution transformer. The drawbacks of oil immersed reactors are large weight and more expensive price. (Elovaara & Haarla 2011)

4.3.2 Connections

There are several possible connection choices available for reactors, which are presented in figure 4.2. The first one from the left is ungrounded wye-connection and the second one is delta-connection. Both of these can be transformed to each other with wye-delta transformation. The third one is grounded wye-connection with grounded wye-connection. The fourth one is the grounded wye-connection with a neutral reactor, which is, however, only used in countries, in which the single phase reclosing is used. (Areva 2011)

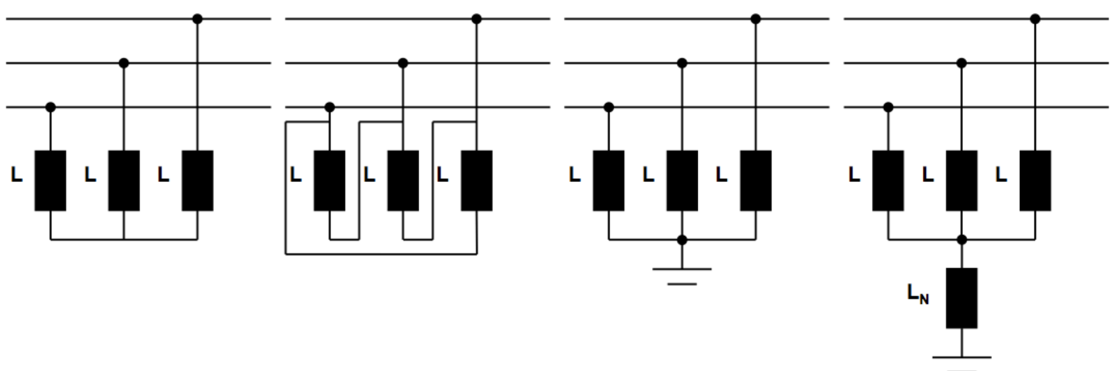

Figure 4.2. *Shunt reactor winding connections*

The grounded wye-connection reactor works as a Petersén coil and it can be used to compensate earth fault current. The coil connects in parallel with the capacitances of the power line and therefore decreases the amount of capacitive power during an earth fault. However, the ability of earth fault current compensation sets requirements on the coils. Firstly, the coils have to withstand the line voltage because the healthy phases will experience the line voltage in the solid earth fault. Secondly, the positive and zero sequence impedances of the coil have to match in order to behave linearly during the fault. Thirdly, if there is a gapped core, it can not saturate so the inductance would not drop. (Virtanen 2012)

The reactance of wye connected reactor can be calculated with the equation (4.8) and the reactance of delta connected with the equation (4.9). The delta- and ungrounded wye-connections operate only as a reactive power compensator. Since there is no ground connection and their zero sequence impedance is infinite, they are invisible in the earth fault situation. However, the delta connection consumes more reactive power because they operate on the line voltage instead of the phase voltage. (Areva 2011)

$$X_{Wye} = \frac{{U_N}^2}{S} \tag{4.8}$$

$$X_{Delta} = 3 \cdot \frac{{U_N}^2}{S} \tag{4.9}$$

4.3.3 Variability of the inductance

Reactors can be divided into three main categories according to their variability: fixed-type, step-type and plunger core reactors. Fixed-type reactors are the simplest ones, which have a constant inductance and they can not be changed afterwards. The insulation can be either oil immersed and air cooled depending on the product. Step-type reactors have a tap changer, which allows to change their inductance manually when they are disconnected from the network. Step-type reactors are also available as oil immersed and dry type. (Trench 2012)

Plunger core reactors are able to adjust their inductance without disconnecting them from the network. The adjusting is implemented by changing the air gap of the core with electric motors. The principle of a variable shunt reactor is described in figure 4.3. The motor drive cabinet controls the worm gear of each coil and moves the cores to the desired position. The control of the consumed reactive power can be done automatically based on the measured reactive power flow. It is possible to vary the power of the reactor between 20 % and 100 % with a delay less than 300 s. The control delay is possible to set less than the delay in on-load tap changers of the main transformers. As a result, the tap changers will not start to work in vain in order

to maintain the voltage level when reactive power flow increases. (Trench 2012)

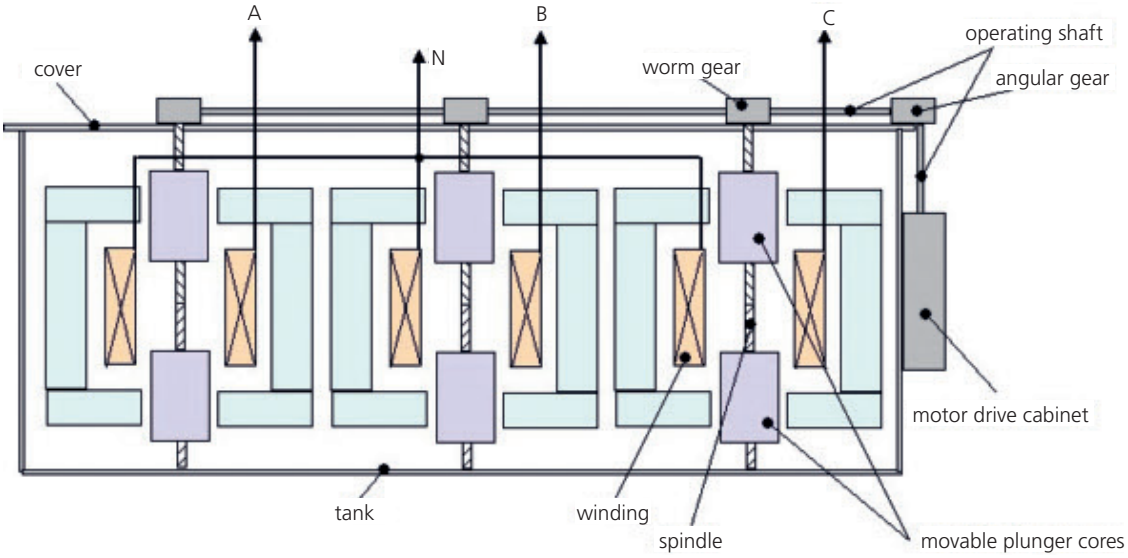

Figure 4.3. *The principle of a variable shunt reactor (Trench 2012)*

5. RESEARCH METHODS

The purpose of the applied part of this thesis is to answer several questions regarding the extensive cabling in rural area networks. Firstly, what is the economic effect of the reactive power increase when the reactive power window and power losses are taken into account. Secondly, should the reactive power be compensated centrally at the substations or locally along the feeders. On the other words, is it profitable to use distributed shunt reactors or should the centralized reactors be used instead. Thirdly, how the earth fault compensation should be implemented in order to avoid the challenges of extensive cabled networks, which were introduced in section 3.3. It should also be decided whether to use traditional Petersén coils, shunt reactors or a combination of them to compensate both reactive power and earth fault current effectively.

The above questions were studied by combining information from PSCAD - simulations, references and different calculations. In this chapter, the initial conditions, assumptions and used tools are declared. In section 5.1, the utilized programs are presented. Section 5.2 presents the examined case substation in detail, which were used in the simulations. Section 5.3 describes the modeling of different components in PSCAD. Section 5.4 presents the pre-assumptions of the economic calculations.

5.1 Programs

Basically two different programs were used in this thesis, which are presented in this section. PSCAD includes more features in the network analyzing compared with Tekla NIS and therefore it was used as a principal program to make simulations. Tekla NIS was a supportive program, which was used as a source of information. Additionally, NIS was used to validate the correctness of the PSCAD simulation model by using power flow and earth fault calculation features.

5.1.1 Tekla NIS

Tekla NIS is a network information system, which is used for the management of the assets. Basically, NIS consists of five components: Tekla NIS Basic, Tekla PSA (Power System Analysis), Tekla Network Planning and Construction, Tekla Asset Management and Tekla Maintenance. Tekla NIS Basic includes the network

model and the basic element such as topology information and detailed information about the components. Tekla Power System Analysis can be used to make steady state power flow calculations, short circuit and earth fault calculations and reliability calculation. Tekla Network Planning and Construction is used to manage the construction and planning process and allows the long term development of the network. Tekla Asset Management can be used to analyze the value of the current network based on different parameters and analyze the economic influences of the investments in the asset. Tekla Maintenance is a maintenance management system, which can be used to plan the maintenance of the components and calculate the cost saving in asset management. In this thesis, only the features of Tekla NIS Basic and Power System Analysis were used. (Tekla 2012)

The load flow calculations are carried out with iterative methods in Power System Analysis by using Newton-Raphson or Gauss-Seidel algorithms. The idea is to make several rounds of calculations and make the result more accurate on every round until the satisfied accuracy has been reached. The earth fault calculation uses the traditional version for calculating earth fault currents. It considers only the susceptance of the power lines, the fault resistance and the parallel resistance of the Petersén coil. However, the zero sequence resistance and inductance of the power lines are not considered in the calculations and therefore NIS does not provide any extra information such as resistive parts of the earth fault currents or zero sequence voltage of the fault location. (Tekla 2012)

Tekla NIS models the loading of the network based on the combination of the measurement information and index series. The active power measurement information is imported to NIS from AMR-meters of the customers. Remote meters provide measurement data hourly by communicating via GPRS-network or other communication channels. Meters could provide reactive power measurement data as well. However, due to communication reasons it is not acquired to the NIS-database. As a consequence, active power results from index series are used to calculate the reactive power with constant $\cos\phi$ for each customer group.

5.1.2 PSCAD

PSCAD is a transient simulation environment, which can be used to simulate fast phenomenon in the electricity networks. In addition to steady state studies, it allows to examine different quantities in the time domain. The calculations are performed by EMTDC-program, which uses differential equations of the components to solve the network. The equations are solved with a fixed adjustable time step, which is 50 μs by default but can be changed by the user. The used program was the X4 version of PSCAD, which does not have node limitations. (Manitoba HVDC Reasearch Centre 2010)

In PSCAD, the simulation model is assembled from blocks, which can represent an electrical or logical component. PSCAD master library includes a number of ready models for the basic components used in the electricity networks such as resistors, coils, transformers, circuit breakers, generators and so on. It is also possible to create different control systems by using non-electrical components like logical ports and signal processing tools. An important feature is the possibility to create blocks, which can include a combination of components or the block can include a script written with Fortran- or C-programming language. This enables building the simulation model to multiple levels, which simplifies the structure of the model and makes it possible to maintain a reasonable size for each module. (Kauhaniemi & Mäkinen 2011)

It is possible to measure a variety of quantities from the simulation model. This is done by either adding a meter component to the model or using internal meters of certain components. After this, the measured signal can be processed further for example by adding it to a Fourier-transformation block. Signals can be visualized with a number of different graphical illustration tools.

The parameters of the components can be either predefined before the simulation or changed during the simulation, which means that they are runtime configurable. It is possible to adjust runtime configurable components for example by using slide controls or switches during the simulation run. However, only part of the components are possible to build as runtime configurable and most of the parameters of the components have to be set before the simulation starts.

5.2 Examined substation

The modeled Substation 1 is based on a real substation, which is located in the rural area. Substation 1 was chosen as a case network since it will have a new straight 26 km cable feeder installed, which is used to feed a switching station from the main substation. The cable is the longest straight cable, which has been installed in Elenia's network so far and the rest of the substation is also likely to be cabled in the future. A schematic diagram of the substation is presented in figure 5.1. There are eight feeders in Substation 1 and feeder 14 is the link cable to the switching station. The lengths of the feeders and the line types are listed at table 5.1 and 5.2.

Table 5.1. *Lengths of the feeders and line types of Substation 1*

	F5 (km)	F6 (km)	F9 (km)	F10 (km)	F11 (km)	F12 (km)	F13 (km)	F14 (km)	Total (km)
OHL	97,0	41,8	49,1	63,0	9,4	75,1	1,4	0	336,8
CC	1,3	0,3	0	3,00	2,5	2,5	3,4	0	12,9
Cable	5,8	0,1	2,5	0,2	1,4	0,7	4,1	25,8	40,5

Table 5.2. *Lengths of the feeders and line types of the switching station*

	FP5 (km)	FP6 (km)	FP7 (km)	FP8 (km)	FP9 (km)	Total (km)
OHL	44,2	16,2	12,4	0,8	12,9	86,6
CC	0	3,5	0	0	1,1	4,6
Cable	1,2	0,1	0,1	8,1	9,6	19,0

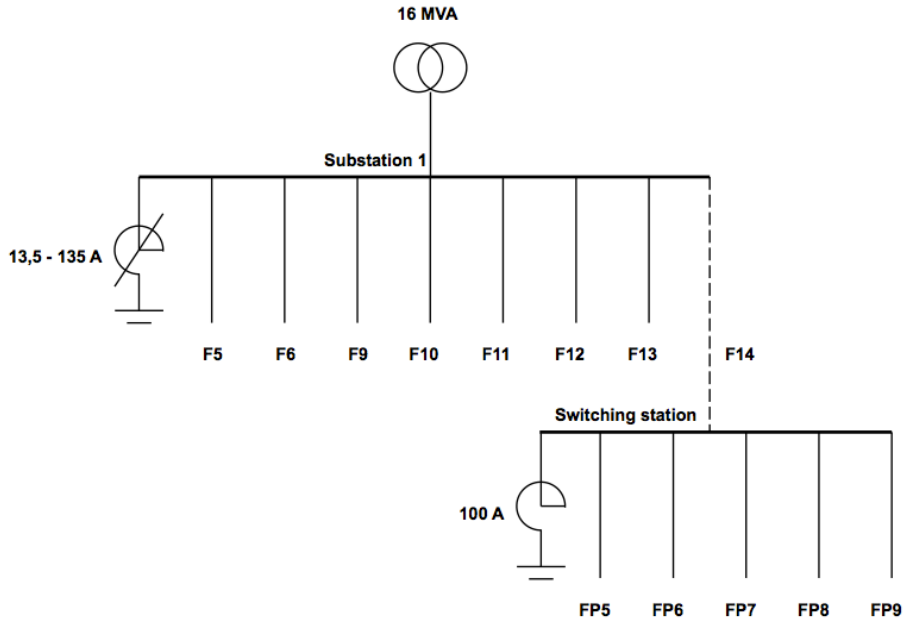

Figure 5.1. *A schematic diagram of Substation 1*

The earth fault compensation of the network is carried out with two Petersén coils. An adjustable coil (13,5 - 135 A) is located at Substation 1 and a fixed 100 A coil is at the switching station. Another one of the coils is fixed, so that two coils would not cross-adjust their inductance with each other. The total earth fault current of the network is approximately 180 A, so there is some extra capacity in the coils to be used for earth fault current compensation. Additionally, there will be a 178 kVAr shunt reactor at the feeder 14 located 15 km from Substation 1, which can be used for earth fault compensation as well.

The substation is connected to Elenia's 110 kV Hawk -overhead line and the connection point to the main grid is 96 km away from the substation. Besides Substation 1, there are also three other substations along the same 110 kV line. The other substations were modeled only as fixed loads because more accurate modeling was not relevant in the scope of this thesis.

Substation 1 was also cabled in order to use it in the simulations as an example case. The cabling was carried out in different stages. At the start, Substation 1 was in the present state with the new long cable feeder 14. Firstly, the trunks of the feeders of Substation 1 were cabled one by one, secondly the branches of the feeders,

thirdly the trunks of all feeders at the switching station and lastly all the branches of the switching station. At the end, the total network was cabled. The cabling was carried out by using the cables introduced in subsection 5.3.1. The lengths of new installed cables to each feeder are listed at tables 5.3 and 5.4. One should consider that the cabling of the network is just an example and it has not been carried out in the most ideal and efficient way. However, this was because the network planning was not the main theme of this thesis.

Table 5.3. *Amount of installed cable types in Substation 1*

	F5 (km)	F6 (km)	F9 (km)	F10 (km)	F11 (km)	F12 (km)	F13 (km)	F14 (km)
AXAL-TT50	53,0	14,2	29,4	43,2	14,2	63,9	-	-
AXAL-TT95	17,7	17,3	19,2	10,5	4,3	13,1	1,4	-
AXAL-TT150	18,0	-	-	11,0	5,9	-	3,9	-
AXAL-TT240	8,5	-	-	-	-	-	-	-

Table 5.4. *Amount of installed cabled in the switching station*

	FP5 (km)	FP6 (km)	FP7 (km)	FP8 (km)	FP9 (km)
AXAL-TT50	25,3	6,5	11,7	0,8	3,3
AXAL-TT95	10,2	-	-	-	8,1
AXAL-TT150	11,3	8,6	-	-	-
AXAL-TT240	-	-	-	-	-

5.3 Network component modeling

This section describes the modeling of different components in the PSCAD model and their specifications. PSCAD has many ready models for basic network components, which were used as much as possible. Only shunt reactors and Petersén coils had to be built from basic components since the master library of PSCAD did not include them. Only those specifications, which are presented in this section, have been changed to PSCAD models. Other settings were left to program's defaults.

5.3.1 Power lines

The power lines of the network model were modeled in two different ways. In Substation 1, all lines were modeled with pi-sections. PSCAD has a ready pi-section model, which allows to insert the positive and zero sequence data as well as the length of the line. Pi-section is accurate enough for steady state simulations when the transient behavior of the lines is not the priority (Manitoba HVDC Reasearch Centre 2010). Parameters of each line type are listed at 5.5.

Table 5.5. *Specifications of the modeled lines*

Type	R $(\frac{\Omega}{km})$	R_0 $(\frac{\Omega}{km})$	X $(\frac{\Omega}{km})$	X_0 $(\frac{\Omega}{km})$	C $(\frac{nF}{km})$	C_0 $(\frac{nF}{km})$	I_{max} (A)
Sw25	1,35	1,50	0,40	1,93	9,2	6,1	155
Sp40	0,85	1,00	0,38	1,91	9,5	6,1	210
Rv63	0,54	0,69	0,37	1,90	10,0	6,1	280
Pg99	0,34	0,49	0,35	1,89	10,0	6,1	360
PAS50	0,72	0,87	0,31	2,03	12,0	5,0	245
PAS70	0,49	0,64	0,30	2,02	12,0	5,0	310
AXAL-TT50	0,64	3,96	0,12	0,17	160,0	160,0	170
AXAL-TT95	0,32	3,64	0,11	0,15	190,0	190,0	240
AXAL-TT150	0,21	3,00	0,10	0,14	230,0	230,0	300
AXAL-TT240	0,13	2,52	0,09	0,11	270,0	270,0	400
AXAL-F-TT240	0,13	2,52	0,09	0,11	260,0	260,0	340

The positive sequence parameters have been gathered from Tekla NIS. The zero sequence resistances and reactances of the cables have been estimated by using equation (5.1). A more detail explanation of the estimation can be found from (Guldbrand 2009). The descriptions of the symbols and the used values of the equation are listed below the equation, the same estimated values have been used as in (Pekkala 2010). The cable specific geometrical values are listed at table 5.6.

$$Z_0 = l \cdot (R_c + 3 \cdot \frac{j\omega\mu_0}{2\pi} \cdot \ln \frac{r_s}{\sqrt[3]{r_c{}' \cdot d^2}}) + \frac{3l \cdot R_s(R_{e1} + R_{e2} + l(R_g + \frac{j\omega\mu_0}{2\pi} \cdot \ln \frac{D_e}{r_s{}'}))}{R_{e1} + R_{e2} + l(R_s + R_g + \frac{j\omega\mu_0}{2\pi} \cdot \ln \frac{D_e}{r_s{}'})} \quad (5.1)$$

- The cable length l
- The equivalent penetration depth $D_e = 659 \cdot \sqrt{\frac{\rho}{f}} = 659 \cdot \sqrt{\frac{2500\Omega m}{50Hz}}$=4659,8 m
- The permeability of a free space $\mu_0 = 4\pi \cdot 10^{-7}$
- The angular velocity $\omega = 2\pi f = 100\pi$
- The earthing resistance of the grid at the end first of the cable $R_{e1} = 8\ \Omega$
- The earthing resistance of the grid at the end second of the cable $R_{e2} = 8\ \Omega$
- The ground resistance $R_g = \frac{\omega\mu_0}{8} = \frac{2\pi \cdot 50Hz \cdot 4\pi \cdot 10^{-7}}{8} = 4,935 \cdot 10^{-5}\ \Omega$
- The sheat resistance R_s
- The conductor resistance R_c
- The geometric mean radius of sheet $r_s{}'$
- The geometric mean radius of a conductor $r_c{}'$

Table 5.6. *Geometrical values of modeled cables (Ericsson 2012)*

Cable	$r_c{}'$ (m)	$r_s{}'$ (m)	R_c (Ω)	R_s (Ω)
AXAL-TT50	0,0039	0,024	0,000641	0,0012
AXAL-TT95	0,0056	0,0275	0,00032	0,0012
AXAL-TT150	0,007	0,03	0,000206	0,0008
AXAL-TT240	0,009	0,035	0,000125	0,0008
AXAL-F-TT240	0,009	0,0365	0,000125	0,0008

There are also more accurate ways to model a power line in PSCAD, which use long line equations. This means that the model assumes that parameters are distributed along the line in differential small parts. In this thesis, Bergeron-model was used, which models a power line accurately with a specific frequency. However, as the line model becomes more accurate, the simulation time gets also longer and the shorter the line is, the shorter has the be to simulation step because of the propagation speed of the electromagnetic wave. Therefore the Bergeron model was only used in the power loss measurements of the straight feeders. Pi-sections would not have been accurate enough with longer lengths because they assume that the capacitance of the line is divided into two parts. When the power losses of the reactive power are measured, the reactive power accumulates gradually along the line and it would be wrong to assume that half of the total reactive power flows through the entire feeder. (Manitoba HVDC Reasearch Centre 2010)

5.3.2 Compensation devices

Shunt reactors were modeled simply with a series connection of an inductance and a resistor between each phase and the neutral point. All reactors were wye-connected with a vector group Yn. Since no shunt reactors have been used in Elenia's network before, the product specifications were asked from the manufacturers. The specifications were asked for 1-3 MVAr air core dry type reactors, which were supposed to be placed in the substation. Additionally, one shunt reactor of 178 kVAr was used for the distributed reactive power compensation. From the modeling point of view, the interesting information was the power losses and the inductance of the coils, which were acquired from the manufacturers' data. Specifications of the used reactors are introduced in table 5.7.

Table 5.7. *Specifications of modeled reactors (Alstom 2012)*

Q (kVAr)	P_{cu} (kW)	I_n (A)	L (H)
178	2,5	5	7,53
1000	12,0	28	1,27
2000	16,8	56	0,64
3000	6,5	84	0,42

Petersén coils were built as a combination of a Zn-grounding transformer and an inductance. Additionally, centralized Petersén coils had an extra parallel of 5 A in parallel with the inductance. The function of the Zn-transformer was only to create a virtual neutral point to the network. Therefore, the transformer was assumed to be ideal and non saturable. The inductance of the Petersén coil was calculated from a desired compensation current values I_{comp} according to the equation (5.2). All distributed Petersén coils were calculated to compensate 15 A of earth fault current and the capacity of the centralized Petersén coils varied.

$$L = \frac{U_{ph}}{I_{comp} \cdot 2\pi \cdot 50} \tag{5.2}$$

5.3.3 Transformers

PSCAD has a ready model for transformers, which was used in all simulations. For Substation 1, six different sizes of distribution transformers were modeled and their specifications were acquired from Tekla NIS. Additionally, the 16 MVA main transformer data was collected from Tekla NIS. The specifications of the used transformers are presented in table 5.8. The transformation ratio of all distribution transformers was 20,6/0,4 kV and the vector group was Dyn. For the main transformer, a ratio of 110/20,6 kV and a vector group Dy was used.

Table 5.8. *Specifications of modeled transformers (Tekla NIS 2012)*

S (kVA)	x_k (%)	P_0 (kW)	P_{cu} (kW)
16	4,00	0,11	0,50
30	4,00	0,14	0,78
50	4,00	0,12	1,10
100	4,00	0,20	1,75
200	4,50	0,34	2,75
315	4,00	0,66	4,00
500	4,50	0,90	5,70
800	4,70	1,35	7,10
1000	5,00	1,45	9,20
16000	10,60	11,00	65,00

5.3.4 Loading

Generally, there are three different ways to model the loading according to the dependency on the voltage. A fixed impedance load has a square dependence to the voltage. It gives the most favorable results from the network point of view. A fixed current load is directly proportional to the voltage and it is often used to describe

motor loads. A fixed power load is independent on the voltage, which means that it always takes the constant power and can be considered as the worst case scenario. Therefore, it is common to use the fixed power load in the power flow calculations in order to get the "worst" results. The fixed power load model was used in this thesis as well. (Elovaara & Haarla 2011)

The loading model of Substation 1 was based on the results from Tekla NIS. The estimation was made separately for each feeder by choosing all the distribution transformers and drawing a loading graph from their data. The measurement data of the transformers is based on the combination of the index series and actual measurements from AMR-meters. The loadings of the feeders were assumed to be correct in Tekla NIS and they were not verified separately from SCADA-measurements. After getting the maximum load for each feeder, the loading was assumed to be distributed evenly to each transformer. It means that all transformers in a single feeder were loaded evenly according to the nominal power of the transformer. The power factor was assumed to be 0,95 for all loads. PSCAD provides a ready fixed load model, which allows the user to choose between fixed impedance, fixed current and fixed power. However, the fixed load is not runtime configurable, which means that the values can not be changed afterwards. Therefore, parameters for the component had to defined manually for each transformer size and each feeder. Since the total amount of loading points was almost 400, it was found to be adequate to simulate the network in the maximum loading and no load situation. No load situation represented the absolute worst case scenario. The loads were put to the low voltage side of the distribution transformers. The maximum loading for each feeder is presented in table 5.9

Table 5.9. *Maximum loadings in Substation 1*

Feeder	P_{max} (kW)	Q_{max} (kVA)
F5	1219	395
F6	544	156
F9	315	118
F10	786	212
F11	1008	322
F12	1189	307
F13	2182	1092
FP5	646	177
FP6	1001	317
FP7	210	69
FP8	214	70
FP9	253	81

In addition to Substation 1, fixed loads had to be also calculated for three different cable types in order to perform power loss calculations in the test network of straight cable feeders. This is explained in detail later in this thesis. The loading of the feeders was calculated in two different ways. Firstly, the loading was calculated to be for 5-20 % from the maximum capacity of the cables with a fixed power factor of 0,95. Secondly, 10 % of the maximum capacity was calculated with power factors 0,9, 0,95 and 1. The calculated parameters of the loads are listed at table 5.10 and 5.11.

Table 5.10. *Calculated active and reactive power loads with a constant power factor*

Cable type	$P_{5\%}$ (kW)	$Q_{5\%}$ (kVA)	$P_{10\%}$ (kW)	$Q_{10\%}$ (kVA)	$P_{15\%}$ (kW)	$Q_{15\%}$ (kVA)	$P_{20\%}$ (kW)	$Q_{20\%}$ (kVA)
AXAL-TT95	414,7	136,3	829,3	272,6	1244,0	408,9	1658,6	545,2
AXAL-TT150	518,3	170,4	1036,6	340,7	1555,0	511,1	2073,3	681,5
AXAL-TT240	691,1	227,2	1382,2	454,3	2073,3	681,5	2764,4	908,6

Table 5.11. *Calculated active and reactive power loads with a constant loading*

	$cos\phi = 1$		$cos\phi = 0,95$		$cos\phi = 0,9$	
Cable type	$P_{10\%}$ (kW)	$Q_{10\%}$ (kVA)	$P_{10\%}$ (kW)	$Q_{10\%}$ (kVA)	$P_{10\%}$ (kW)	$Q_{10\%}$ (kVA)
AXAL-TT95	872,9	0,0	829,3	272,6	785,7	380,5
AXAL-TT150	1127,6	0,0	1036,6	340,7	982,1	475,7
AXAL-TT240	1454,9	0,0	1382,2	454,3	1309,4	634,2

5.4 Economic calculations

One large part of the thesis was to evaluate the costs of using different compensation devices. There are several costs, which are related to network components but only the investment price and the cost of losses were considered relevant in this scope. The investment prices of used compensation devices are listed at table 5.12 and the prices include the devices, installation and other necessary equipment. The prices of centralized shunt reactors are estimates from the manufacturer. Both of centralized Petersén coils are list prices from Energy Market Authority. Distributed compensation units are estimates from Elenia's staff.

Power losses have been calculated with certain assumptions, which are listed at table 5.13. Since the calculated power losses are due to the reactive power flow, the peak usage time has set to 8760 h. If cables are installed in the network, they generate the same amount of reactive power every hour, which creates the losses. Therefore, it is also more convenient to assume the loading increase rate to zero.

Table 5.12. *Investment prices of different compensation devices*

Device	Q (kVAr)	I_c (A)	Price (€)
Distr. Shunt reactor	178	15	30 000
Centr. Shunt reactor	1000	84	51 000
Centr. Shunt reactor	2000	168	61 000
Centr. Shunt reactor	3000	252	94 000
Distr. Petersén coil	-	15	10 000
Centr. Petersén coil	-	140	170 000
Centr. Petersén coil	-	250	186 000

Table 5.13. *Parameters of power loss calculations*

Review period T	20 years
Interest rate p	4 %
Loss price H	50 €/MWh
Loading increase rate r	0 %
Peak usage time t	8760 h

The costs of power losses can be discounted to present by using equations (5.3) and (5.4). κ is the capitalization factor, which is calculated for a fixed time period with a certain interest rate. When κ is known, the present value of the power losses can be calculated with equation (5.5).

$$\Psi = \frac{(1 + r/100)^2}{1 + p/100} \tag{5.3}$$

$$\kappa = \Psi \cdot \frac{\Psi^T - 1}{\Psi - 1} \tag{5.4}$$

$$C_l = \kappa \cdot t \cdot H \cdot P_{losses} \tag{5.5}$$

6. RESULTS

The results chapter consists of five different sections, which are different perspectives to the compensation issue. The first section discusses power losses due to increasing reactive power flow and different ways to reduce them. The second section studies whether the loading capacity of the cables will become a problem due to the reactive power. The third section considers if Ferranti-effect is significant in the medium voltage network. The fourth section discusses the principle of estimating the reactive power window exceeding costs when more cables are installed in the network. The fifth section considers different phenomena of earth fault situations in the extensive cabled network. In the sixth section, all studied perspectives are taken into account and an optimal compensation strategy is suggested. The last section reveals the possible inaccuracy of the study and evaluates the used programs.

6.1 Power losses in cabled networks

As discussed, cables generate a significant amount of reactive power, which causes power losses on long power lines due to the increasing current. In this section, shunt reactors' capability to decrease power losses consequent from reactive power flow were studied. Simulations were done for both straight and branches feeders with different reactor placements. Straight feeders were assumed to be straight without any branches and branched feeders were acquired from Substation 1. Additionally, transformers' power losses were examined. The main purpose was to define whether it is economically profitable to compensate reactive power locally by using distributed shunt reactors or should the shunt reactors be located at the substation from the power losses point of view.

6.1.1 Ideal placement for distributed shunt reactors

The first task was to find out the best possible situation for using a distributed shunt reactor, where it reduces power losses the most. The ideal case would show if the distributed shunt reactors were profitable at all and give advice to the effective use of the reactors. The ideal situation was defined based on two main factors; the topology, where the reactive power flow creates the largest power losses and the placement of the reactor in this topology, which decreases power losses the most.

At first, the maximum power losses were simulated with different topologies,

which are introduced in figure 6.1. All feeders in the figure have the same total length of 50 km and the cable type of AXAL-TT150. The feeders were simulated in no load situation in order to define the power losses caused by the reactive power flow. The voltage was constant 20,6 kV at the beginning of the feeder. The power losses of each topology are presented in table 6.1. Evidently, the losses of a straight line are the greatest and the losses get smaller when the topology gets more branched. However, the total generated reactive power varies very little between the topologies and it is practically constant. The reason is that the reactive power accumulates differently along the line between the topologies. As the power losses are square proportional to current, currents are smaller in branches and their sum is not the same even though the total amount of generated reactive power is equal.

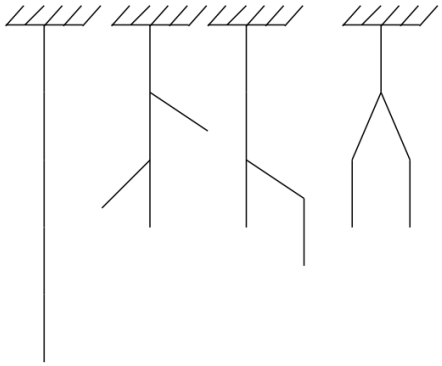

Figure 6.1. *Different topologies for test simulations*

Table 6.1. *Power losses on no load of different topologies*

	Straight line	2 short branches	1 long branch	2 long branches
P_{loss} (kW)	19,98	13,41	12,48	17,15
Q (kVAr)	-1544,00	-1541,01	-1540,58	-1542,73

Next, the ideal placement of the reactor was studied with the same straight 50 km AXAL-TT150 feeder. 178 kVAr distributed shunt reactor was placed every 10 km to the feeder and power losses were measured from each case. The measurements were made with no load and 10 % of the maximum loading with three different power factors; 0,9, 0,95 and 1. The results are presented in table 6.2. As can be seen, the most beneficial place of the reactor would be at the end or at the latter part of the feeder. However, the variation of the losses is actually quite small when the coil is further placed than 30 km. This would indicate that the influence of the placement is rather irrelevant if the reactor is placed in the latter part. The actual ideal placement for the reactor would be the place, at which the length of the line on the load side generates the amount of reactive power, which corresponds to the

inductive part of the loading. In order to simplify and justify the results, the place of the reactor was chosen to be at the end of the feeder. Another reason relates to the limitation of the Bergeron-model. For example, if the power losses of a 20 km cable line compared with two 10 km parts, they are not equal. Therefore it would have been difficult to optimize the reactor placement and maintain the comparability with the results.

Table 6.2. *Power losses in a straight feeder with different reactor placements*

Length (km)	$P_{\cos\phi=1}$ (kW)	$P_{\cos\phi=0,95}$ (kW)	$P_{\cos\phi=0,9}$ (kW)	P_{Noload} (kW)
10	50,65	36,61	31,84	19,43
20	49,02	35,58	31,04	17,70
30	47,92	35,06	30,75	16,50
40	47,33	35,07	30,99	15,84
50	47,29	35,61	31,76	15,73

6.1.2 Straight cable feeders

After the most beneficial situation was found out, different cable types were tested with and without the reactor in the straight feeders. Straight feeders were studied with three different 20 kV cables, which are widely used in Elenia's distribution network; AXAL-TT240, AXAL-TT150 and AXAL-TT95. The specifications of the cables were introduced in subsection 5.3.1. The profitability analysis was done by first measuring power losses from each cable feeder with and without the shunt reactor at the end of the feeder. After that the difference of the losses was converted to discounted costs in 20 years by using the parameters introduced in section 5.4. The measurements were first made by varying the loading with a fixed power factor and after that varying the power factor with a fixed load. All straight feeder measurements were done with the same basic set up, where the voltage was set to 20,6 kV at the beginning of the feeder and the power losses were measured as a difference of active power at the start point and the end point of the line. In order to justify the results and measure the worst case scenario, the loading was placed at the end of the feeder.

The results of fixed power factor loadings are presented in figure 6.2, 6.3 and 6.4. The figures describe how much economic profit is gained from decreased power losses due to a single shunt reactor. Each bar represents the difference between the situation with and without the reactor. Green bars represent economic benefit and red bars represent economic loss. If there is no bar at some points of the figure, it means that the voltage dropped under 95 % of the nominal voltage and the feeder could not be used.

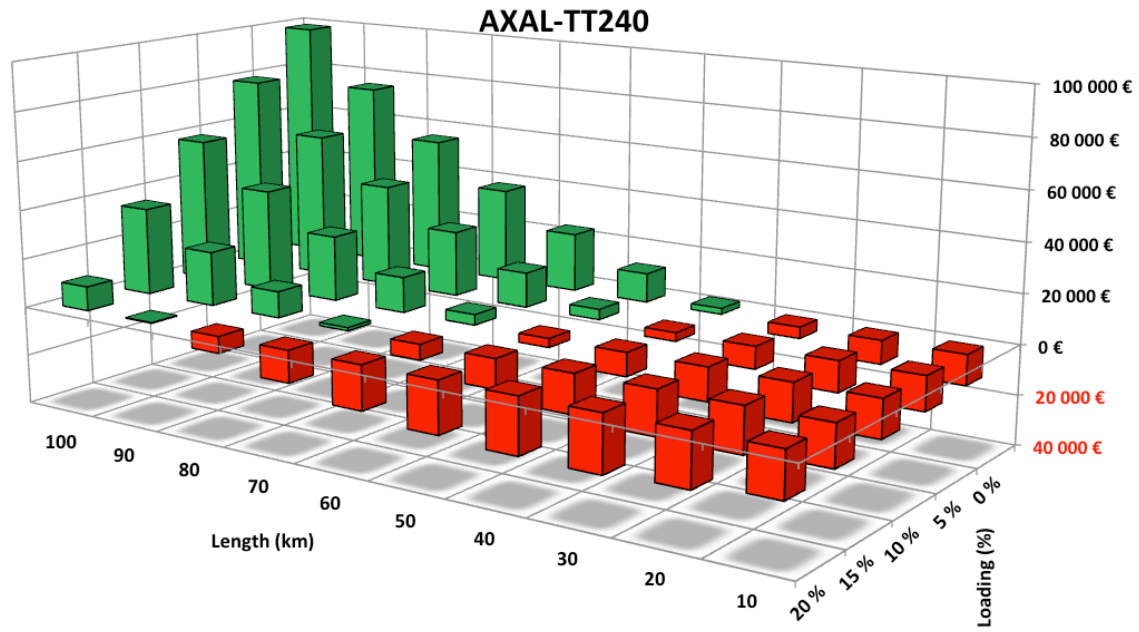

Figure 6.2. *Profit of using a shunt reactor in AXAL-TT240 feeder,* $\cos\phi$*=0,95*

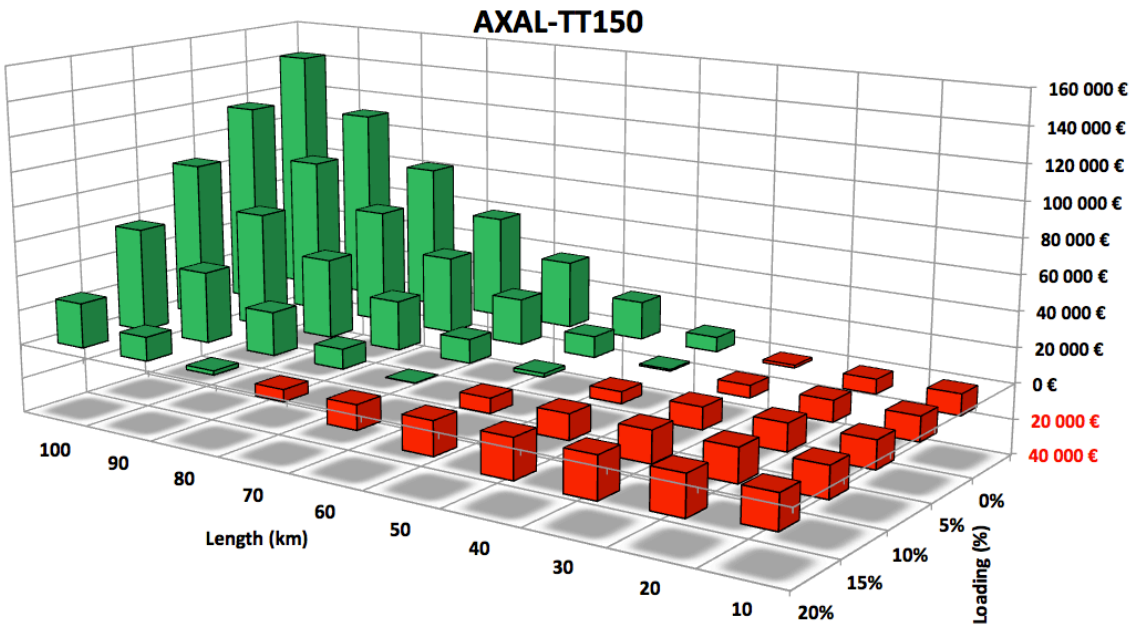

Figure 6.3. *Profit from using a shunt reactor in AXAL-TT150 feeder,* $\cos\phi$*=0,95*

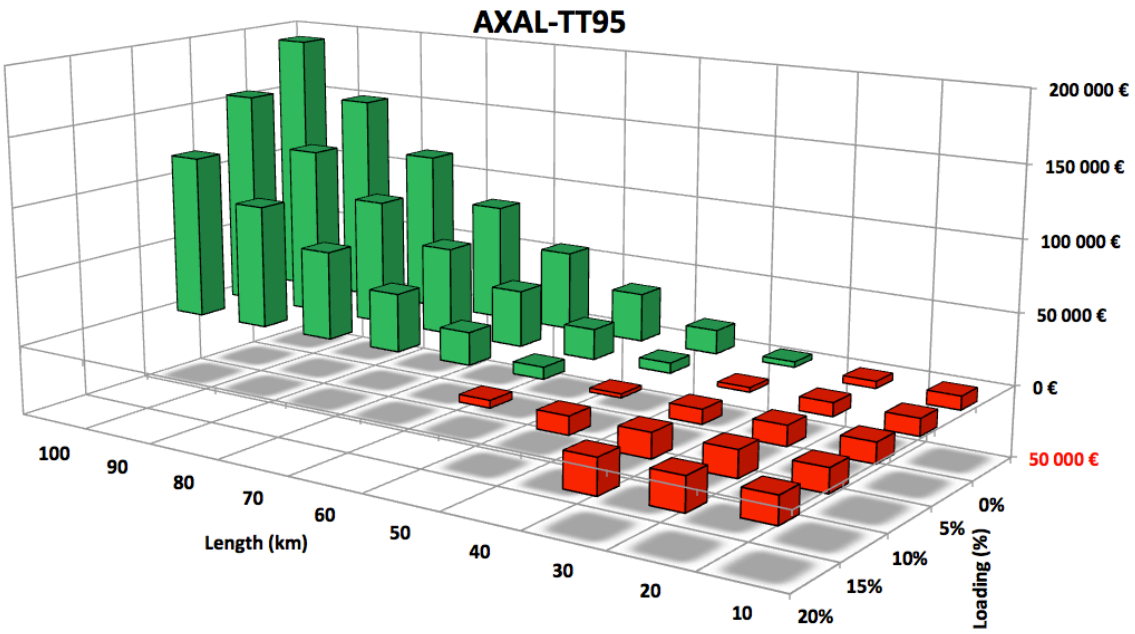

Figure 6.4. *Profit from using a shunt reactor in AXAL-TT95 feeder,* $\cos\phi$*=0,95*

It can be noticed that the profitable usage of the reactors depends highly on the loading and the length of the feeder. As the length of the feeder increases, the usage of the reactors becomes more beneficial. Additionally, the smaller the load is, the greater the economic benefit is. This is natural because as the loading percentage is increased with a fixed power factor, the inductive part of the load increases. As a result, more reactive power is flowing to the load and the need for the compensation decreases. The economic benefit seems to be also greater with smaller cable sizes, which is a consequence of the greater characteristic resistance value of cables. The greater resistance value causes greater power losses and therefore the relative benefit from the reactor is larger since the losses are square proportional. Also, the losses increase linearly as the loading increases with a fixed power factor.

Next, the power factor was varied between 0,9 and 1 and the loading percentage was kept constant. These results are presented in figures 6.5, 6.6 and 6.7. Again, the longer feeder lengths result in greater economic benefit. However, the power factor seems to affect the profitability as well. When the power factor gets lower, also the profit gets smaller. The reason is basically the same as with the fixed power factor; when more inductive power is flowing to the loading, the need for compensation decreases. Evidently, the benefit is the greatest with the pure resistive load. Based on these simulations, the distributed shunt reactors appear to be profitable when the straight feeder is over 50 km. Additionally, the loading should be relatively small and the power factor as high as possible.

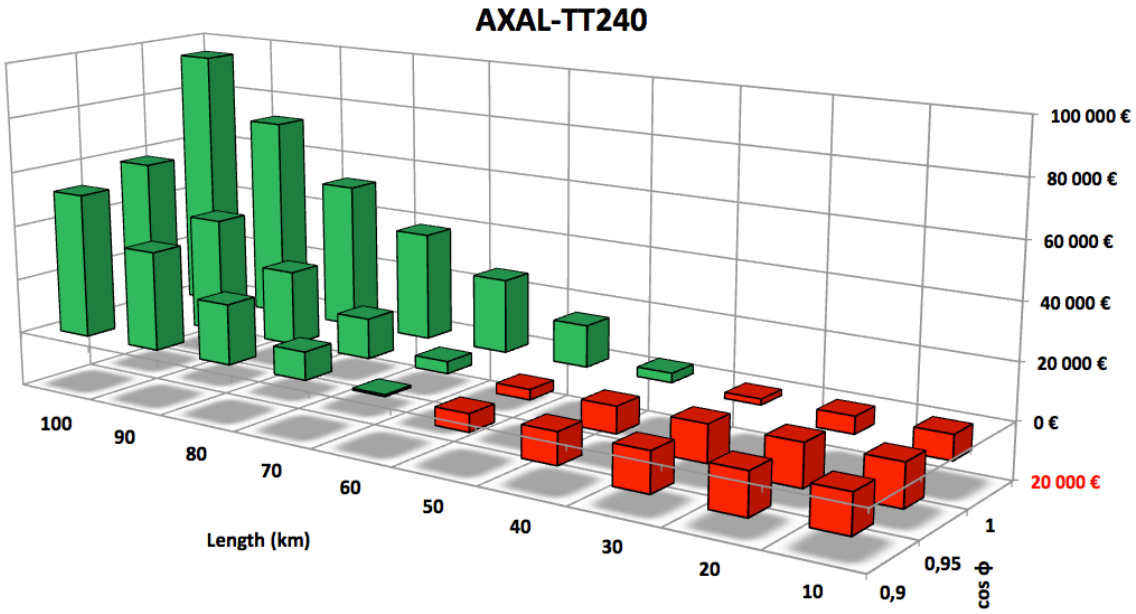

Figure 6.5. *Profit from using a shunt reactor in AXAL-TT240 feeder, 10 % loading*

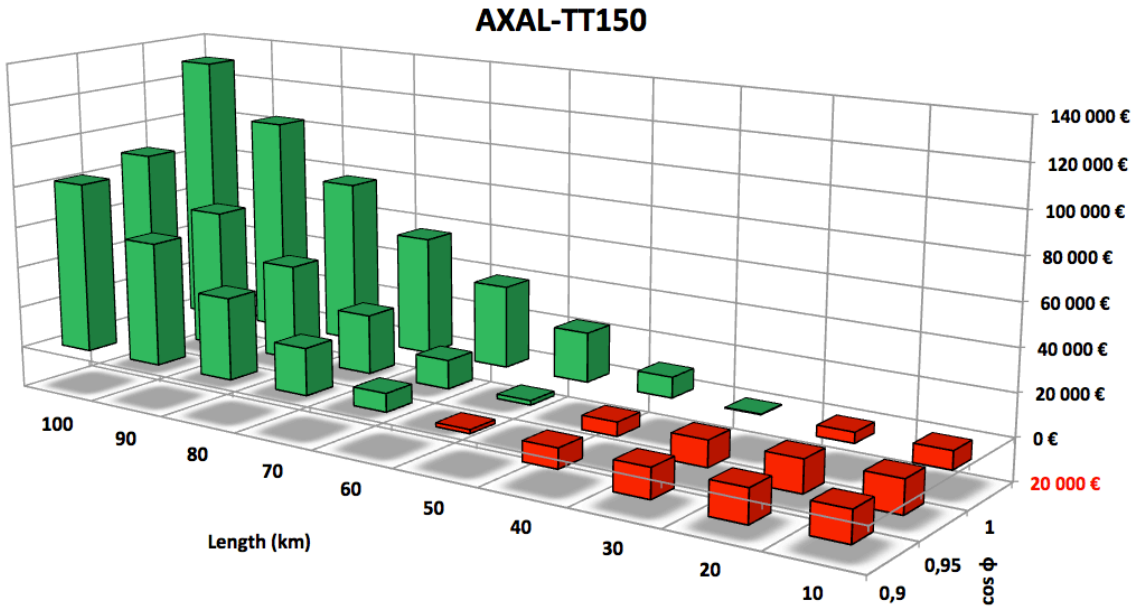

Figure 6.6. *Profit from using a shunt reactor in AXAL-TT150 feeder, 10 % loading*

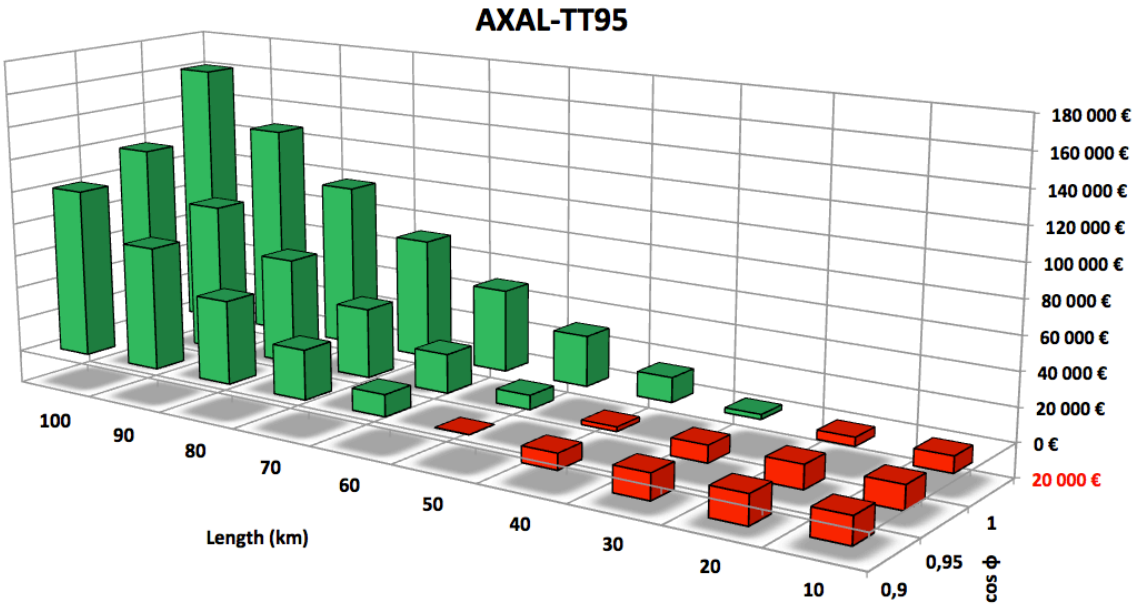

Figure 6.7. *Profit from using a shunt reactor in AXAL-TT95 feeder, 10 % loading*

6.1.3 Branched cable feeders

Distributed shunt reactors' ability to decrease power losses was also studied with branched feeders in Substation 1 when the network was totally cabled. Since the whole simulation model was quite large, each feeder was examined separately by connecting only one feeder to the bus at the same time. The absolute value of the losses on power lines was not practically possible to accomplished due to the size and the detail of the modeled network. The simulation model would have needed a measurement point at every load in order to separate the actual line losses on the pi-sections and the simulation would have slowed down remarkably. Therefore, the loss calculation was done by calculating the difference of the total active power between different cases. As different cases are compared with, the change of the active power describes how much the power losses have increased or decreased.

Feeders 5, 9, 10 and 12 were chosen to be observed since their reactive power surplus was over 1 MVAr at the substation, which can be considered as remarkable. The placement of the distributed shunt reactors was chosen to be at the latter part of the feeder based on the result from section 6.1.2. Totally 4 reactors were placed in each feeder. Figure 6.8 presents the economic profit gained from the decreased power losses on the maximum load and figure 6.9 on no load. The profit is calculated in the same way from the period of 20 years as with the straight cables.

As can be seen, the gained benefit from the reactor usage is actually quite small. Not surprisingly, the most beneficial feeders are 5 and 12, which are also the longest ones and have the largest reactive power generation. As the investment price of a distributed shunt reactor is approximately 30 000 €, they can not be considered as

economic from the power losses point of view in branched feeders. The problem of the distributed shunt reactors is probably their small size and losses. In order to decrease power losses due to the cables' reactive power generation, the compensated reactive power has to be enough the win reactor's own power losses. As the power losses are square proportional, the amount of reactive power has to be particularly significant in order to create real benefit.

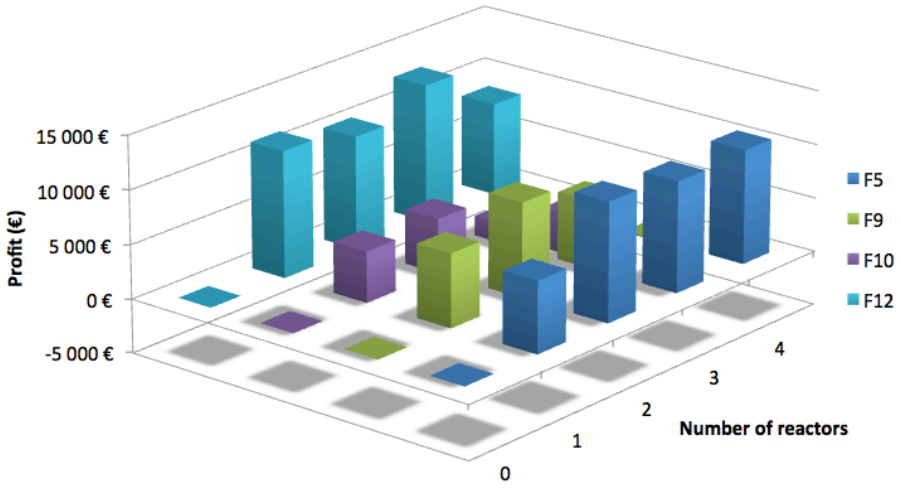

Figure 6.8. *Benefit from using shunt reactors on feeders 5, 9, 10 and 12, max load*

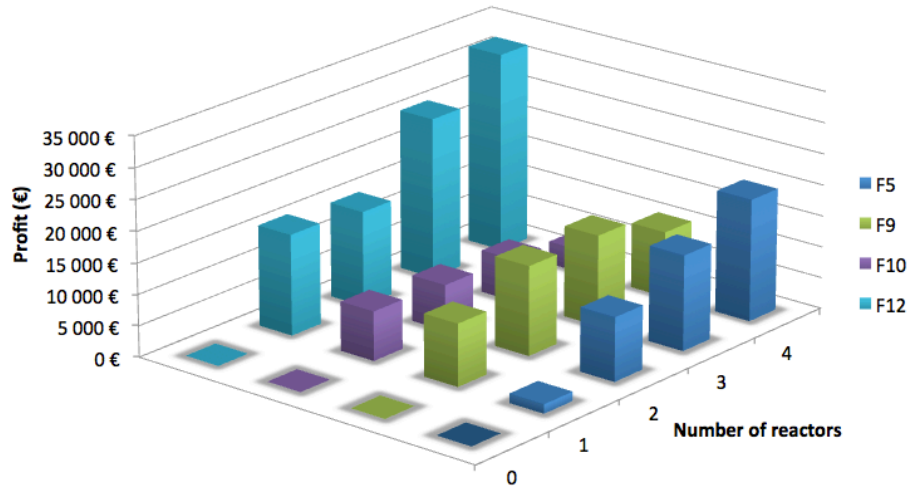

Figure 6.9. *Benefit from using shunt reactors on feeders 5, 9, 10 and 12, no load*

Feeder 14 was simulated separately from other feeders since it is a link cable between the substation and the switching station. The feeder is quite heavily loaded since it feeds the whole switching station. The loading and consequently the power losses were tried to reduce by placing centralized shunt reactors at the switching station. When the whole network was cabled, the reactive power flow towards the substation was varied between 2,5 MVAr and 3,5 MVAr in maximum and no loading

respectively. The surplus was tried to reduce by placing four sizes of shunt reactors at the switching station. Figure 6.10 presents the profit gained from the power losses with different reactor sizes. In the first case, the reactors were modeled as ideal inductances without any resistance. As can be expected, the benefit increases as the reactor size increases and the decrease is larger in the minimum loading.

Figure 6.11 presents the same situation when the power losses of the shunt reactors are taken into account according to the specifications in subsection 5.3.2. As can be seen, the reactors' own losses have a remarkable effect on the profitability. Only 178 kVAr and 3000 kVAr reactors are profitable on both minimum and maximum loading situations. The reason is the structure of the 3000 kVAr reactor since it is a low loss reactor, which is more expensive than normal 1000 kVAr and 2000 kVAr reactors. The price of the low loss reactor is approximately double to normal but according to these measurements, the low loss construction will pay itself back quickly.

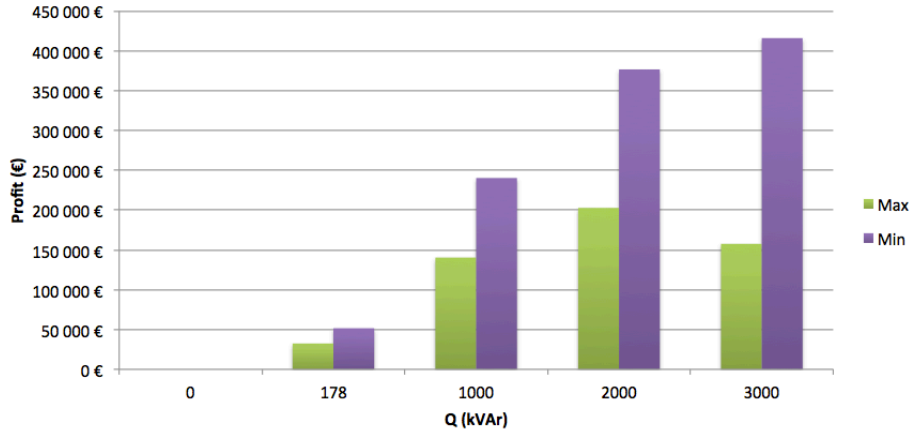

Figure 6.10. *Decreasing of power losses on feeder 14 with different reactors*

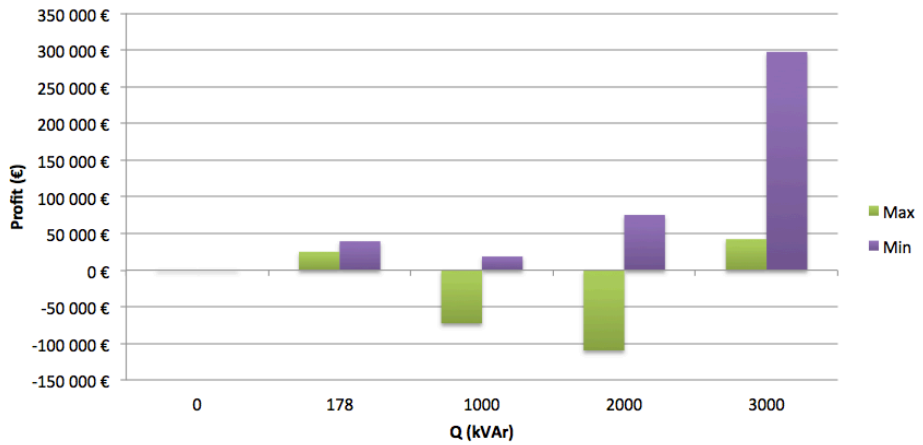

Figure 6.11. *Decreasing of power losses on feeder 14 with different reactors concerning reactors' losses*

6.1.4 Losses of the main transformer

In addition to power lines, the reactive power flow through the main transformer creates remarkable losses. As more cables are installed in the network, more power flows through the transformer continuously and the power losses of the main transformer will increase. It is possible to compensate the losses with both centralized and distributed shunt reactors by simply decreasing the amount of reactive power flow. The level of transformer's losses depends on the impedances and quality of the main transformer. It has to be concerned that distribution transformers are also inductances, which consume reactive power. However, the measurement was made only for the 16 MVA main transformer because the distribution transformers were considered as loads in Substation 1 model.

The power losses of the transformer were simulated with different capacitive loads behind the transformer. In this case, the capacitive load represents a certain amount of installed cables. The active power load was kept at constant 9,9 MW, which is approximate of the maximum loading of Substation 1. In the starting situation, the transformer had no capacitive load. Figure 6.12 presents how much the costs of power losses increase when capacitive load is added with 1 MVAr steps. Losses have been calculated again in a period of 20 years. From this figure, the savings of the reactors can be calculated by decreasing the Q with compensation capacity. For example, if the capacitive load was 10 MVAr, a 3 MVAr decreasing would save approximately 100 000 €.

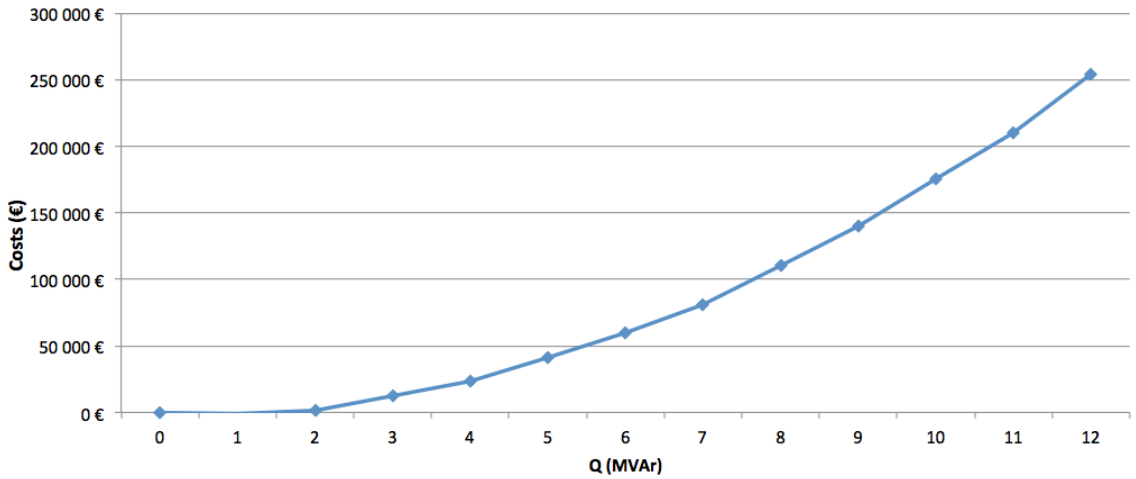

Figure 6.12. *Costs of increasing power losses in 16 MVA main transformer*

However, the decreasing of the capacitive load has to be made with shunt reactors, which have their own losses to consider. Figure 6.12 illustrates how much can be spent on the losses of a centralized shunt reactor in order to be profitable. Granted that all the excess reactive power is compensated with an adequate amount

of 178 kVAr, 1 MVAr, 2 MVAr reactors and their losses are taken into account. With this method, the real profit of decreased transformer losses can be calculated. Figure 6.13 presents the profit, which would be gained by using different reactors. Clearly, 3 MVAr shunt reactor is the only one, which is barely profitable from power losses perspective. The figure might look quite bad from reactors' perspective but it has to remember that this considers only the power losses of the main transformer. In some cases, it might be compulsory to compensate the reactive power flow anyway if the transformer is close to become overloaded by the reactive power flow. In this case, the main transformer would become overloaded after 12,6 MVAr.

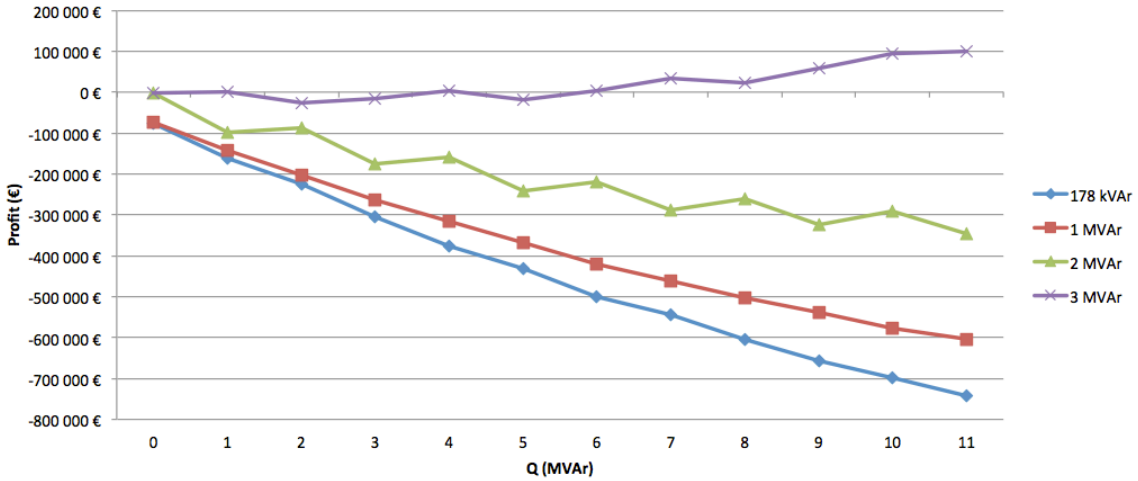

Figure 6.13. *Profit from compensating the power losses of the main transformer with different sizes of reactors*

6.2 Cables' loading capacity

The loading capacity of the cables was the second possible limiting technical factor, which can result from the increase of the reactive power. It is possible that the natural reactive power generation of the cable feeders limits the loading capacity of the cables. This is because the current in the cable is increased due to reactive power and therefore the bandwidth of the active power decreases. Since the reactive power accumulates along the line, the loading capacity decreases the most in the sending end of the feeder.

This was studied with the straight cable feeders by increasing the length of the feeders, which were on no load. The idea was to measure how much the loading capacity decreases due to reactive power flow. The reactive and active power flow were measured at the sending end of the feeder and the measured values were compared with the maximum loading capacity of the cables. The simulations were carried out for same three cable types, which were used in section 6.1. Figure 6.14 presents the available loading capacity of each cable type at the sending end of the feeder.

As the feeder length increases, the available loading capacity decreases at the sending end. This is natural since more reactive power is generated. However, the decreasing is relatively small and practically it is not possible to overload the cable due to the reactive power flow with normal feeder lengths. Practically, the values in the y-axis show how much active power could be fed to the feeder if the series inductance of the feeder is neglected and the load is assumed to be purely resistive. This would represent the worst case scenario. If the load was slightly inductive, more loading capacity would be available in the sending end since the cable generates the necessary reactive power for the load. Additionally, the simulation results would be the same even though the feeder would be branched instead of straight. This is because the reactive power generation does not depend on the shape of the feeder as was proven in subsection 6.1.1. In conclusion, the loading capacity will not be a problem with radial feeders.

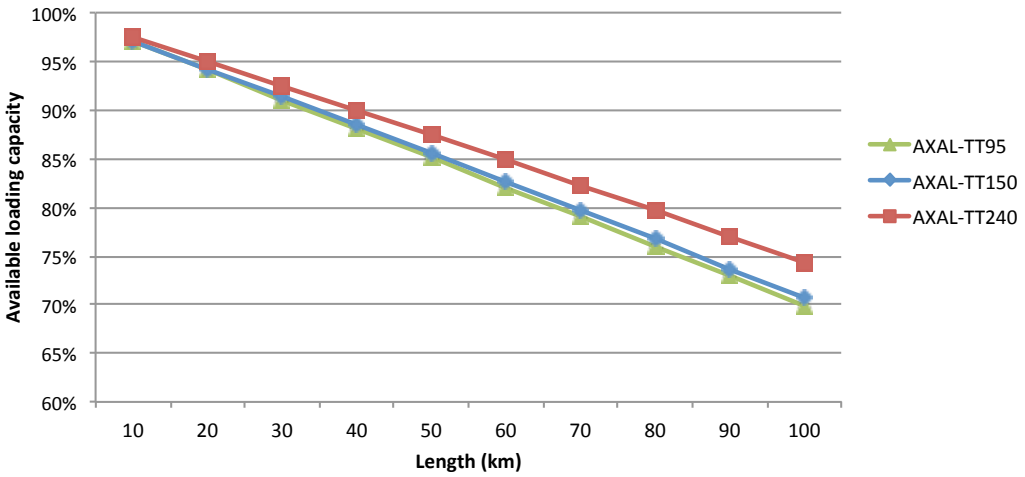

Figure 6.14. *Available loading capacity at the sending end with three cable types on no load*

It should be remembered that these simulations represent the situation with radial feeders. The cables between the substations and switching stations are a different case, which was considered in subsection 6.1.3. The overloading of the link cables can simply be avoided by compensating the reactive power at the switching station. Practically, the installation of the shunt reactor would always be sensible from the power losses point of view when the overloading of the cable is possible.

6.3 Voltage rise due to Ferranti-effect

Ferranti-effect was the third issue, which relates to the increase in reactive power. It was introduced as a phenomenon in subsection 2.2.2. Ferranti-effect has mainly been a concern with long transmission lines and cables in the high voltage network. The problem with the Ferranti-effect is the fact that it is usually not possible to

control with the on-load tap changer in the substation. If the voltage rise would be compensated by lowering the voltage at the bus, other feeders of the substation would suffer from it. Additionally, the voltage rise can not be seen from the substation and it might cause dangerous voltages to the customers.

Ferranti-effect was studied without loading with the same three cable types, which were introduced in section 6.1.2. At first, the simulations were made with pure cable feeders and the length of feeders was increased from 10 km to 100 km. The receiving end voltages are presented in figure 6.15. As can be seen, the voltage rise is quite small and it would be significant only with over 80 km cables. These kind of straight cables are naturally really rare and therefore the phenomenon could seldom become a practical problem.

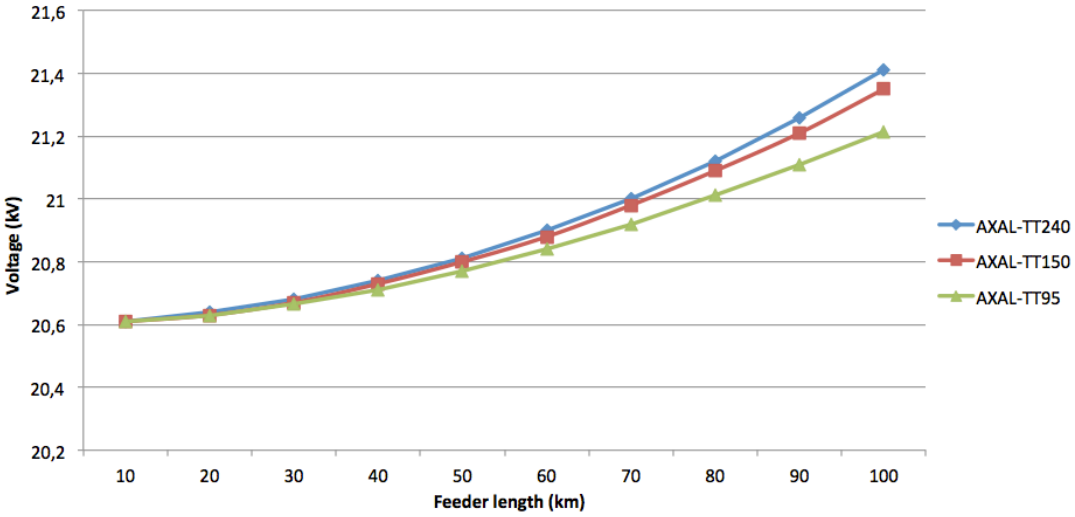

Figure 6.15. *Voltage rise with different feeder lengths on pure cable feeders*

Next, the voltage rise was simulated in a mixed network. As stated in 2.2.2, Ferranti-effect was at its highest when 1/3 from the beginning of the feeder was overhead line and 2/3 was cable according to (Elforsk 2006) and (Pekkala 2010). These kind of mixed feeders were also simulated in this thesis. Pigeon 99 overhead line was added to the beginning of the above feeders so that 1/3 of the feeder was overhead line. The receiving end voltages are drawn in figure 6.16. The addition of overhead line changes the situation slightly. The voltage rise becomes remarkable already after a 50 km lengths. In this kind of cases Ferranti-effect can become a problem. However, it has to be remembered that replacing overhead line with cables from the end of the feeder is not a good choice from the distribution reliability point of view. In most cases, the cabling would be started from the beginning of the feeder, which does not cause any problems. This is because the non-cabled overhead line part would have a large inductance compared to its capacitance and it would limit the voltage rise.

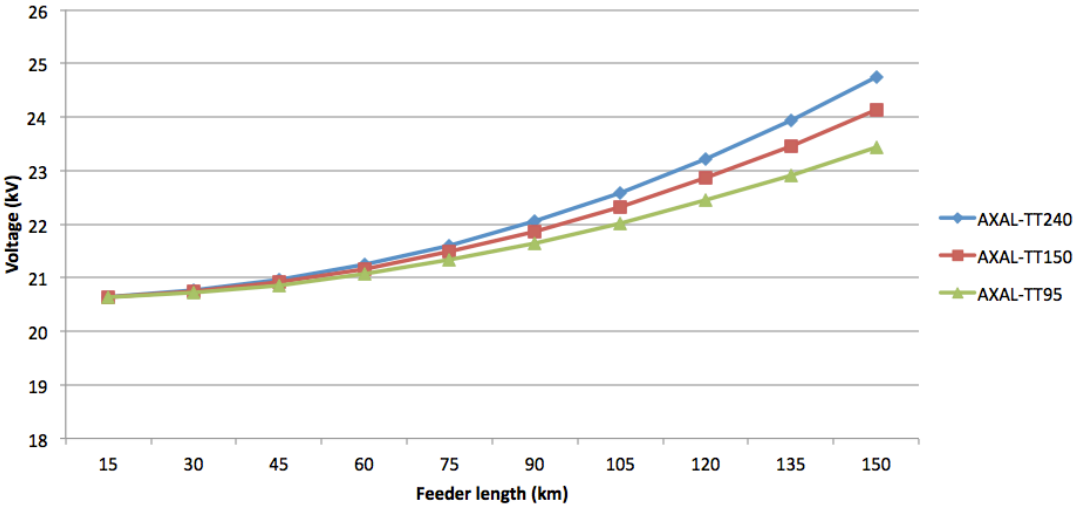

Figure 6.16. *Voltage rise with different feeder lengths on 2/3 cable feeders*

6.4 Fingrid's reactive power window

Fingrid's reactive power limit was the fourth important factor affecting on the compensation strategy of reactive power. As discussed in section 4.1, Fingrid has set an input and output limit for each connection point. The exceeding of these limits will result in extra costs to Fingrid's customers, like DSOs. Although the limits have been defined for each connection point, several connection points are observed together as one monitoring area, which has a common reactive power window. Since the exceeding of the reactive power window will bring costs, the reactive power generated by cables will also result in additional costs to the DSO if the reactive power is not controlled or compensated. The purpose of this section was to define how much the cabling increases the exceeding costs of the reactive power window. This was done by first defining the meaningful reactive power generation of the cables and using the result to calculate the costs from the window exceeding. At the end, an example calculations were made to Substation 1.

6.4.1 Estimation of cables' reactive power generation

Theoretically, the reactive power generation of the cables is close to constant as the voltage level of the distribution network substations is kept close to 20,6 kV. Granting that new cables are being installed in a substation network and they have a constant reactive power generation of Q_{gen}. The power and energy consumption of the connection point is measured hourly and they can be described with discrete functions $P(t)$ and $Q(t)$. As the reactive power generation of the cables can be assumed to be fairly constant over time, it will shift the measured reactive power at the substation and at the connection point with the amount of $\Delta Q = Q_{gen} - Q_{losses}$.

Therefore the new function of reactive power would be $Q(t) + \Delta Q$. The shift will result in every hour measurement comparatively to the original amount. Q_{gen} is easy to calculate from the capacitance values of the cables but Q_{losses} have to be defined with simulations. If Q_{losses} can be defined as the percentage, it would provide a tool for estimating how much the window exceeding costs will change when a number of cables are installed in the connection point area.

Q_{losses} was defined for Substation 1 with PSCAD-simulations. Original overhead lines were replaced with cables and all compensation devices were removed from the network. After each phase of cabling, the new reactive power was measured at the connection point, at the substation and at the bus. At the end of the cabling, the measured results were compared with the calculated reactive power generation values of the installed cables. The calculation of the nominal reactive power generation was done purely based on the capacitance value of installed cables. The simulations were done in both maximum loading and no load situations.

The reactive power difference between the starting situation and different phases of cabling is presented in figure 6.17. The same figure is drawn with percentage difference in figure 6.18. FG MAX and FG MIN represents the values at the connection point, 110 kV MAX and 110 kV MIN represent the values before the main transformer and 20 kV MAX and 20 kV MIN represent the values after the main transformer at the bus. The percentage figure has some steps and variation at the curves. The reason is the tap changer of the transformer, which was used manually when the bus voltage was differing over 0,2 kV from the nominal level. As the tap changer changes the voltage at the bus, also the reactive power generation changes according to the voltage level. Tap changes can be seen from the climbs of the curves.

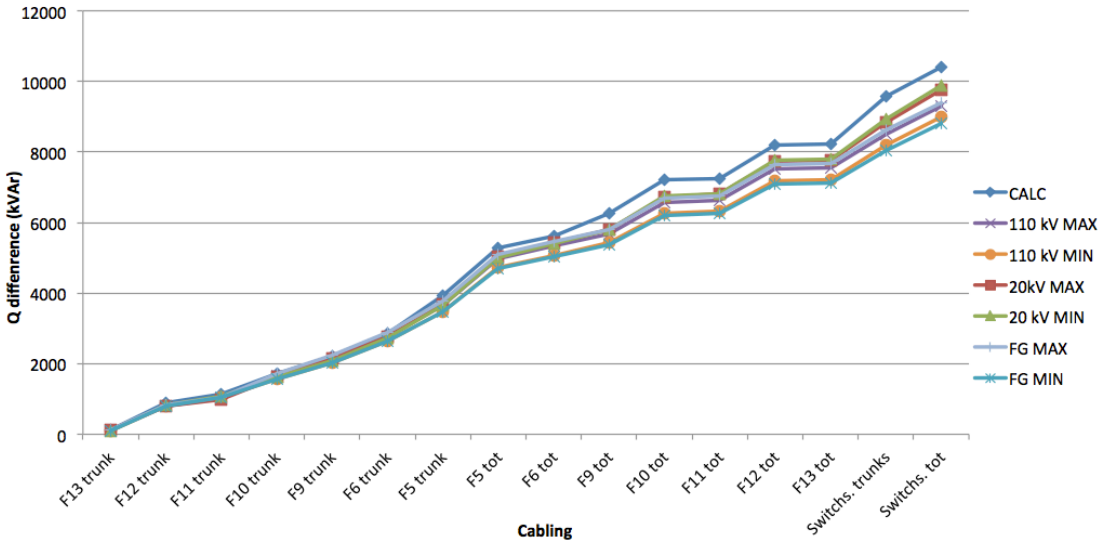

Figure 6.17. *Difference between the calculated and simulated values*

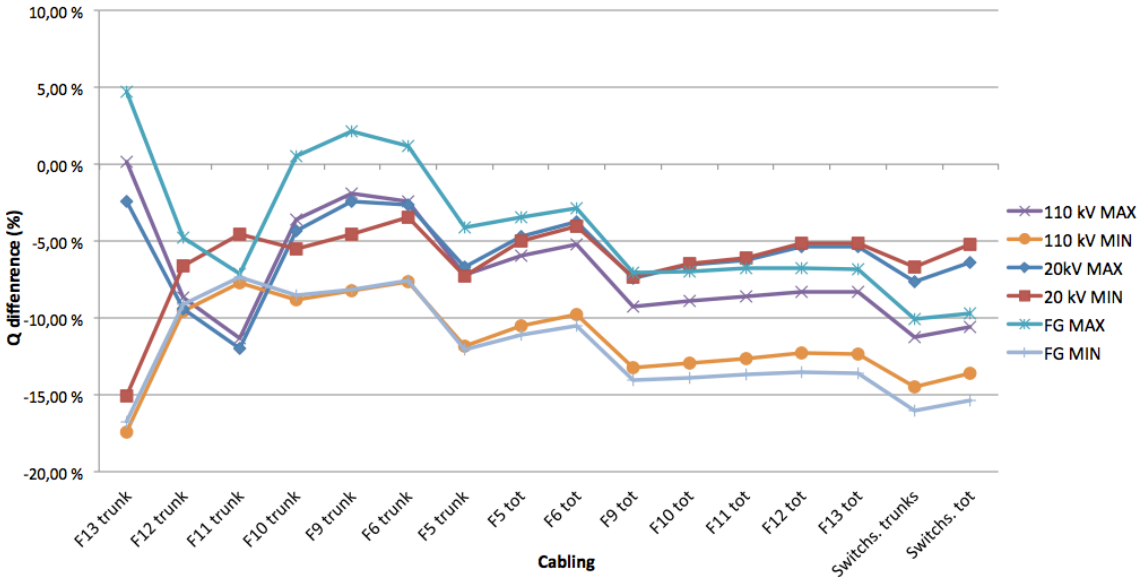

Figure 6.18. *Percentage difference between the calculated and simulated values*

It can be seen that the curves have quite a small difference after all. The influence of the 110 kV network is small and the biggest decreasing of reactive power comes from the main transformer. At the bus, the difference is approximately only 6 % from the calculated value. When the main transformer and 110 kV losses are taken into account, the percentage would increase to approximately 12 %. In this case, Q_{losses} would be equal to $0,12 \cdot Q_{gen}$. Therefore according to these simulations, 88 % of cables' nominal reactive power generation could be added to Fingrid's connection point measurement. Now it is possible to estimate how much the window exceeding costs will rise due to cabling of a certain amount. A more practical way is to convert the megavars to equivalent cable lengths, which have the equally reactive power generation. Table 6.3 presents the corresponding cable lengths if MVArs are converted to installed cable amounts with the 12 % decreasing.

Table 6.3. *Corresponding cable lengths of the added reactive power*

Q (MVAr)	AXAL-TT50 (km)	AXAL-TT95 (km)	AXAL-TT150 (km)	AXAL-TT240 (km)
1	41	35	29	24
2	83	69	57	49
3	124	104	86	73
4	165	139	115	98
5	206	174	143	122
6	248	208	172	147
7	289	243	201	171
8	330	278	230	196
9	371	313	258	220
10	413	347	287	244

6.4.2 Principle of estimating the exceeding costs

As stated in the previous subsection, cables can be regarded as an almost constant capacitive load at the network and their reactive power generation can be added to the measured reactive power. This addition is seen not only at the connection point but also in the measurement of the monitoring area. Practically this means that every hour reactive power measurement can be increased with the ΔQ. The graphical demonstration is presented in figure 6.19. The diagrams are examples of PQ-diagrams, which show the reactive power measurements from a certain time. The left hand vertical line is the input limit Q_{s1} and the right hand line is the output limit Q_s. If these lines are crossed, it will result in exceeding costs. The real diagrams consist of a number of dots, each of which describe a single hour measurement. In order to show the principle, the dots are replaced with areas in this example. The old measured points are drawn with a solid line and the new measurements with a dashed line after the cabling.

All dots will move with the amount of ΔQ regardless of the shape of the area when cables are installed in the connection point area. The increase speed of window exceeding costs depends highly on the monitoring area and the shape of the PQ-diagram. It can be seen that the costs increase with a different speed in each diagram depending on the shape. If the shape is a narrow ellipse, the costs increase slower and vice versa for a circle. It is important to notice that this is exactly correct only when all the other consumption is assumed to be exactly the same as before. Naturally this rarely happens but it gives a good estimate. The accuracy of the calculation can be specified if the history data is available from a longer period.

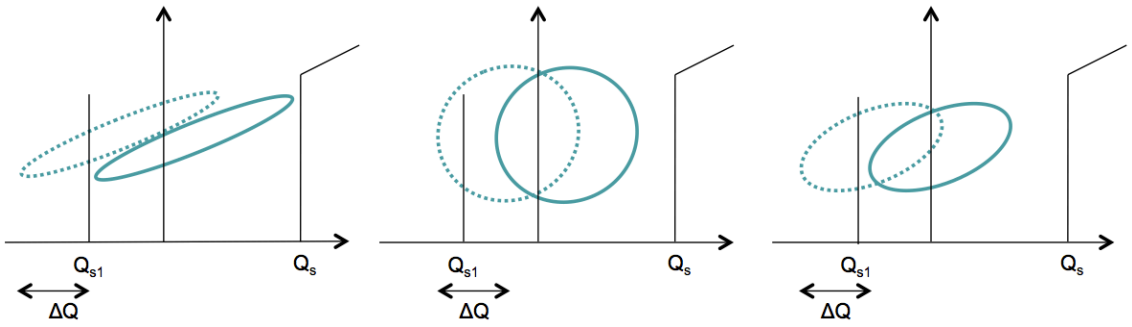

Figure 6.19. *Different shapes of PQ-diagrams*

However, the payer of the window exceeding fees is not always obvious. One monitoring area includes several connection points and usually they do not belong to the same customer. The measurement data of other customers is not available so their window exceeding fees or limits are not known by the others inside the same monitoring area. Only the total measurement data of the monitoring area is available for everyone in addition to every customer's own connection points'

data. Nevertheless, if the limit of the monitoring area is exceeded, the payer of the exceeding fee is always one who has exceed the limit of his own connection point.

The problem can be understood by example. Granting that Monitoring area 1 consists of Customer 1 and Customer 2. Figure 6.20 presents the PQ-diagram of both customers and the monitoring area. Customer 2 installs a significant amount of cable to the network, which is seen at his connection point and at the monitoring area measurements as an addition ΔQ to the reactive power. This will shift both areas with an amount of ΔQ. Customer 1 has already exceed his connection point limits but he has not paid anything before because the monitoring area has staid within limits. Now the cabling of Customer 1 will result in fees for Customer 1. Customer 2 does not have to pay anything for monitoring area exceeding until his own Qs1-limit has been reached. Also, it is possible that two or more connection points exceed their window limits at the same time and the fees are shared but it has not included in this study for simplicity. Instead, if reactive power is added to the appropriate connection point and it causes the monitoring area limit to exceed, all costs are assumed to fall on the owner of the appropriate connection point.

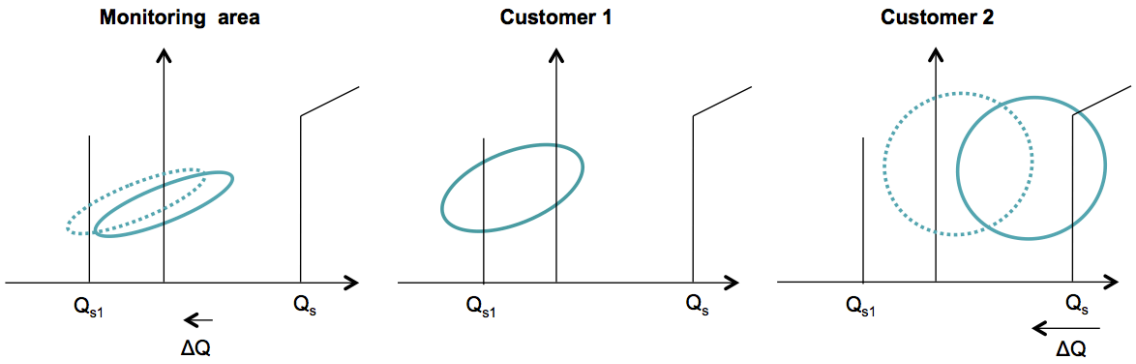

Figure 6.20. *PQ-diagrams of the example case*

6.4.3 Example calculation for Substation 1

Next, the goal was to estimate the reactive power window costs of Substation 1 when more cables are installed in the substation. The first task was to collect reactive power measurement history data from Fingrid's LTJ-Ekstranet, which is Fingrid's web-based measurement information service. The measurement data was collected regarding to the monitoring area and the connection point of Substation 1 from the past year. The PQ-diagram of the connection point is presented in figure 6.22 and the monitoring area in figure 6.21. The diagrams are drawn from the past year and every blue dot represent a single measurement hour. As can be seen, the monitoring area is inside the limits so there are no present exceeding costs even though the connection point has several dots over Qs-limit.

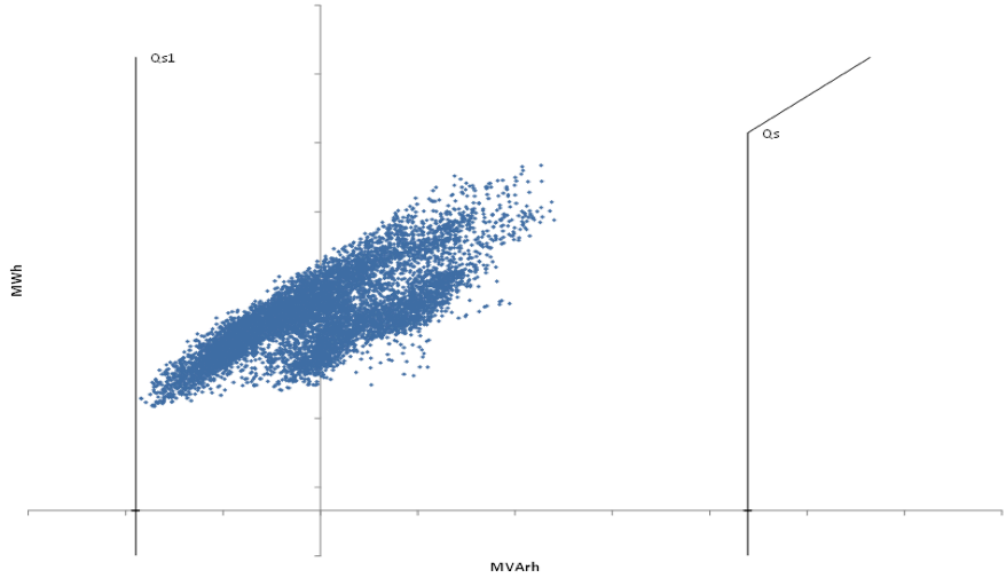

Figure 6.21. *Reactive power measurement from the monitoring area (Fingrid 2012)*

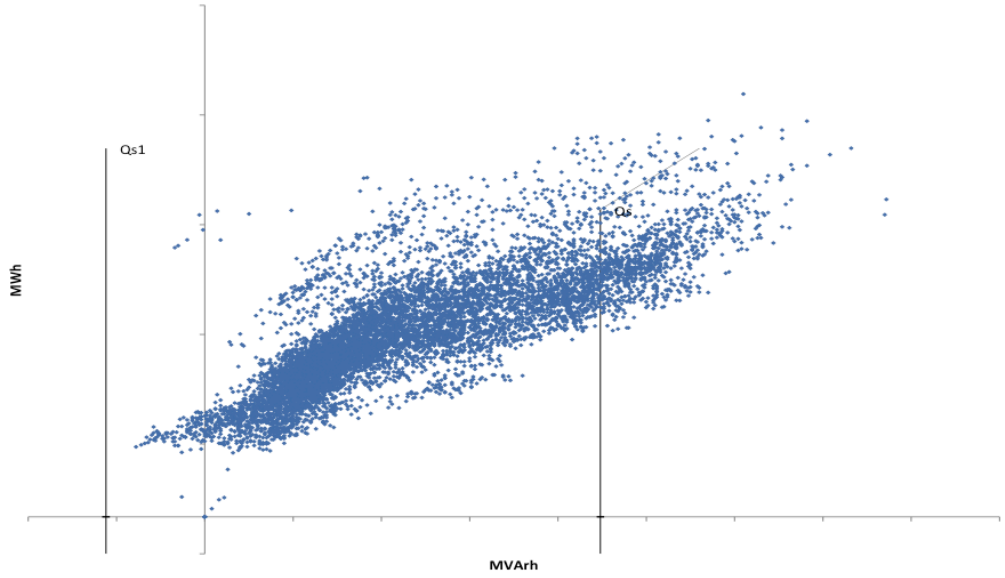

Figure 6.22. *Reactive power measurement from the connection point (Fingrid 2012)*

The amount of installed cable can be used to calculate the nominal reactive power generation Q_{calc} by multiplying it by 0,88. ΔQ is equal to the reactive power seen at the connection point and in the monitoring area. Figure 6.23 shows both of these values in each phase of the cabling. These reactive powers can be added to the connection point and monitoring area measurement. The corresponding exceeding fees of the monitoring area are calculated in figure 6.24. The numbers on the x-axis represent the reactive power addition to the original value and the costs are

calculated for one year. In this monitoring area, the costs will rise quite slowly. If the costs are wanted to calculate for a longer period, they could be multiplied with the equivalent number of years.

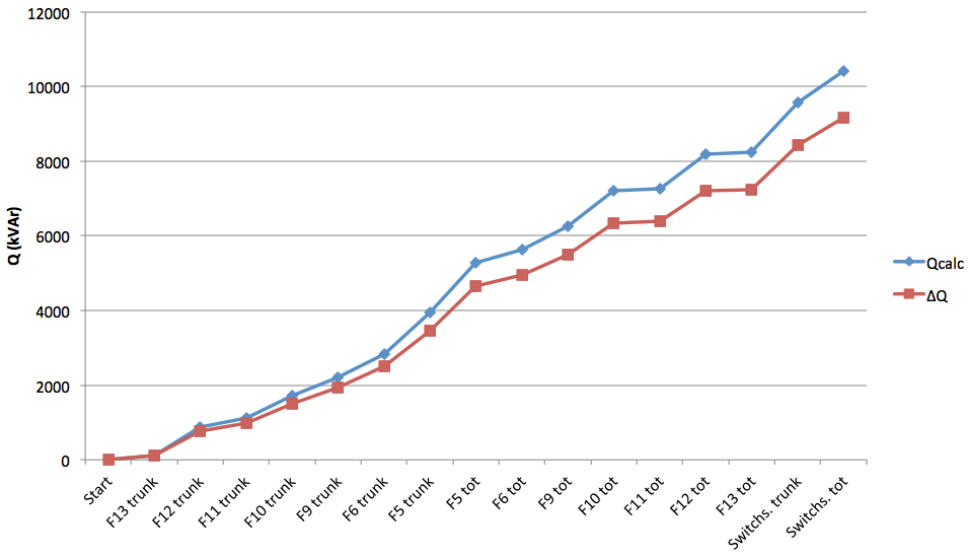

Figure 6.23. *Calculated reactive power generation and ΔQ in each phase of cabling*

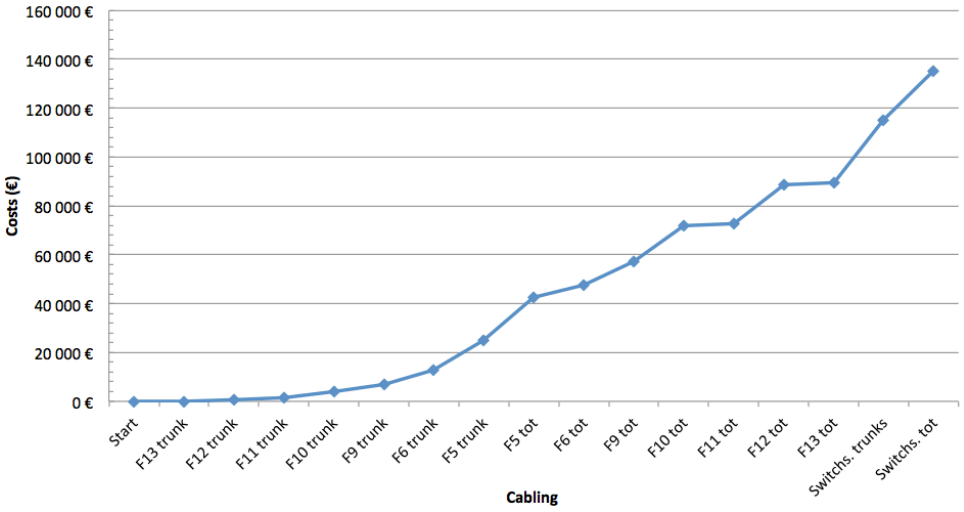

Figure 6.24. *Calculated costs for reactive power window exceeding per year*

It is evident that the excess of reactive power has to be compensated. Granted that the whole excess of the reactive power is compensated with either 178 kVAr, 1 MVAr, 2 MVAr or 3 MVAr shunt reactors. If the investment price and the power loss price of the necessary reactors are taken into account from 20 year period with each type of reactors and it is compared with the costs from the reactive power window, the total profit from the reactors can be calculated. Figure 6.25 represents how much profit the compensation of the whole reactive power makes with different

reactors in 20 years. The reactive power window costs are assumed to be constant at each cabling phase. In conclusion, all of the over 1 MVAr shunt reactors seem to be really profitable when the purpose is to stay inside the reactive power window. Also, this shows that the window exceeding costs are really significant part of the total costs and they are important to keep at a low level even with the cost of larger power losses.

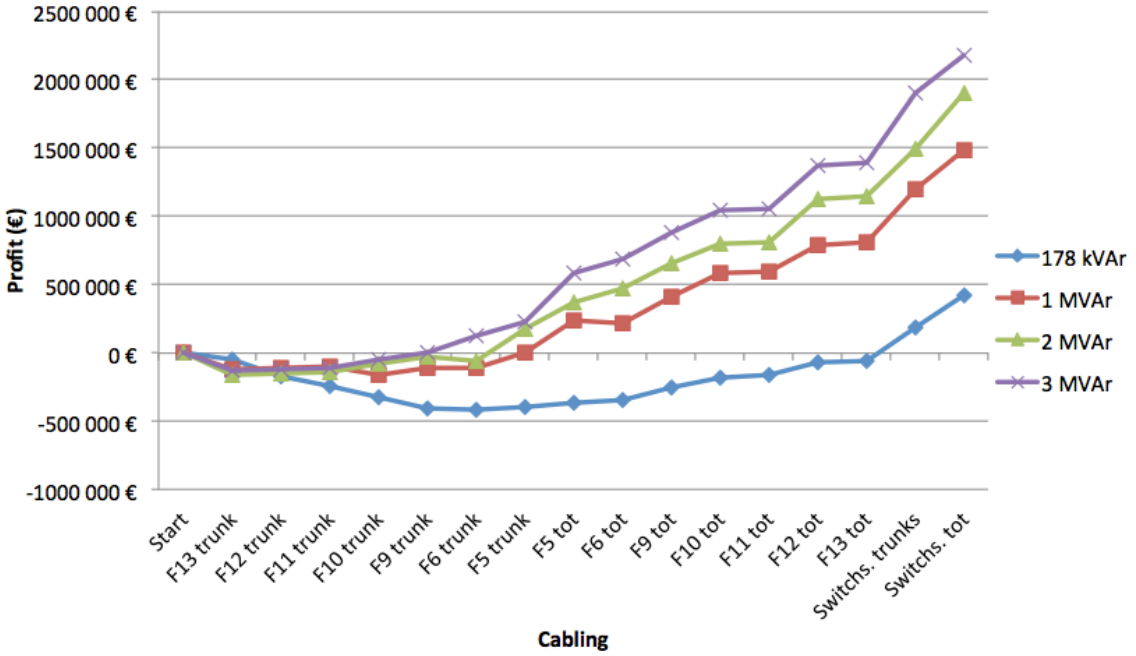

Figure 6.25. *Profit from compensating the reactive power flow to the main grid with different reactor sizes concerning the investment price and the loss price*

6.5 Earth fault current compensation in extensive cabled network

The compensation of the earth fault current was another issue related to extensive cabling, which was studied in this thesis. In this section, shunt reactors' behavior was simulated during an earth fault. Additionally, the behavior of earth fault current was studied in Substation 1 in totally cabled network and two alternative compensation solutions were created. In the last subsection, a discovered transient phenomenon regarding earth faults is presented and simulated.

6.5.1 Behavior of shunt reactors during earth faults

The behaviour of the shunt reactors was examined in detail during an earth fault since it is a fairly new device used for earth fault compensation in the medium voltage network. In the testing environment, 1 MVAr wye-connected shunt reactor

was connected to the bus, which had four 10 km feeders of AXAL-TT95 on no load. The specifications of the shunt reactor were introduced in subsection 5.3.2. The fault was a solid bus bar fault at phase c and it lasted from 0,2 s to 0,4 s. The following quantities were measured; I_a, I_b and I_c represent the phase currents of the reactor, I_0 represents the zero sequence current of the reactor, I_f represents the fault current and U_a, U_b and U_c represent the phase voltages. All measured quantities are RMS-values of 50 Hz wave.

Firstly, the neutral point of the shunt reactor was floating and therefore not grounded. Figure 6.26 presents the currents and voltages during the fault. In the current diagram, I_a, I_b and I_c stay at the level of 28 A during the whole simulation and zero sequence current I_0 stays at zero. This is the steady state current, which compensates the capacitive current in a normal situation. The fault current is approximately 104 A. Since the fault is solid, the phase voltage c drops to zero and other two phase voltages rise to the magnitude of line voltage.

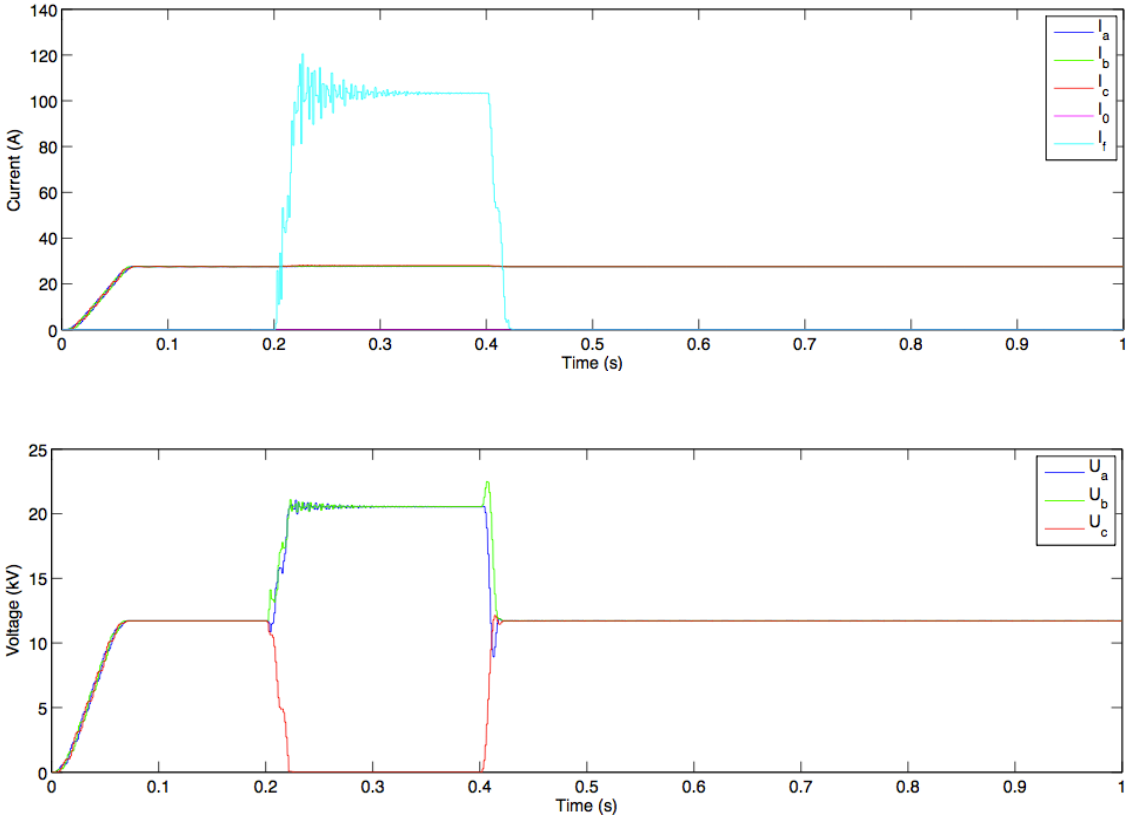

Figure 6.26. *Ungrounded 1 MVAr shunt reactor during a solid earth fault*

Next, the neutral point of the shunt reactor was grounded. Figure 6.27 represents the same current and voltage curves. When the fault occurs, the current in two healthy phases I_a and I_b rises to magnitude of 47 A and current I_c drops to zero. I_0, which is the earth fault compensation capacity, rises to a level of 84 A and the same drop of 84 A can also be seen in the fault current. Actually, 84 A is equal to the sum

of steady state currents and only the magnitudes and phase angles change between the phases. After the fault has ended, the currents and voltages start to resonate with the network, which is seen as a small variation in the curves. The damping speed of the currents depends on the zero sequence resistance, which is greater with larger resistance values.

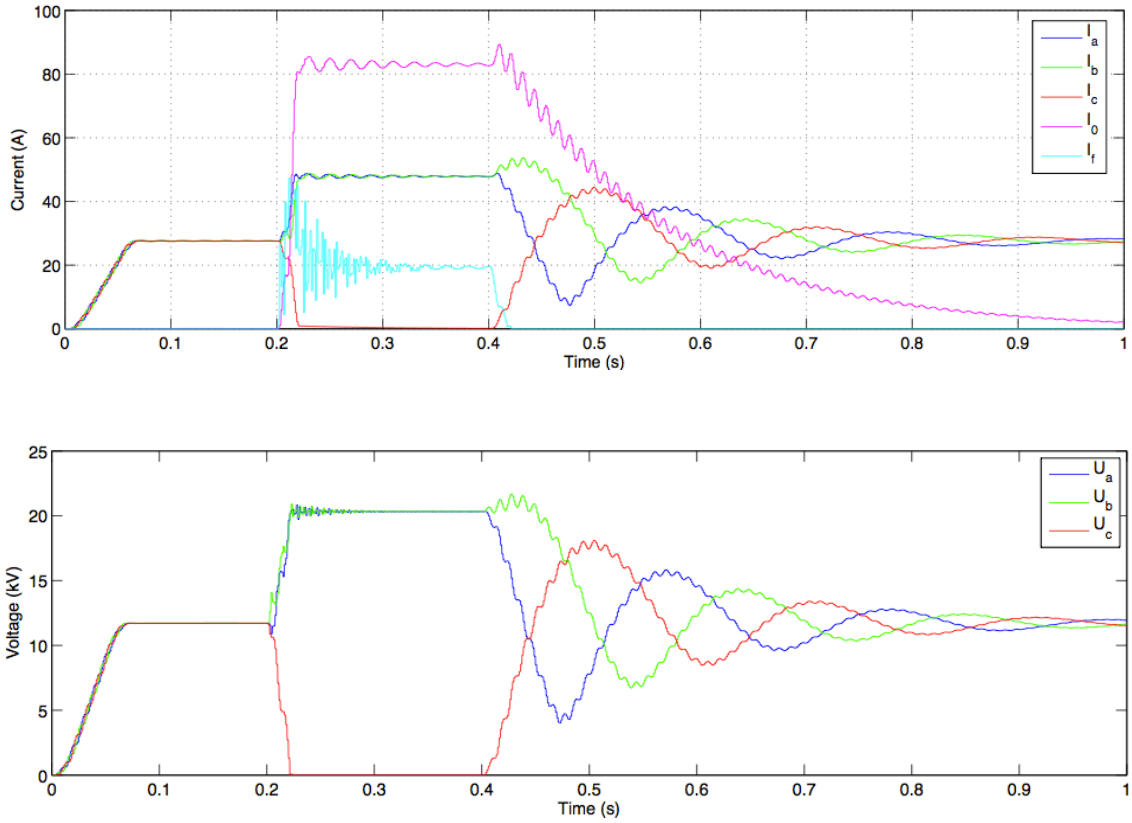

Figure 6.27. *Grounded 1 MVAr shunt reactor during a solid earth fault*

The same fault was simulated with a Petersén coil, which was tuned to 84 A. Voltage and current curves are presented in figure 6.28. Phase voltages U_a, U_b and U_c; zero sequence current I_0 and fault current I_f look almost identical to the grounded shunt reactor curves. However, phase currents are identical to each other unlike in a grounded shunt reactor. This is because there is a grounding transformer before the Petersén coil and the voltage displacement over the Petersén coil affects on every phase. In the grounded shunt reactor, each reactor is directly connected between the phase and ground and therefore the voltages are different over each coil.

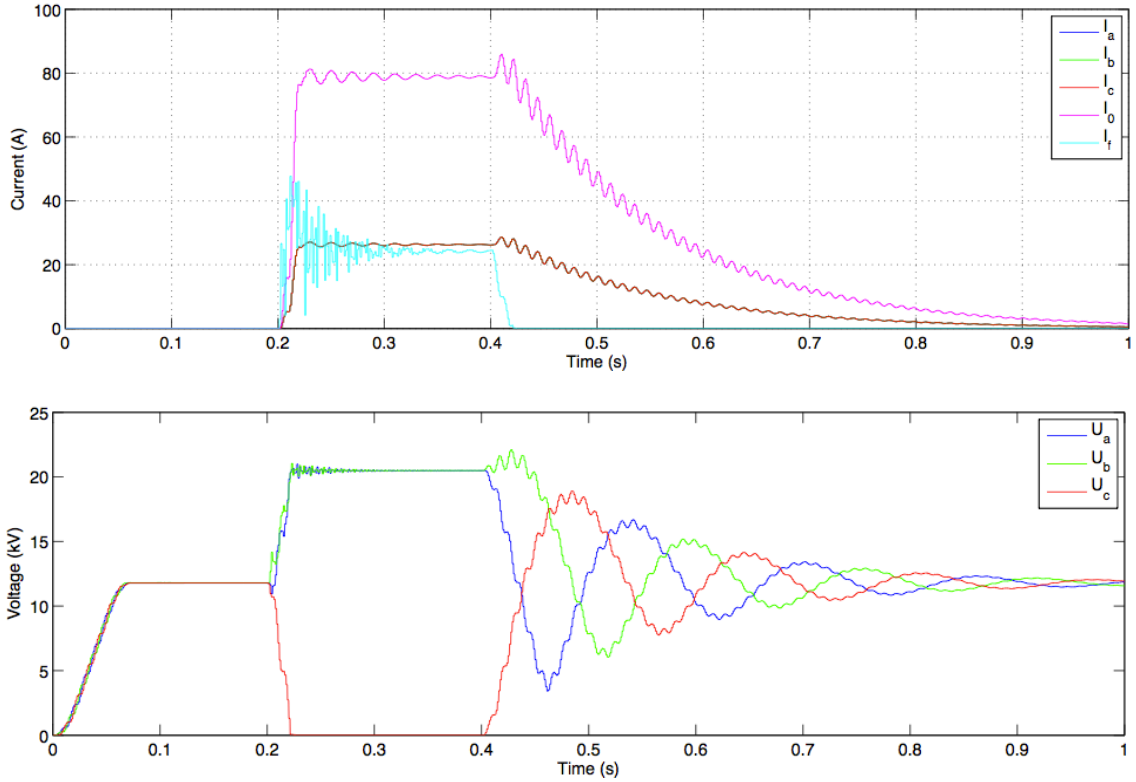

Figure 6.28. *84 A Petersén coil during a solid earth fault*

In conclusion, the grounding of the neutral point defines the participation of the shunt reactor to the earth fault compensation. As there is no technical requirement of grounding the neutral point, the grounding can be chosen freely (Fälldin 2012). This widens the use range of the shunt reactors and gives a possibility to ground when needed. For example, it would be possible to place a remote controlled disconnector to the neutral point. This would be possible since there is no current through the neutral line in the normal situation. It could provide extra compensation capacity for example in case of substation replacements. Another opportunity is to install the shunt reactor and leave the neutral point ungrounded if the earth fault current compensation capacity is not needed at the moment. If more cables are installed in the substation later, the neutral point can be grounded later to get extra earth fault compensation capacity.

The compensation capacities can be directly calculated from the inductance or the power of the shunt reactors. If the power of the shunt reactor is Q_s, the earth fault compensation capacity is

$$I_{comp} = 3 \cdot \frac{Q_s}{3 \cdot U_{ph}} = \frac{Q_s}{U_{ph}}, \tag{6.1}$$

in which I_{comp} is the earth fault compensation capacity and U_{ph} is the phase voltage.

6.5.2 Behavior of earth fault current in totally cabled network

The increase of the earth fault currents due to cabling was studied in Substation 1 by cabling the network in phases. The intention was to find the maximum earth fault current generation of the network and therefore the fault was carried out as a solid bus fault without any compensation devices at the network. The growth of the earth fault current in different cabling phases is presented in figure 6.29. The simulated earth fault current values were compared with the calculated values, which have also been drawn in the figure. The simulated values correspond the calculated values really well as can be expected. Figure 6.30 divides the earth fault current values to resistive and capacitive parts. As can be seen, the resistive part increases remarkably as more cables are installed. However, as the total current is the vector sum of the capacitive and the resistive part, the increase of the resistive current does not have a remarkable effect on the total current. Nevertheless, the resistive part becomes dominant if the fault current is tried to compensate with centralized Petersén coils and almost all of the capacitive current has been compensated.

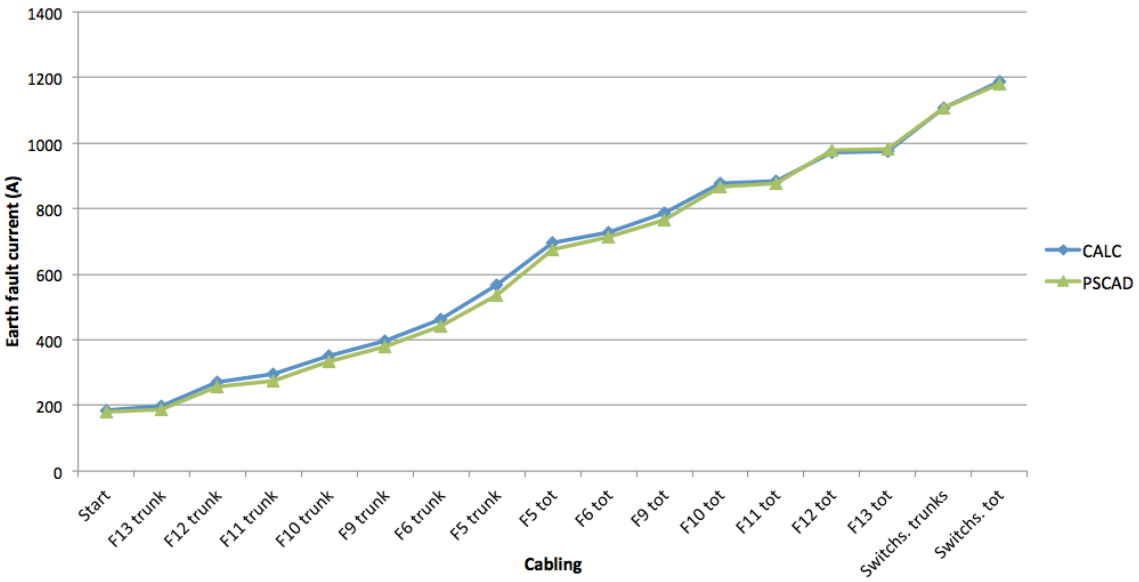

Figure 6.29. *Simulated and calculated maximum earth fault current in Substation 1*

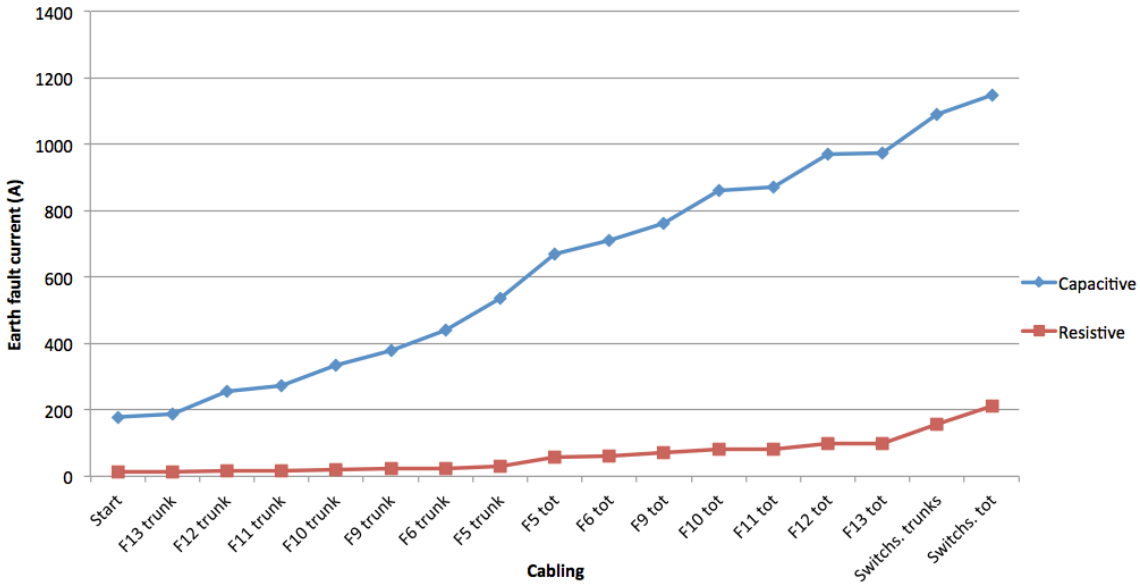

Figure 6.30. *Capacitive and resistive parts of the maximum earth fault current in Substation 1*

After the network was totally cabled, the behavior of the earth fault current was studied by varying the fault location with two fault resistances; 0 Ω and 500 Ω. In addition to the bus bar fault, faults were placed at the end of feeder 9, at the switching station and at the end of feeder FP6. Zero sequence voltage and zero sequence currents were measured from the beginning of each feeder in order to measure the quantities, which are seen by the protection relays. Additionally, zero sequence voltage and fault current were measured at the fault location. Figure 6.31 presents the resistive and capacitive parts of the fault currents from the measured fault locations whereas figure 6.32 shows the zero sequence voltages at the bus bar and at the fault location. It can be seen that the earth fault current is not constant in all fault locations unlike the conventional earth fault analysis suggests. Also, the zero sequence voltage drops to a very low value at the bus bar when the fault is located elsewhere than at the bus bar. If the voltages of 500 Ω fault are observed, the voltage displacement is barely seen in the bus. This could lead to a failure to detect the fault if the zero sequence displacement voltage is below the setting value. Both of these observations are consequences of the zero sequence resistance of the cables, which causes a voltage drop in the zero sequence system.

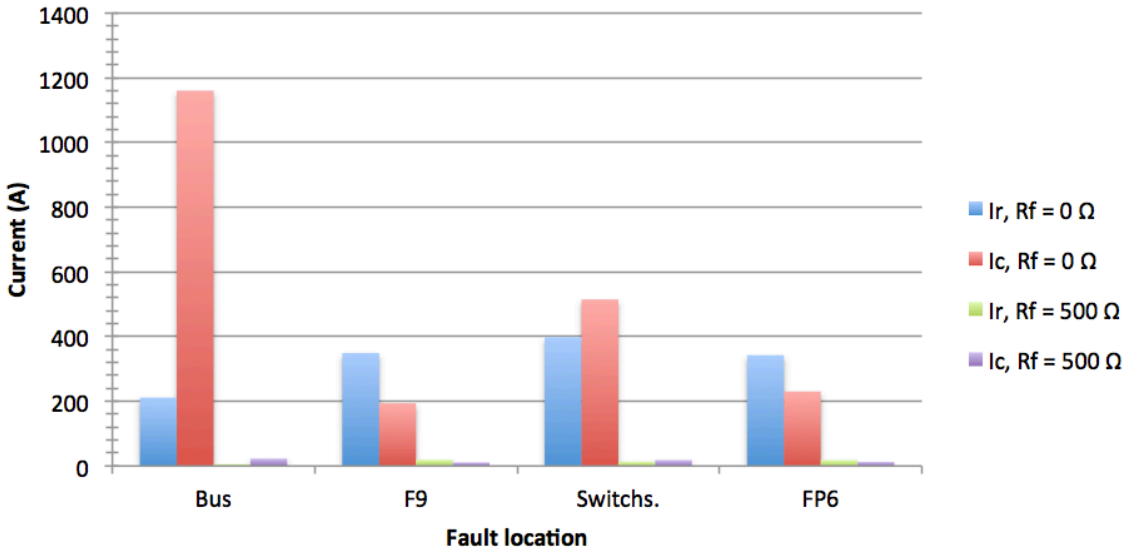

Figure 6.31. *Fault currents in non compensated network*

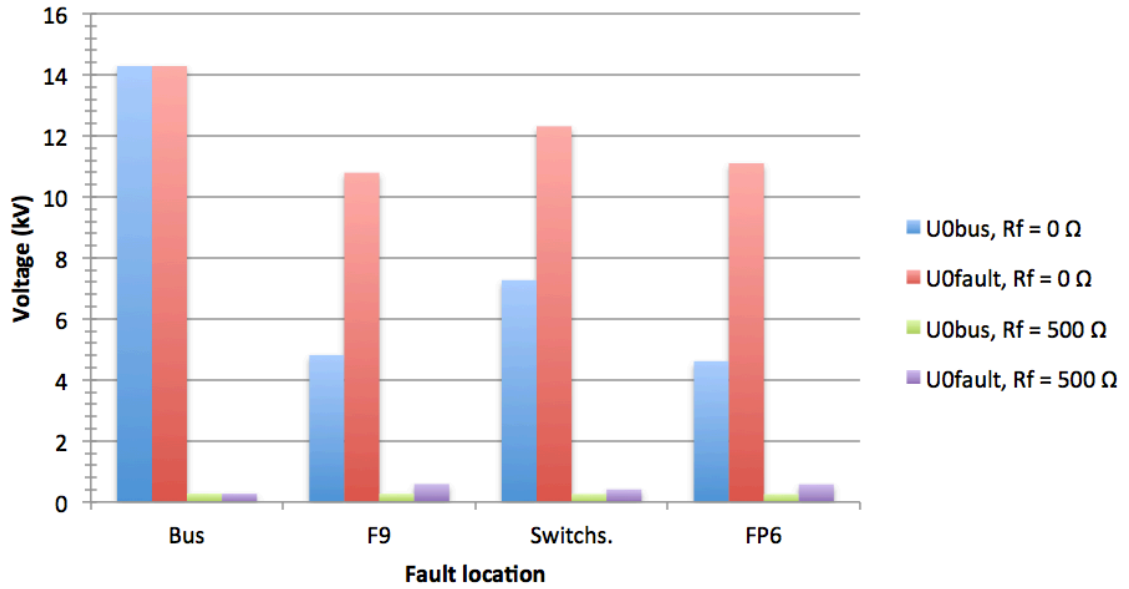

Figure 6.32. *Zero sequence voltages in non compensated network*

The generation of the earth fault current was examined in detail. The fault was decided to place in four parts of feeder 9 and the earth fault current generation of each feeder were measured. The results are presented in table 6.4. As can be seen, the fault current drops really significantly as the fault location is taken further to the feeder. This kind of phenomenon is familiar from short circuit currents, whose magnitude is dependent on the distance of the fault. The reason is probably the non negligible zero sequence series impedance of the cable, which affects on the fault current. When the fault occurs deeper in the network, the impedance seen from the other feeder increases and as a result, the fault current decreases as in the short

circuit calculations.

Table 6.4. *Zero sequence currents of Substation 1 feeders with different fault locations*

Distance (km)	I_f (A)	$I0_{F5}$ (A)	$I0_{F6}$ (A)	$I0_{F9}$ (A)	$I0_{F10}$ (A)	$I0_{F11}$ (A)	$I0_{F12}$ (A)	$I0_{F13}$ (A)	$I0_{F14}$ (A)
4,5	965,8	207,4	84,0	868,9	130,9	29,5	139,3	21,4	265,1
8,3	763,3	163,8	66,3	686,6	103,4	23,3	110,3	16,9	209,4
14,3	535,0	114,8	46,5	481,6	72,5	16,3	77,7	11,8	146,8
20,1	399,5	85,7	34,7	359,8	54,1	12,2	58,2	8,8	109,6

The behavior of the earth fault current was also measured in a more simplified network. The network was constructed from two AXAL-TT95 cable feeders; F1 and F2, which were 30 km 40 km long respectively. A single phase earth fault was placed to F1 every 10 km from the bus bar and the generation of earth fault current was measured at F2 in three different measurement locations every 10 km. The results are presented in table 6.5. As can be seen, the current at the fault locations drops by 10 A when the fault is further in the feeder. The same trend can be seen from the I_0 measurements. In order to give comparison results, the same measurement was made with Raven 63 line by keeping the line lengths the same. The results are presented in table 6.6. A slightly similar trend can also be seen with Raven but the phenomenon is barely noticeable and the fault current is independent on the location.

Table 6.5. *Earth fault measurements in the testing network with AXAL-TT95*

Distance (km)	I_f (A)	$I0_{F1}$ (A)	$I0_{F21}$ (A)	$I0_{F22}$ (A)	$I0_{F23}$ (A)
0	151,63	86,51	64,91	43,30	21,66
10	150,96	86,09	64,60	43,09	21,55
20	147,60	84,23	63,20	42,15	21,09
30	141,10	80,54	60,43	40,31	20,16

Table 6.6. *Earth fault measurements in the testing network with Raven 63*

Distance (km)	I_f (A)	$I0_{F1}$ (A)	$I0_{F21}$ (A)	$I0_{F22}$ (A)	$I0_{F23}$ (A)
0	2,75	2,75	1,37	0,69	4,81
10	2,76	2,76	1,38	0,69	4,82
20	2,77	2,76	1,38	0,69	4,83
30	2,78	2,77	1,39	0,69	4,85

6.5.3 Earth fault current compensation in Substation 1

The earth fault compensation to Substation 1 was implemented in two different ways; centralized compensation and a combination of centralized and distributed

compensation. Both of these options were implemented into the totally cabled network, which was simulated also in the previous section. At first, only centralized devices were used for earth fault compensation. As the maximum earth fault current generation of the network was 1180 A, it had to be divided into the switching station and into the substation. The feeders of the switching station generated around 245 A of earth fault current and feeder 14 generated 80 A. Therefore, 300 A Petersén coil was decided to place in the switching station and the rest of the fault current was compensated with 520 A Petersén coil, 3 MVAr shunt reactor and 1 MVAr shunt reactor, which were located at the substation. According to the equation (6.1), the compensation capacity of the 3 MVAr reactor is 252 A and the capacity of the 1 MVAr reactor is 84 A.

After the compensation devices were placed in the network, the same four faults were simulated with four locations and two resistances as was done in the previous section. Figures 6.34 and 6.33 present the fault current and zero sequence voltages with the centralized compensation. As can be expected, the capacitive fault currents drop significantly but also the resistive part of the current drops by 120 A. This happens because the one of the coils was placed at the switching station and it limits the growth of the resistive part in feeder 14. Nevertheless, there is still around 70 A of resistive earth fault current left, which comes from other feeders and can not be compensated centrally. However, the dependency on the fault location decreases and the total current is now close to constant in all fault locations. The uncompensated resistive part can also be seen in zero sequence voltages. There is approximately 1 kV difference between the bus bar and the fault location. This does not appear to be a problem with a 500 Ω fault resistance but it might be difficult to detect high resistance faults.

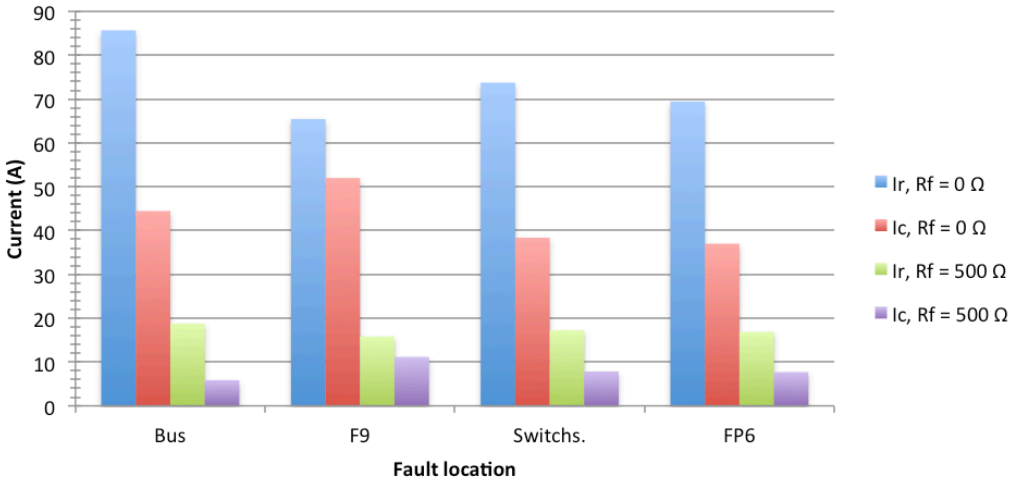

Figure 6.33. *Fault currents in the compensated network (centralized compensation)*

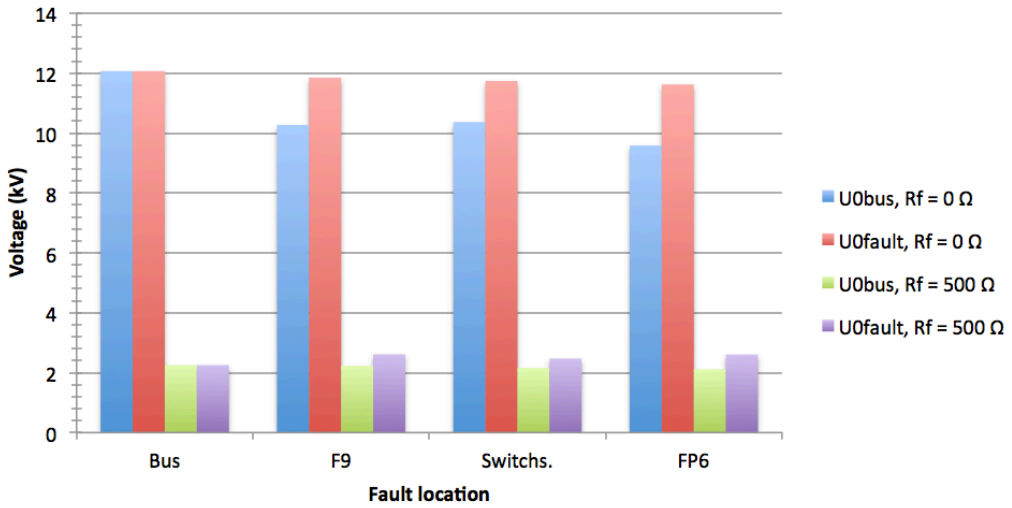

Figure 6.34. *Zero sequence voltages in the compensated network (centralized compensation)*

The second compensation solution was made as a combination of centralized and distributed compensation units. The solution was made by following the guidelines from Pekkala's M.Sc. thesis, where the appropriate limits of using centralized and distributed earth fault compensation were studied. According to the thesis, centralized compensation should compensate the lines 10 km from the substation and every next 5,7 - 6,7 km a distributed compensation unit should be placed. By following these limits, the resistive part of the earth fault current can be limited adequately and the feeders do not become overcompensated.

Firstly, all cables which are over 10 km from the substation were compensated with distributed Petersén coils. Totally 39 distributed 15 A Petersén coils were placed in the feeders, their distribution is presented in table 6.7. After the distributed Petersén coils had installed, the sizes of the centralized Petersén coils were defined by compensating the rest of the earth fault current and leaving 5 % to the resonance point. Eventually, a 2 MVAr shunt reactor with a 168 A earth fault compensation capacity was decided to put in the switching station and a combination of adjustable 180 A Petersén coil and 1 MVAr shunt reactor with a capacity of 84 A were put to the substation.

Table 6.7. *Installed distributed Petersén coils*

Feeder	F5	F6	F9	F10	F11	F12	F13	F14	FP5	FP6	FP7	FP8
Coils	10	4	5	6	0	7	0	3	2	0	1	1

The same simulations were made with 0 Ω and 500 Ω fault resistances in four different fault locations. Figure 6.35 and 6.36 present the new fault currents and zero voltages after the compensation implementation. Now the currents were limited

to a lower level and they are also fairly constant at all fault locations. The resistive current is around 16 A and the capacitive part is 33 A, which is quite the same as with only centralized coils. Zero sequence voltages are also almost similar at the bus bar and at the fault location, which also allows to detect the fault with higher fault resistances. Naturally, the solution is not the best possible one and it could be fine adjusted by changing to places of distributed coils to more suitable locations. However, this shows that the distributed compensation coils are extremely useful in the extensive cabled network.

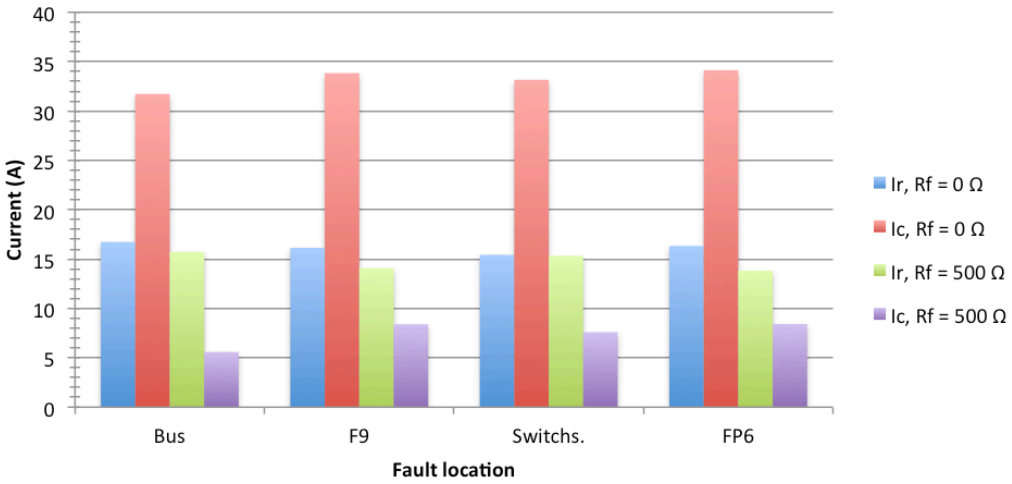

Figure 6.35. *Fault currents in the compensated network (centralized and distributed compensation)*

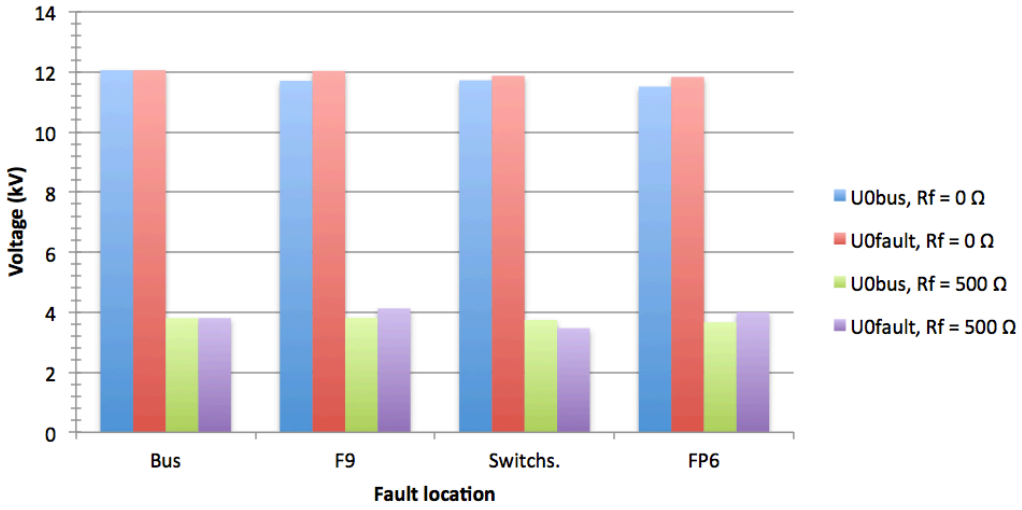

Figure 6.36. *Zero sequence voltages in the compensated network (centralized and distributed compensation)*

6.5.4 Transient phenomenon after an earth fault

The last earth fault issue was a transient phenomenon, which was recognized last year in Elenia. There had been unexplainable relay protection failures in one of Elenia's substation during earth faults. The substation had totally 6 feeders, of which one had approximately 6 km of cable and others consisted of mixed lines. There was no centralized compensation installed in the substation but the cable feeder had a distributed Petersén coil installed. When an earth fault occurred in a mixed feeder, the faulted feeder was correctly disconnected from the network by the breaker. However, also the feeder with a distributed Petersén was disconnected from the substation after the earth fault although there was no fault in it.

Since the phenomenon had happened several times, PQ-measurements were made on the location by Tampere University of Technology. The reason for the protection failures appeared to be the transient current in the zero sequence network, which was due to the capacitance change of the network. As the faulted feeder was disconnected from the substation, the distributed Petersén coil was connected to the line capacitances of the other feeders. As a result, damping resonance currents started to flow between the inductance and the capacitances. Since the phenomenon happened in the zero sequence, it increased the zero sequence current of the feeder with the distributed coil and the resulted current was adequate to exceed the current setting of the earth fault relay.

The zero sequence current and zero sequence voltage measurements are presented in figures 6.37 and 6.38. The measurements were made for four feeders. Feeder 8 is the one with the distributed Petersén coil, the earth fault happened in feeder 18 and the other two feeders are healthy. The phases of the phenomenon are marked to the figures with red lines and boxes. When the first FRO starts, the actual fault is disconnected from the network and the healthy feeders should remain in the normal state. However, I_0 starts to resonate in feeder 8 with feeder 10 and feeder 14 so that $I0_{F8} = I0_{F10} + I0_{F14}$. The magnitude of the current is still approximately 10 A after 0,5 s, which is the relay setting of Feeder 8. As a result, feeder 8 is disconnected from the bus by the false triggering. Another important thing is the change of the frequency as the resonating starts. As the feeder is under compensated, the frequency of the wave is below 50 Hz. If the feeder had been over compensated, the frequency would have been over 50 Hz.

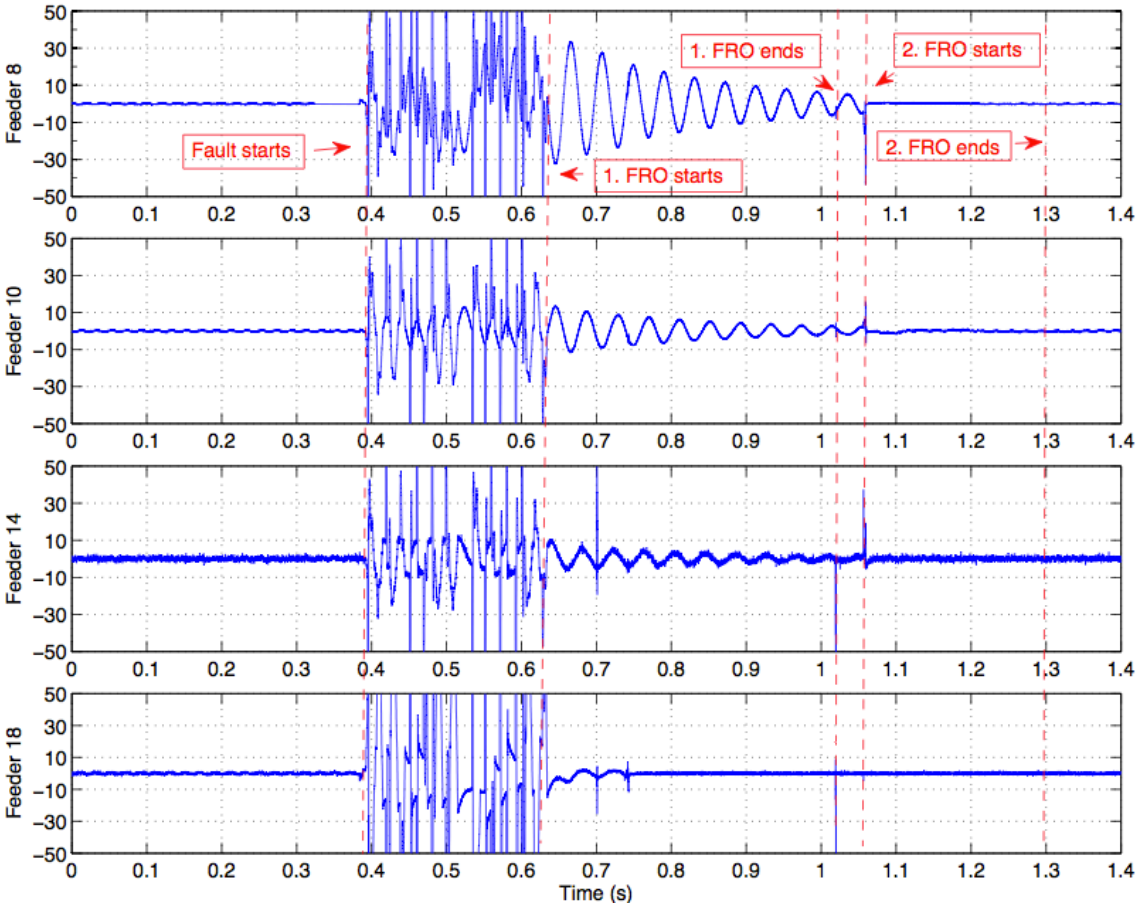

Figure 6.37. *Measured zero sequence currents (DEEE 2012)*

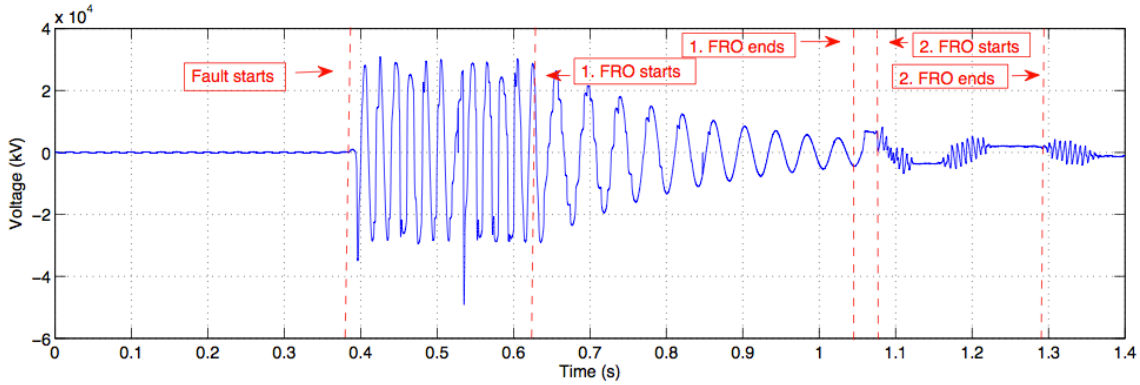

Figure 6.38. *Measured zero sequence voltage (DEEE 2012)*

The same situation was simulated in the PSCAD-environment. Since the phenomenon was not the main focus of the thesis, the PSCAD model was constructed as simplified. Figure 6.39 and 6.40 presents the same zero sequence currents and zero sequence voltage as in the measurements. Simulation results do not correspond exactly the measurements but the same phenomenon can be seen from the figures. The feeder with the distributed Petersén coils starts to resonate with other two feeders and the resonating can also be seen in the zero sequence voltage.

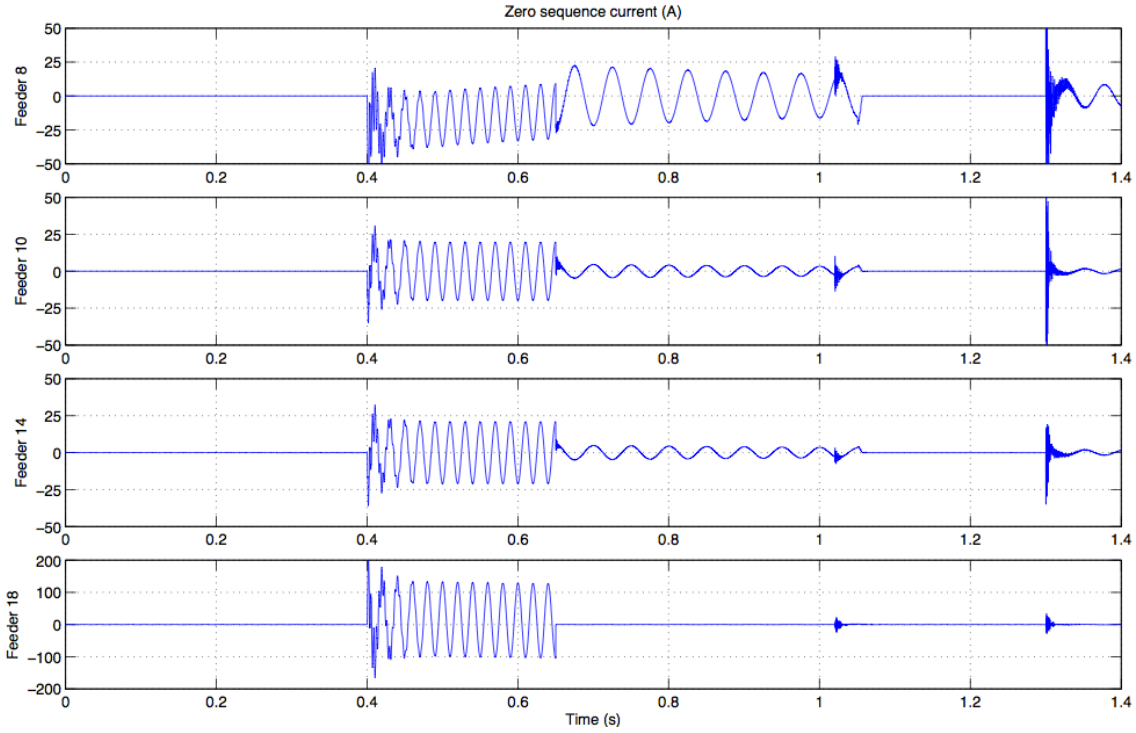

Figure 6.39. *Simulated zero sequence currents*

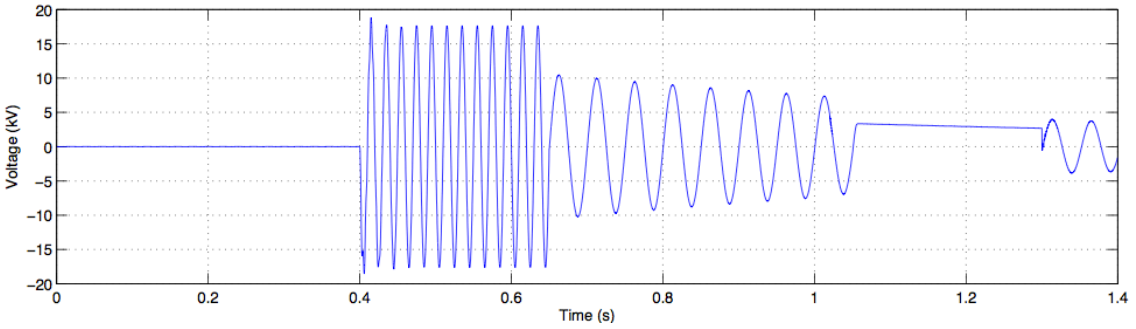

Figure 6.40. *Simulated zero sequence voltage*

One way to decrease the affects of the phenomenon is to add resistance to the network. This was accomplished by adding a centralized Petersén coil to the network with a compensation capacity of 70 A in addition to the distributed Petersén coil. Firstly, a 5 A parallel resistance was connected in parallel with the centralized coil. Figure 6.41 presents the zero sequence current of feeder 8 and the zero sequence voltage of the bus. It can be seen that the wave damps quicker. The resonating is much smaller and in practice it would not cause a false triggering. If a 15 A parallel resistance would be connected, the damping is even quicker. Figure 6.42 presents the corresponding curves. In this case, there would be not problems caused by the transient current.

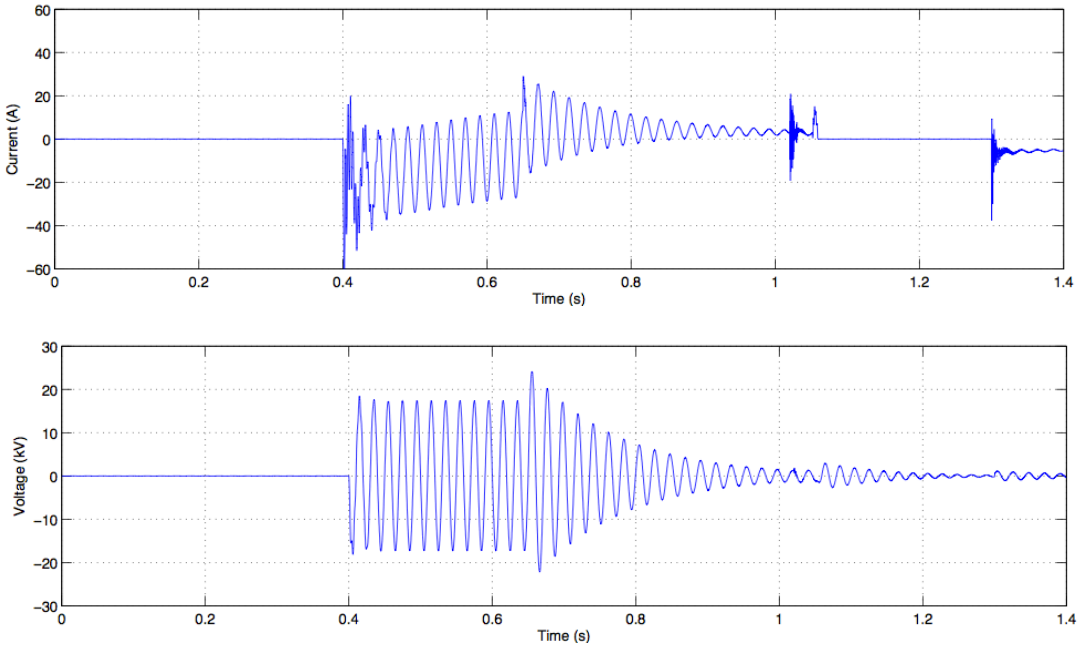

Figure 6.41. *Simulated zero sequence current and zero sequence voltage in feeder 8 with centralized compensation and a 5 A parallel resistance*

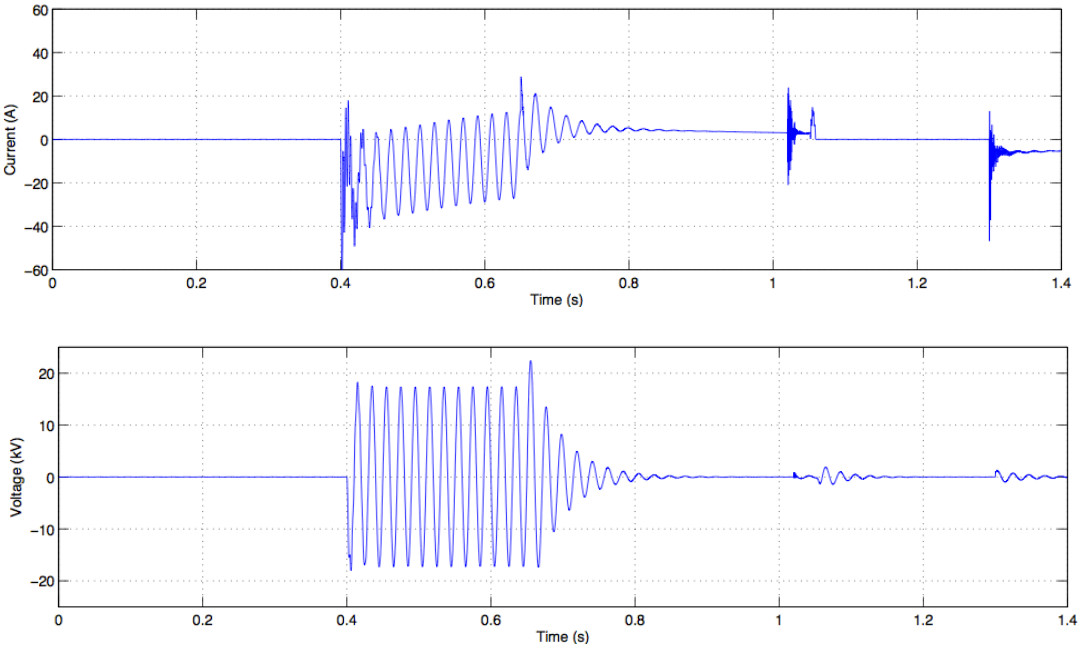

Figure 6.42. *Simulated zero sequence current and zero sequence voltage in feeder 8 with centralized compensation and a 15 A parallel resistance*

In conclusion, it can be said that the transient phenomenon can be limited by adding resistance. Although the measurements and simulations results did not match perfectly, the same phenomenon could also be seen in the simulations. An easy way to avoid the resonance in the zero sequence network is to use the centralized Petersén coil to compensate the first kilometers from the substation. On the other

hand, the usage of parallel resistance would also damp the transient phenomenon of distributed Petersén coils if it is necessary to use them.

6.6 Optimal compensation strategy

In the introduction of chapter 5 several questions were asked regarding extensive cabling. The purpose of this section is to conclude all sections of the result chapter and answer the questions based on the acquired information. Several different compensation devices have been studied in this thesis and a good base for the answers is a price table of them, which is presented in table 6.8.

Table 6.8. *Summary of prices and compensation capacities of different compensation devices*

Device	Q (kVAr)	I_{comp} (A)	€/MVAr	€/A	Price (€)
Distr. Shunt reactor	178	15	169	2005	30 000
Centr. Shunt reactor	1000	84	51	607	51 000
Centr. Shunt reactor	2000	168	32	363	61 000
Centr. Shunt reactor	3000	252	31	373	94 000
Distr. Petersén coil	-	15	-	667	10 000
Centr. Petersén coil	-	140	-	1216	170 000
Centr. Petersén coil	-	250	-	743	186 000

Firstly, it was studied whether it is profitable to use distributed shunt reactors for the reactive power compensation or should it be done centrally. As the distributed shunt reactors can also be used in earth fault compensation as well, their prices were compared with distributed Petersén coils. As stated, the number of needed distributed compensation units to earth fault compensation can be assumed to be constant for decreasing the resistive component by an adequate amount. Therefore, if the price of the needed distributed Petersén coils is assumed to be $x\cdot$ 10 000 €, the price of the equal number of distributed shunt reactors is $x\cdot$ 30 000 €. Therefore, shunt reactors should bring extra benefit at least with an amount of $x\cdot$ 20 000 € in order to be profitable.

As proven in subsection 6.1.3, the economic benefit from the decreased power losses is not remarkable in a branched network. According to the simulations in the case network, the first installed shunt reactor has the largest benefit and the benefit gets smaller when more shunt reactors are installed in the single feeder. The maximum benefit of the first reactor was 10 000 €, which was accomplished by placing one reactor in the latter part of feeder 12 in the totally cabled network. The benefit in other feeders was under 5000 €.

Distributed shunt reactors were also simulated with straight feeders. In this case, shunt reactors can be profitable if they are placed correctly. An optimal placement

for distributed shunt reactors would be at the latter part of over 50 km straight cables, which are low loaded and they have a relatively high power factor. As the length of the feeder gets longer, the economic benefit gets larger. At the same time, Ferranti-effect might become a problem especially if the length of the feeder is close to 80 km. Also, the overloading of the cables was proven not to be a problem due to reactive power flow. Therefore, distributed shunt reactors can be recommended to use in especially long feeders. However, over 50 km straight cables are quite rare and therefore distributed Petersén coils should be used in most situations for earth fault current compensation.

This means that reactive power compensation should mostly be carried out by using centralized shunt reactors. A lot of attention should be paid on the losses of centralized shunt reactors and low loss reactors should be favored. Low loss coils can be profitably used to decrease the power losses of the main transformer and high loaded link cables between a substation and a switching station, for example. However, as was shown in subsection 6.4.3, the costs from Fingrid's window limit exceeding are much more significant compared with the power losses. If the input limit of the reactive power window is crossed, it can result in over 120 000 € costs per year. According to the simulations, all examined 1-3 MVAr reactors saved a lot of money as they limited the exceeding costs when the cabling degree increased. Both investment price and the loss price were considered in the calculation. A straight consequence from the need of shunt reactors is the decreasing need of shunt capacitors. As the cabling increases, many of the capacitors in the substations will become relatively useless especially in low loaded rural areas.

Since the reactive power window exceeding is the major defining factor of using shunt reactors, also the placements of the reactors have to be chosen according to it. When single cabling projects are accomplished, the decision about the reactive power compensation can not only be made based on a single project. Instead, the cabling projects inside a monitoring area should be observed as an entity in order to know if there is a need of investing to shunt reactors. However, it is important to notice that this study has been made with the current reactive power window exceeding prices, which are possible to change in the future.

Shunt reactors should naturally be placed in potential cabling locations, where it is likely to install more cables in the future. In principle the location of the shunt reactors is indifferent from the window limits perspective as long as it is located inside the same monitoring area. The only real requirement is that the compensation should be made on the medium voltage side. Otherwise the main transformer would age faster and even the loading capacity of the transformer can become a problem at some locations. Therefore, €/MVAr price defines the cheapest option for the preferred compensation device from the window perspective. From

this point of view, centralized shunt reactors would be an easy choice.

Centralized earth fault compensation can be implemented as a combination of centralized shunt reactors and centralized adjustable Petersén coils. As proven in subsection 6.5.1, shunt reactors can be used for earth fault current compensation. The grounding of the neutral point of shunt reactors define their behavior during an earth fault. If the neutral point is ungrounded, shunt reactors do not participate in the fault compensation. If the neutral point is grounded, shunt reactors participate in the earth fault current compensation. The compensation capacity of shunt reactors is practically constant since it can be calculated straight from the inductance value. Therefore, the shunt reactor works in the same way as a fixed Petersén coil during an earth fault. If desired, the neutral point of the shunt reactor can also be left ungrounded and ground later since there are no technical barriers of leaving the neutral point ungrounded. One option would be to place a remotely connected disconnector between the neutral point and ground, which could provide extra earth fault compensation capacity if needed. Another good possibility is to purchase a large shunt reactor, which is off line adjustable. This enables increasing the reactive power and earth fault current compensation capacity as more cables are installed in the same substation.

However, it is really important to first have an adjustable Petersén coil in the substation before grounding shunt reactors. Petersén coils adjust their inductance according to the connection situation and keep the correct compensation degree. This is vital for the correct function of protection relays, which have been set for an under compensated network. If the compensation degree of the network crosses 100 %, it can result in non-selective relay operations. For example, if a substation would only have a fixed centralized compensation coil and the topology of the network changes so that a part of the network is moved behind another substation, the earth fault current generation of the network decreases. In this case, a fixed coil could cause the network to become over compensated. As a result, the relays of the feeders would not recognize to an earth fault and the neutral point voltage relay would disconnect the whole substation when an earth fault occurs.

6.7 Evaluation of results and tools

This section presents possible sources of inaccuracies, which should be noticed when the results are inspected. The first issue is the cost calculation and the prices of compensation devices. One should consider that the prices of the devices are estimates and they can differ between different manufacturers. Also, the power loss calculations include a lot of assumptions. It is possible that the price of the electricity will change remarkably or the interest rate changes. Additionally, the power losses due to reactive power flow were assumed to accumulate from the whole

year by assuming the peak usage time to be 8760 h and loading increase rate to zero. In fact, the situation is not that simple because the loading will increase in time. However, it would be have been difficult to concern the surge impedance loading of the cables. If a cable operates under its surge impedance loading, it is possible that the increase in the loading actually decreases the losses because the cable operates closer in its surge impedance loading.

When the exceeding costs of the reactive power window are evaluated, a few things should be considered. Firstly, the history data from the measurements should be collected from a long period of time in order to get valid information. In this thesis, history data was collected from one-year period of time but the accuracy would increase if the average value was used from several years. However, Fingrid has just renewed its reactive power control method so not much history data is available yet. Furthermore, it is harsh to assume that all other consumption would be constant in the monitoring area. Again, history data would provide a more accurate guess if it was available. Fingrid is also justified to change the exceeding fees, which would influence the results.

The modeling of loading is also an issue to discuss. The modeling of the loading was based on the combination of AMR-measurements and index series since AMR-meters provide only active power measurement information. Therefore, the reactive power was calculated based on the index series of different customer groups and the actual $\cos\phi$ is not exactly known. However, it was assumed that the index series will provide a sufficient accuracy in the scope of this thesis. Additionally, the loading of each feeder was assumed to be distributed evenly to the distribution transformers according to their nominal power, which was regarded to provide adequate accuracy.

The earth fault behavior of the cables can also not be known exactly. The zero sequence impedance of the cables is calculated with an estimation formula and no real measurements have been made in the field. Therefore, the actual amplitude of resistive and capacitive parts is not known. However, the results from this thesis are similar to earlier studies related to the same subject.

The main tool used in this thesis was the PSCAD-simulation program, which is mainly intended to use for simulating fast transient phenomenon in power networks. Additionally, Tekla NIS network information system was used as a supportive program for creating the PSCAD-models. From the network calculation point of view, these two programs have been programmed from a different perspective compared and therefore they should be used for different purposes. Tekla NIS is more suitable for the daily use in the DSO for several reasons. Firstly, it already includes information about the network, which does not exist in PSCAD. At the moment, there is no way to transfer and convert the network information directly from Tekla NIS to PSCAD. This means that the user have to create the PSCAD-model manually

by checking the correct parameters of all network components and power lines first from Tekla NIS and then create a suitable component for PSCAD. This is really time consuming especially if the network is large. Large simulation models will also increase the time needed for the simulation run. For example, Substation 1 model took approximately 5 minutes to run a simulation time of 0,5 s. Secondly, the creation and the usage of the PSCAD models are not necessarily straight forward for new users since PSCAD is a fairly new program in Elenia. The program is sensitive to user errors and the search of the them can be complicated. However, the basic use can be learned quickly especially if a ready network model is available but the more advanced use requires time to learn.

However, in some cases it is not possible to use Tekla NIS due to the restrictions of the program. For example, Tekla NIS is not capable of doing transient studies and the accuracy of the component models is limited. PSCAD is an excellent tool for these purposes, where the time domain analysis is required or more accuracy is needed for the modeling. For example, the earth fault phenomena in the extensively cabled network or the transient phenomenon after an earth fault would not have been possible to conduct with Tekla NIS. Another usage targets could be distributed generation or voltage dips in the short circuit faults.

7. CONCLUSIONS

The purpose of this thesis was to find an optimal combination for reactive power and earth fault current compensation in extensive cabled networks. This was accomplished by defining the actual need for compensation and developing a techno-economic compensation solution for it. The study was mainly carried out by using PSCAD-simulation software and making calculations based on the results.

The study showed that there is a certain need for reactive power compensation. The most important reason is the reactive power window of Fingrid, which can cause major costs when the cabling of the medium voltage network is taken forward. The installed cables can be noticed as a constant capacitive addition to reactive power measurements at the connection point in every hour and they effect on the exceeding costs of the whole year. This means that the reactive power balance in the connection points should carefully be observed when more cables are installed in the network. Practically, the installation of the cables will partly remove the need for capacitors in the substations at some point.

The second reason for compensation is the possibility to reduce the power losses. It is possible to limit the reactive power flow through the main transformer and therefore decrease its power losses. The second possibility is to decrease the reactive power flow in the link cables between a substation and a switching station. As the amount of reactive power is decreased, it also gives more bandwidth for active power transmission. However, the cost savings depend highly on the power losses of the shunt reactors and a lot of attention should be paid on the low loss construction of the reactors even by the costs of the investment price.

It was studied whether to compensate reactive power with distributed or centralized shunt reactors. According to the simulations, distributed shunt reactors did not appear to be profitable in the normal branched feeders. Instead, distributed shunt reactors should only be used with straight cable feeders, which are over 50 km long and low loaded with a high power factor. This means that the power losses due to reactive power flow are not generally profitable to compensate in single feeders with distributed shunt reactors.

Therefore, the economic way to compensate reactive power appeared to be the usage of centralized shunt reactors, which are installed in the substations or at the switching stations. Besides reducing the reactive power flow to the main grid and

reducing the power losses, wye-connected shunt reactors can also be used to compensate earth fault currents. Shunt reactors' participation in earth fault compensation depends on the grounding of their neutral point. In case the neutral point being grounded, the shunt reactor compensates earth fault current according to its inductance value. In case the neutral point being ungrounded, the shunt reactor does not participate in the earth faults. It could be possible to place a remote disconnector between the neutral point and the ground if the earth fault behavior of the shunt reactor is desired to choose. Additionally, it would be possible to buy a large off line adjustable shunt reactor, which could be adjusted according to the need.

Earth fault compensation should be implemented by using centralized and distributed Petersén coils. It is practically compulsory to have distributed earth fault compensation units since the resistive component needs to be compensated by an adequate amount in order to assure the safety of the network. As distributed shunt reactor did not turn out to be profitable, distributed Petersén coils should be used for compensation instead. Centralized earth fault compensation should be implemented as a combination of adjustable Petersén coils and shunt reactors. However, shunt reactors can not be used solely for centralized compensation since they have a fixed earth fault compensation capacity. Instead, networks should always first have an adjustable Petersén coil at the substation to keep the correct compensation degree. This is required since the topology of the network can change and network can become overcompensated, which causes relay protection to become non-selective.

7.1 Further study

According to the results from this thesis, there will be challenges of controlling the excess of reactive power in the future. In order to control the reactive power, it would be useful to get real-time data about the reactive power consumption of the customers. At the moment, reactive power measurement data is not available from the customers under 63 A connection and their load calculation is based on the index series. It should be studied if it was possible to start to gather reactive power measurement information also from the AMR-meters of the customers.

In order to control the balance of reactive power in the medium voltage network, it would be useful for network operators to have graphical real-time reactive power measurements for each connection point and substation. Therefore, they could be aware of the reactive power window and make switching operations in order to operate within the window limits. This could be carried out as a SCADA-extension. The balance of reactive power could be followed in the substation level by utilizing the relay measurements. The measurement information could be used to optimize the compensation of the reactive power to the locations, where the excess is the largest. Therefore the operators could make the switching operations of the compensation

devices more optimally. Additionally, the relay measurements could be utilized to verify the validity of the index series of the loading models.

In addition to the presented compensation solutions in this thesis, other ways should be studied to compensate the reactive power. One way to ease the reactive power excess could be to change the reactive power tariffs for medium voltage customers. It could be possible to allow them to consume a certain amount of reactive power without having to pay for it. Therefore, the customers would have a similar reactive power window, which is used by Fingrid. This possibility should be studied closer as a business case.

The behavior of the earth fault current should also be studied more in totally cabled networks. The simulation results showed that the zero sequence resistance of the cable changes the behavior of the earth fault current remarkably. It would be interesting to verify these results with field measurements. The transient phenomenon is another earth fault issue, which should be studied more specifically. As the transient phenomenon was a secondary subject of this thesis, the results were only shallow. Additionally, it should be studied if there are other transient phenomena, which are caused by an extensive use of Petersén coils or shunt reactors.

REFERENCES

Alstom. Specifications of reactors. Offer, 7.11.2012.

Areva. Shunt Reactors in Power Systems. T&D Tech News.

Aro, M., Elovaara, J., Karttunen, M., Nousiainen, K., Palva, V. Suurjänniteteknikka (in Finnish). Bookwell Oy, Jyväskylä 2011. Gaudeamus Helsinki University Press. 520 p.

Bastman, J. Sähköverkkojen mallintaminen ja -analyysi, study materials 2011 (in Finnish). Tampere University of Technology, Finland. Department of Electrical Energy Engineering.

Department of Electrical Energy Engineering. Unpublished material. Tampere University of technology 2011.

Elenia Oy. Verkkopalveluhinnasto 1.5.2012 (in Finnish). [Cited 11.7.2012] Available at: `http://www.elenia.fi/sites/default/files/Verkkopalveluhinnasto_en_0.pdf`

Elforsk rapport 06:64. Nätkonsekvenser vid kablifiering av luftledningsnät (in Swedish). Stockholm, Sweden 2006.

Elovaara, J. & Haarla, L. Sähköverkot I (in Finnish). Tallinna Raamatutrükikoda 2011, Tallinna 2011. Gaudeamus Helsinki University Press/Otatieto. 520 p.

Elovaara, J. & Haarla, L. Sähköverkot II (in Finnish). Tallinna Raamatutrükikoda 2011, Tallinna 2011. Gaudeamus Helsinki University Press/Otatieto. 551 p.

Ericsson. AXAL-TT PRO 12/20(24 kV) Product information. 2012.

Fingrid. Kantaverkkopalvelu 2012-2015 (in Finnish). [Cited 10.7.2012] Available at: `http://www.fingrid.fi/portal/suomeksi/palvelut/kantaverkkopalvelut/`

Fingrid. Yritysinfo. [Cited 9.7.2012] Available at: `http://www.fingrid.fi/portal/suomeksi/yritysinfo/`

Sederlund, J. Telephone interview. 15.8.2012.

Fälldin, A. Interview. KKM Power, 15.11.2012.

Grainger, J J. & Stevenson W D. Power System Analysis. McGraw-Hill Inc., 1994. 787p.

Guldbrand, A. System earthing. Report, Sweden 2006. Lund University, Department of Industrial Electrical Engineering and Automation.

Guldbrand, A. Earth Faults in Extensive Cable Networks. Licentiate thesis. Lund, Sweden 2009. Lund University. Department of Measurement Technology and Industrial Electrical Engineering.

Guldbrand, A & Samuelsson, O. Central or Local Compensation of Earth-fault Currents in Non-Effectively Earthed Distribution Systems. Conference Power Tech 2007. Lausanne, Switzerland, July 1-5 2007. [Cited 6.6.2012]

Kannus, K. Suurjännitekniikka 2, lecture material (in Finnish). Tampere University of Technology, 2012.

Kauhaniemi, K. & Mäkinen, O. PSCAD-simulointi ohjelma - käytön perusteet (in Finnish). Available at: http://lipas.uwasa.fi/~kauhanie/PSCADV4_opus40.pdf

Korpinen, L. Muuntajat ja sähkölaitteet, 2012 (in Finnish). Available at: http://www.leenakorpinen.fi/archive/svt_opus/9muuntajat_ja_sahkolaitteet.pdf

Kothari, D. P. & Nagrath, I. J. Modern Power System Analysis, 3rd edition. New Delhi, 2010. Tata McGraw Hill Education Private Limited. 694 p.

Lakervi, E. & Partanen, J. Sähkönjakelutekniikka, 3rd edition (in Finnish). Hakapaino Oy, Helsinki 2008. Gaudeamus Helsinki University Press/Otatieto. 295 p.

Manitoba HVDC Research Centre. EMTDC User's guide. Canada 2010. 233 p.

Manitoba HVDC Research Centre. PSCAD User's guide. Canada 2010. 492 p.

Ministry of Employment and The Economy. Työ- ja elinkeinoministeriön ehdotus toimenpiteistä sähkönjakelun varmuuden parantamiseksi sekä sähkökatkojen vaikutusten lievittämiseksi (in Finnish). Memo, 16.3.2012.

Mörsky, J. Relesuojaustekniikka, 2nd edition (in Finnish). Karisto Oy, Hämeenlinna 1993. Otatieto Oy 1992. 459p.

Nikander, A. Novel Methods for Earth Fault Management in Isolated or Compensated Medium Voltage Electricity Distribution Networks. Doctoral thesis. Tampere, 2002. TTKK-paino. 200p.

Nikander, A. Smart Grids, lecture materials 2012. Department of Electrical Energy Engineering. Tampere University of Technology. [Cited 2.7.2012] Available at:http://webhotel2.tut.fi/units/set/opetus/kurssit/SET_1520/Materiaalit-2012/Ari_SET_1520_lecture_material_earth-faults.pdf

Pekkala, H. Challenges in Extensive Cabling of the Rural Area Networks and Protection in Mixed Networks. Master of Science Thesis. Tampere 2010. Tampere University of Technology. Department of Electrical Energy Engineering.

Pekkala, H. Katkeilevien maasulkujen aiheuttamat suojaushaasteet. Elenia Oy, unpublished material.

SFS-6001 + A1. High voltage electrical installations. 15.8.2005. Finnish Standards Association (SFS).

Tekla. Tekla products and applications, 2012. Available at: http://www.tekla.com/international/products/tekla-solutions-for-infrastructure-and-energy-industries/Pages/Default.aspx

Tekla NIS. Network information data, 2012.

Trench. Variable Shunt Reactors for Reactive Power Compensation. Product brochure 2012.

Virtanen, E. Email message, sent 8.10.2012. ABB.